**Analyzing Wound Induced Polyploidy**

By

James Sebastian White

Dissertation

Submitted to the Faculty of the

Graduate School of Vanderbilt University

in partial fulfillment of the requirements

for the degree of

DOCTOR OF PHILOSOPHY

In

Cell and Developmental Biology

May 10, 2024

Nashville, Tennessee

Approved:

Andrea Page-McCaw, Ph.D

M. Shane Hutson, Ph.D

Irina Kaverina, Ph.D

Guoqiang Gu, Ph.D

Jared Nordman, Ph.D

Gregor Neuert, Ph.D

*“The story so far:*

*In the beginning the Universe was created.*

*This has made a lot of people very angry and been widely regarded as a bad move.”*

-Douglas Adams, The Restaurant at the End of the Universe

*“If you look for the light, you can often find it.*

*But if you look for the dark that is all you will ever see.”*

-Iroh, The Legend of Korra

**ACKNOWLEDGMENT:**

What an incredible experience this has been! So many ups, downs, successes, panics, celebrations, and genuine moments of joy. Without question it has been the people around me that made this journey possible and for that I will be forever grateful.

Firstly, I cannot imagine a better lab to conduct my PhD research in than the Page-McCaw lab. Andrea, you have been such an incredible mentor there to celebrate exciting data, academic milestones, as well as strategize and plan when we were confronted with the unexpected. By pushing me to achieve academic excellence while being understanding and supportive when I was struggling, I have truly grown as a scholar and individual and I will carry the lessons I have learned with me into everything else I do. To our lab manager Kimi, I have to say that this work would not have been possible without the support you have given me as an individual, but also for everything that you do to keep the lab running, you truly make all our projects possible! To the other members of the lab, Indrayani, Aubrie, Junmin, Elkie, our previous rotation students, and high school mentees, thank you for making the lab such an accepting and exciting environment to work in. Jasmine and Ivy, you were fantastic mentees, and it was such a privilege to have you working with me in the lab. Thank you for all the work you did towards my project, and I look forward to all the amazing things you shall both go and do in the future. To my co-mentor Shane and the trainees past and present in the Hutson lab thank you for helping to shape my work with new insights and perspectives I could not have gleaned otherwise. I greatly appreciate Nick and Kari at the COE, my analysis wouldn't have been possible without you. Thank you to the Losick lab for allowing me to attend your lab meetings and discuss new findings and insights in the field of wound induced polyploidy. I also thank my committee Irina Kaverina, Guoqiang Gu, Jared Nordman, and Gregor Neuert for their guidance and expertise throughout my PhD career as well as all the faculty and students in the CDB and PDB departments who have weighed in on my project during retreats and seminars.

To all my friends, your support through my PhD has made it possible. James O'Connor I couldn't imagine a better grad student mentor to have. You're a brilliant scientist and one of the smartest people I know. I've benefitted so much from your support and guidance, and I am so privileged to be able to call you a friend. You're the kindest and most genuine person I know, and I'm so happy that we met. To Mary I'm so glad we've become best friends since we rotated together, our excursions have continually brought me joy and I'm so glad to have had your comradery through the years. Jonathan and Esther, it's been a delight getting to know each of you and I wish you both the best of luck with your future endeavors and look forward to rendezvousing for dinner parties. To Kavya thank you for not only being a fantastic friend but helping to create the spaces for academics to branch into industry, I look forward to seeing all that you build. Ryan, the Sunday dinners have been such a tremendous grounding force for me during my studies, through thick and thin a delicious meal was often exactly what I needed to pick myself up and face the coming week.

Finally, I'd like to thank my family. Mom and Dad thank you for all the sacrifices you've made and the time you've put into raising me to be the person I am today. Reaching this stage in my academic career would not have been possible without your support and belief in me. Alex thanks for being a great brother, your support through my PhD, and your expertise with coding has been fantastic. Lastly thanks to Preston, I've learned so much about myself by fostering you and am so happy you're a permanent part of the family, you are and will always be the goodest boy.

**TABLE OF CONTENTS** **Page**

**LIST OF TABLES** **Page**



**LIST OF FIGURES** **Page**

**CHAPTER 1: INTRODUCTION**

Life on earth has not only evolved highly complex biological systems but developed strategies to repair those systems when they become injured. This thesis will endeavor to briefly summarize a number of these repair strategies before delving deeply into two specific mechanisms that aid in wound closure in the fruit fly, *Drosophila melanogaster.*

*What is a wound and why repair it?*

An organism is defined as a self-organizing, self-replicating, entity made up of at least one cell. So, an organism can be as small as a single bacterium, such as the Mycoplasma genitalium which is approximately 200-300 nm in size. This is about the distance between the peak and trough of a wavelength of ultraviolet light. On the opposite end of the spectrum, we have the Blue Whale, which is estimated to be made up of ~1 quadrillion cells. For scale, it would take approximately 1 quadrillion average burritos (5" x 3") placed next to each other to cover the entire surface of the United States of America. To add further complexity, multicellular organisms are comprised of many different cell types, arranged in separate organs, with highly specific functions. These separate organs and the cells that make them up must work in concert with one another to perform the business of being alive. It should also be noted that organisms do not simply pop into existence as fully formed entities. The 1 quadrillion cells of a Blue Whale started as a single fertilized egg that developed by sequential programmed divisions. As they divided the cells took on new characteristics, behaviors, and functions as they became tissues that migrated, folded, deformed, and expanded into the organs that made up the whole blue whale.

As it takes a considerable amount of effort to manufacture a fully developed organism, it is no surprise that defenses have been erected to protect them. Bacteria produce strong outer walls made of peptidoglycans that protect them from microscopic assaults (Silhavy et al., 2010). Arthropods surround their bodies with a waxy cuticle (Vincent, 2002). This cuticle protects insects from dehydration and acts as a physical barrier preventing the invasion of microorganisms. In some insects this cuticle is reinforced to become fully fledged armor, such as the Ironclad beetle whose armor is so strong it can survive being run over by a car (Rivera et al., 2020)! A cursory glance at the side of the road will demonstrate that mammals generally have less success when being run over by a car, though some instances of success in this area have been colloquially noted. We are less resilient to high-speed vehicular encounters because mammals forgo an armored exoskeleton (it should be noted the armored armadillo is encased in bone not an exoskeleton (Chen et al., 2011)). All animals have an external barrier made up of epithelial cells including a layer of tight junction proteins (Anderson & Van Itallie, 2009; Mandel et al., 1993). These tight junction proteins create a seal that dissuades microbes and even water from passing between cells(Kovbasnjuk et al., 1998).

However, despite investing in defenses, injury still comes in many forms. Exposed tissues are at the mercy of debris like stray sticks and sharp boulders (or a tenacious piece of paper) which can slice through the layers of epithelium. Predatory organisms have evolved many tools to cause injury like

microscopic spears, found in jellyfish tentacles, or sharp teeth of the defunct sabretooth tiger, mosquitoes and ticks have evolved needle like olfactory protrusions to stab into their victims and feast on a blood meal. In all these instances, the disruption of the outer barrier for the prey presents many problems. For larger injuries, the immediate threat is that the ability of the epithelium or exoskeleton to keep blood or hemolymph within the body is compromised. A resulting loss of bodily fluids and death can occur rapidly. Clotting factors in the blood of mammals (Palta et al., 2014), and the hemolymph of insects (Dushay, 2009), have evolved to clog the injury site, preventing bleeding out. After dealing with the immediate loss of bodily fluids, the next issue is that the microorganisms that the barrier layer had neatly kept in the outside, have now been invited to the inside. Some microbes like those in the gut work symbiotically with the host (Ghosh et al., 2022; Sasso et al., 2023). However, many of the microbes introduced through breaches in the barrier layer are terrible guests and launch full scale invasions (Doron & Gorbach). As these microbes proliferate, they disrupt the function and homeostasis of the tissues causing further cell death and destruction around the injury site. To combat invaders, multicellular organisms have evolved complex immune systems tasked with detecting and destroying problematic microbes (Chaplin, 2010). This thesis, will explore how epithelia reacts to injury.

*What are epithelial cells?*

Epithelial cells 'did it first' as they were the first organized tissues in evolution predating metazoans which evolved about 600 million years ago (Miller et al., 2013; Morris, 1993). They form the foundation for multicellularity because of their ability to form polarized sheets of cells, holding onto one another with specific attachments (Bryant & Mostov, 2008). These attachments are controlled through several proteins localized to the lateral domain of epithelia, most predominantly cadherin proteins (Chapter 1, Fig 1) (Miller et al., 2013). Cadherins are transmembrane proteins which embed into the plasma membrane bridging both the interior and exterior environments of the cell. The intercellular domain of cadherins connects to the actin-cytoskeleton via catenins (Buckley et al., 2014; Perez-Moreno & Fuchs, 2006). The extracellular domain of cadherins bind to the extracellular domain of cadherins on neighboring cells mechanically holding the two cells together (Perret et al., 2004).

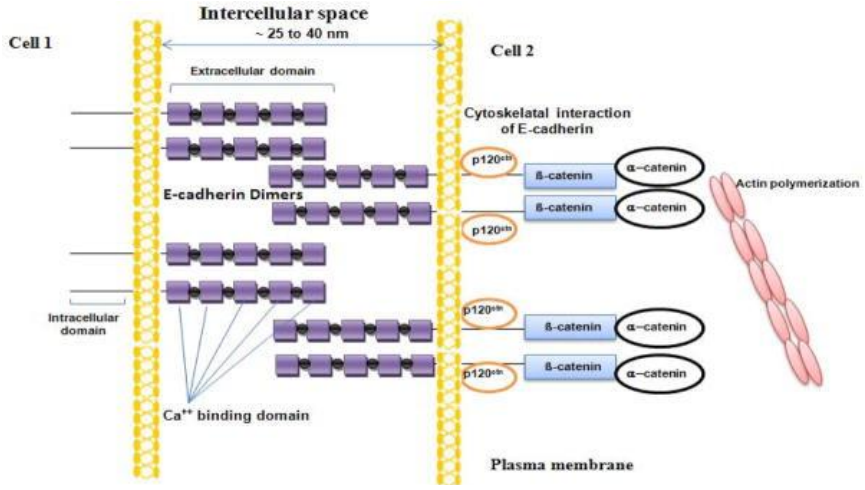


**Chapter 1, Figure 1: Diagram of adherens junction.** Extracellular E-cadherin domains bind cell 1/2 together, while catenin proteins allow the intracellular domain of E-cadherin to interface with the actin cytoskeleton. Figure from (Baranwal & Alahari, 2009).

One of the main hallmarks of epithelia is that they are polarized, and this is one of the evolutionary inventions that allowed for multicellular life to flourish. Briefly, epithelial cell polarity is maintained by several core protein complexes. It should be noted that these core proteins are generally conserved through the animal kingdom (Assémat et al., 2008; Goldstein & Macara, 2007; Rodriguez-Boulan & Macara, 2014; Tepass, 2012; Yamanaka & Ohno, 2008) but they are not necessarily required in every epithelium. Apical cell polarity is dependent on the Par and Crumbs complexes that establish and maintain the localization of the adherens junctions, which demarcate the apical-basal boundary (Bazellières et al., 2018; Halaoui & McCaffrey, 2015; Médina et al., 2002; Morais-de-Sá et al., 2010; Pieczynski & Margolis, 2011). More recently, the Crumbs complex has been implicated in the trafficking of Crumbs and cadherin to the apical domain, (Hao et al., 2020) and the regulation of the lipid phosphatase levels at the apical membrane (Lattner et al., 2019). Additionally, Crumbs and the Pak complex component aPKC have been implicated in regulating the correct apical/lateral membrane ratio in concert with a number of other factors to regulate cortical tension and subsequently allow for the formation of epithelial structures (Biehler et al., 2021). The basal compartment is defined by the Scribble complex, which has been implicated in the initial assembly of adherens junctions (Bonello et al., 2019), but has been better characterized as antagonizing apical and junctional proteins, preventing their spread into the basolateral compartment (Bilder et al., 2003; Bonello et al., 2019; Laprise et al., 2006; Laprise et al., 2009; Tanentzapf & Tepass, 2003).

By holding onto each other through junctional proteins, and polarizing, epithelia allow for the formation of a critical structure in biology: tubes! Epithelial tubes are very common in the animal kingdom and have generalizable polarized domains: the apical side faces an internal lumen space, or the inside of the tube. Whereas the basal side connects to surrounding tissues or extracellular matrix holding the tissues in place. For example, the intestinal tract of *Drosophila* is made up of polarized intestinal epithelial cells. The apical domain faces into the gut tube and produces microvilli which have many roles including nutrient absorption. The basal domain faces out from the gut and through the use of integrins, connects the epithelium to the basement membrane providing stability to the tissue (Klunder et al., 2017). Although the exact architecture changes, similar mechanisms of polarized epithelia are observed in the podocytes of the kidney (Schlüter & Margolis, 2012), uroepithelium of the urinary tract (Khandelwal et al., 2009), multiple cells types of the respiratory epithelium in the lung (Mescher, 2018; Waters et al., 2012), uterine luminal epithelium (Ye, 2020), and hepatocytes of the liver (Tanimizu & Mitaka, 2017). Although epithelial tubes are frequently observed throughout the animal kingdom, we are generally most familiar with the epithelial tissues that forms our outer-most layers: our skin.

Skin specification occurs very early during development, just after gastrulation (Fuchs, 2007) when a subpopulation of the neuroectoderm is essentially blocked from becoming a neuronal and instead become a single layer of epithelial cells. (Bleuming et al., 2007; Böttcher & Niehrs, 2005; Hu et al., 2018; Kashgari et al., 2018; M'Boneko & Merker, 1988; MacDonald et al., 2009; Moll et al., 1982; Stern, 2005). This single layer of epithelial cells eventually develops into the basal layer of the epidermis, the stratum basale (Hu et al., 2018). This layer contains the epidermal stem cells whose progeny differentiate and migrate up forming the other layers of the epidermis (Kuri et al., 2019). In the adult epithelium, the stratum basale is covered by the stratum spinosum, which is comprised of irregularly shaped keratinocytes linked together with desmosomes which help to maintain the structural integrity of the skin. Next the stratum granulosum is made up of flatter keratinocytes loaded with keratohyalin

granules which will be deployed in the next two layers. Thick tissues contain stratum lucidum which is characterized by the presence of eleidin, a product of keratohyalin and an intermediate for the final layer of the skin. The stratum corneum is the outer most layer, the keratohyalin granules expand to become a homogenous keratin matrix as the keratinocytes lose their organelles and nuclei forming a semipermeable barrier to UV radiation, toxins, and mechanical assaults. (Barbieri et al., 2014; Maynard & Downes, 2019).

Outward-facing epithelia, are conserved throughout the animal kingdom, but unsurprisingly they do not all appear exactly like the mammalian skin. The epidermis of *Drosophila melanogaster* is one such case. One of the most striking differences is that *Drosophila,* and all holometabolous insects (Truman, 2019; Truman & Riddiford, 1999), develop two epidermises during their lifetimes. The first is formed during embryogenesis via a process called cellularization whereby the approximately 5000 nuclei that make up the syncytial (or multinucleated) embryo become separated by plasma membranes (Loncar & Singer, 1995). The embryonic epidermis is maintained through to the larval stage of development. During this time the epidermis secretes the cuticle (Hillman & Lesnik, 1970; Kaznowski et al., 1985) which protect the embryo and larva from abrasion and dehydration. At the end of the larval stage, *Drosophila* undergo pupariation, whereby the larval cuticle is ejected and forms the opaque ridged pupal case. Underneath the case, the pupa undergoes impressive renovations, supplanting the original structures that made up the larval body plan by creating the new adult tissues from the imaginal discs. The imaginal discs are adult precursor cells embedded throughout the larva. During pupation the imaginal discs evert out of the larval body (Mirth, 2005; Riddiford et al., 2010), undergoing massive cytoskeletal reorganizations and expanding, as the larval tissues are removed, forming the adult body plan (Athilingam et al., 2021). The entire process of pupation is far too vast for the scope of this thesis, however, a brief review of how the epidermis of the pupal thorax forms will be relevant for future chapters.

The dorsal epidermis of the pupa, the notum, forms during pupation as a result of the eversion of the wing imaginal discs (Fristrom, 1993). The early wing disc is essentially a flattened epithelial tube made up of cuboidal epithelial cells with a thin internal lumen. As the wing disc develops cells of one side of the tube stretch into large but thin peripodial epithelial cells (Auerbach, 1935; McClure & Schubiger, 2005). Cells of the other side divide becoming tightly packed and elongating along the apico-basal axis, forming a columnar epithelium referred to as the disc proper (Tripathi & Irvine, 2022). Keeping to the hallmarks of epithelial cells, the disc proper is polarized on the apico-basal axis. Within the apical marginal zone of the epithelium, polarity factors such as the Crumbs and Par complexes work antagonistically with the basolateral Scribble complex to specify the location of the adherens junctions (Bazellières et al., 2018; Bilder et al., 2003; Bonello et al., 2019; Halaoui & McCaffrey, 2015; Laprise et al., 2006; Laprise et al., 2009; Médina et al., 2002; Morais-de-Sá et al., 2010; Pieczynski & Margolis, 2011; Tanentzapf & Tepass, 2003). Concentrated microtubule and actin networks localize to the apical domain of the columnar epithelial cells near the adherens junctions (Eaton et al., 1995; Sui et al., 2012). On the basal side, the wing disc is surrounded by a basement membrane comprised of collagen, laminin, perlecan, and nidogen (Bonche et al., 2021; Hynes & Zhao, 2000; Ramos-Lewis & Page-McCaw, 2019). However, it is the transmembrane integrin proteins that connect the basal side of the epithelium to this basement membrane (Hynes, 2002) and loss of integrins is associated with a collapse of the wing disc into a cuboidal epithelium (Domínguez-Giménez et al., 2007). Upon pupation a strong ecdysone pulse arrests growth in the wind disc and signals for the eversion of the wing disc (Mirth, 2005; Riddiford et al.,

2010). During eversion, the stalk cells at the dorsal tip of the wing disc in concert with the peripodial cells invade the larval epithelium. A pore is then created through which the notal epithelium migrates behind a wavefront of peripodial cells which crawl between the larval epithelium and the cuticle. As the new pupal epithelium migrates from the two wing discs on either side of the larva, the original larval epithelium delaminates and undergoes apoptosis. (Aldaz et al., 2010, 2013; Athilingam et al., 2021; Fristrom, 1993; Martin-Blanco et al., 2000; Pastor-Pareja et al., 2004). The two migrating halves of the notum meet at the midline and fuse leading to thorax closure and a continuous monolayer epithelium (Martin-Blanco et al., 2000; Zeitlinger & Bohmann*, 1999). This pupal notum has become an excellent model system for studying how epithelia respond to injury (Chapter 1, Fig. 2).

*How do epithelial cells respond to injury?*

The notum was first used as a wounding model in 2013 by Antunes *et al.* In this work they describe an actomyosin 'flow' where mCherry-labelled Moesin could be seen filling the apico-medial space within a ring of cells 3-4 cell diameters out from the wound site. This mCherry-Moesin relocalization appeared to flow from distal cells in towards the wound and correspond with the apical contraction of the cells. This 'wave' of actin coalesced at the leading edge in an actomyosin purse string structure (Antunes et al., 2013). This purse string has been observed in a number of epithelia during wound repair and through its constriction helps to draw the wound closed. First observed in the epidermis of the chick embryo (Brock et al., 1996; Martin & Lewis, 1992), this structure has also been observed around wounds in the early embryo of the frog *Xenopus laevis (Davidson et al., 2002)*, the mouse embryo (Martin et al., 1994), *in vitro* human intestinal epithelium (Bement et al., 1993a; Russo et al., 2005), the *Drosophila* embryo (Abreu-Blanco et al., 2012; Kiehart et al., 2000; W. Wood et al., 2002), and has also been observed in the jellyfish *Clytia hemisphaerica (Kamran et al., 2017)* a member of the phylum Cnidaria which evolved almost 600 million

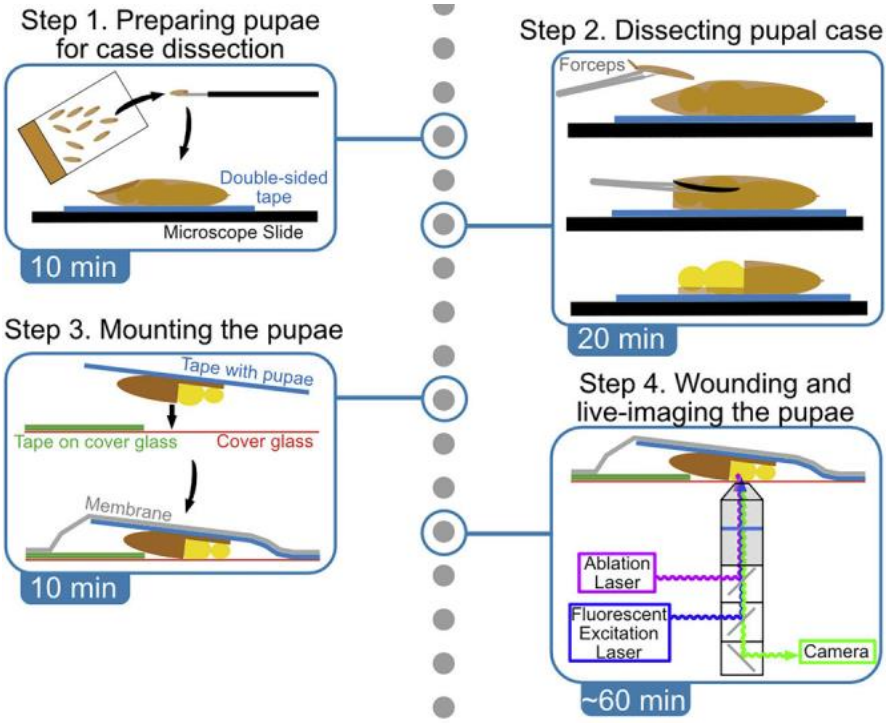


**Chapter 1, Figure 2: *Drosophila* mounting for laser ablation.** The *Drosophila* pupae is an immobile model system making it highly tractable for mounting, wounding, and monitoring for hours or days after injury. Figure from (O'Connor et al., 2022)

years ago, thus epithelial repair via purse strings has likely been utilized by species for hundreds of millions of years.

Wood *et al.* showed that purse string contraction drives an initial stage of wound closure which is then completed by filopodia protrusion at the last stages of closure (W. Wood et al., 2002). However, if either the purse string or filipodia protrusions were inhibited the wounds still closed but on a longer time scale indicating that these behaviors can compensate for one another (W. Wood et al., 2002). This result is consistent with reports in *Drosophila* larva where a purse string was not observed and instead epithelial spreading, likely due to lamellipodial expansions, drove wound closure (Galko & Krasnow, 2004). The use of lamellipodia and filipodia during would closure is also a highly conserved phenomenon observed in canine kidney epithelial cells (Cochet-Escartin et al., 2014; du Roure et al., 2005; Fenteany et al., 2000; Poujade et al., 2007; M. Tamada et al., 2007; Trepat et al., 2009), rat liver epithelial cells (Omelchenko et al., 2003) immortalized human corneal limbal epithelial cells (Klarlund, 2012), and *Drosophila* embryos (Abreu-Blanco et al., 2012; Meghana et al., 2011). So, many behaviors are deployed to bring cells into the wound bed. However, as cells migrate into the wound space becomes limited and another behavior, intercalation, is required to remove cells from the leading edge.

Intercalation refers to coordinated reorganization of cell-cell contacts and is observed through development (Walck-Shannon & Hardin, 2014) and during wound repair (Razzell et al., 2014; Tetley et al., 2019; White et al., 2023). In the context of injury, intercalations often occur between neighbors at the leading edge of repair, where the tricellular junctions of the intercalating cell are brought together establishing a single tricellular junction between its neighbors leading to the ejection of the intercalating cell from the leading edge and advancement of its neighbors. Without intercalation cells at the leading edge would need to continue elongating towards the wound drawing to a point like slices of a pizza. Instead, intercalation allows for cell removal at the leading edge allowing remaining cells to maintain a more typical shape during closure. Through modeling and experiments in the *Drosophila* wing disc, Tetley *et al.* were able to determine that intercalation is the rate limiting step in their system and by modulating purse string and junctional tension the tissue becomes more fluid, allowing for rapid wound closure (Tetley et al., 2019).

Tension has long been implicated in the wound healing process, as early as 1861 guidelines for minimizing mechanical force exerted on wounds have existed to improve patient outcomes (Berry et al., 2023; Carmichael, 2014). More recently, we are understanding that increased mechanical force on a healing wound correlates with increased scarring and reduced functionality in the healed tissue (Gurtner et al., 2011; Wong et al., 2012). Consistent with this, pathological scarring such as hypertrophic scars or keloids are more common in areas subject to higher mechanical strain (Akaishi et al., 2008; Ogawa et al., 2012). The cells responsible for sensing and responding to mechanical forces during wound healing in mammals are mainly dermal fibroblasts (Chiquet et al., 2007; Duscher et al., 2014; Eckes et al., 2006; Kadi et al., 2008; Wang et al., 2005). Fibroblasts expand during the proliferative phase of wound closure (Thulabandu et al., 2018) and contribute to angiogenesis (Li et al., 2003; Tonnesen et al., 2000), and extracellular matrix remodeling (Mirastschijski et al., 2010). Fibroblasts then differentiate into myofibroblasts which regulate many of the processes of the remodeling phase of wound healing (Desmoulière et al., 2005). Interestingly, this differentiation has been linked to tensile forces in an in vitro microtissue model (Kollmannsberger et al., 2018). Myofibroblasts continue to remodel the extracellular matrix, stiffening it while also taking on contractile properties by generating stress fibers (Bernardo & Fibbe, 2013; Grinnell & Petroll, 2010; Sawant et al., 2021). As the tissue recovers and the extracellular

matrix stiffening restores, in part, the tissues tensile strength, cellularization within the scar begins to decrease through apoptosis (Bainbridge, 2013). Thus, mechanical tension plays a critical part in the wound closure process either through the active migration of cells, or as signaling mechanism that cells can use to coordinate the phases of wound closure.

Mechanical tension has also been theorized to play a role in early wound detection (Antunes et al., 2013; Cao et al., 2017; Enyedi & Niethammer, 2015; Franco et al., 2019; Xu & Chisholm, 2011). Our lab has begun to explore tension changes early during wound closure (Han et al., 2023). Ivy Han who was an undergraduate mentee in the lab performed, in an exceedingly diligent and meticulously impressive manner, hundreds of laser recoil experiments in the pupal notum after wounding. We were able to determine that after wounding there was a loss of tension uniformly around the wound. We were then able to determine that tension is restored after injury beginning distal to the wound and moving inward toward the wound center over time. At ~135 µm from the wound it took 5-6 min for tension to be restored, whereas at the ~70 µm mark it took 15-18 min for tension to be restored to normal levels. Unwounded samples had uniform tension across the control and experimental *pnr* domain (an hourglass stripe in the middle of the pupal thorax) in which we were able to express gene knockdowns. When RNAi against *Rok* was expressed in the *pnr* region tension was lost uniformly across 70 - 110 - 210 µm measurements. Given the similar timing and dynamics of this tension restoration we explored its relationship to the actomyosin wave that had been previously observed (Antunes et al., 2013). Interestingly, tension was restored after the wave of cellular contractility passed through. We also determined that the restoration of tension was dependent on the G-protein-coupled receptor Methuselah-like 10 (Mthl10). Our lab previously characterized Mthl10s role in the protease initiated intracellular calcium release after wounding and following large wounds. Depletion of *Mthl10* by RNAi resulted in a 30% decrease in survival (O'Connor et al., 2021). When *Mthl10* RNAi was expressed in the *pnr* region, the contractile wave still passed through the tissue, but tension was not restored. Thus, Mthl10 is not required for the actomyosin wave initiation, however, it is required to maintain high tension in the wake of the wave (Chapter 1, Fig. 3). Further studies will be needed to elucidate the mechanisms of how Mthl10 maintains tension in the wake of the actomyosin wave. However, these studies highlight how fundamental mechanical tension is during the wounding process, not just for a cell's ability to physically migrate into the wound bed, but as a critical part of restoring homeostasis after injury.

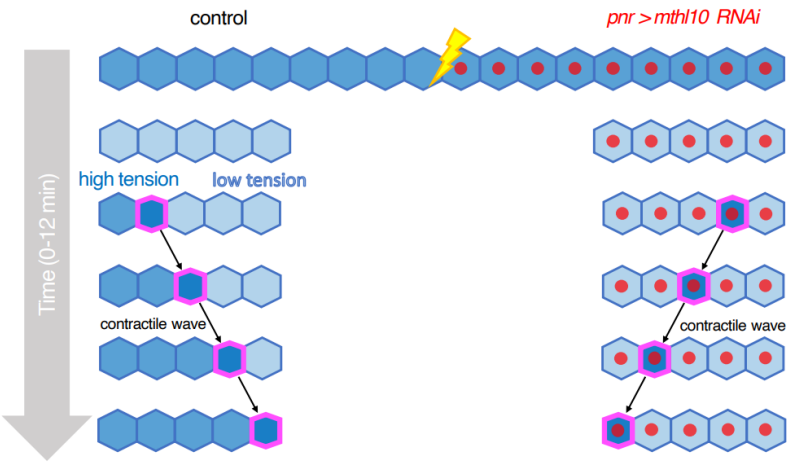


**Chapter 1, Figure 3: *Mthl10* is required to restore tension in epithelial cells after wounding.** From (Han et al., 2023)

*Wound healing, cancer metastasis, and polyploid giant cancer cells*

Mechanisms of wound healing allow organisms to resist an often-hostile world, repairing damage, defeating infection, and restoring function and homeostasis. However, this suite of behavioral and molecular tools cells deployed during injury proves catastrophic when they become dysregulated. In fact, the proliferative, invasive, and migratory behaviors that are critical for rapid wound closure, become the hallmarks of metastatic tumors.

Metastatic tumors occur when cancer cells from a primary tumor within the body escape their original location and invade other parts of the body (Dymerska & Marusiak, 2023). The processes of tumor formation and metastasis are extremely complicated, as different tissues throughout the body utilize different mechanisms to know what cell type they are supposed to be, and thus the nature of their dysregulation is often also different. It is becoming appreciated that metastasis can be driven by the induction of M2 like macrophages within the tumor which help to stimulate epithelial to mesenchymal transition of the primary tumor cells (Duan & Luo, 2021; Pan et al., 2020; Takase et al., 2016; Zhou et al., 2020). This is similar to the role M2 macrophages play during mammalian wound healing where they promote the loss of epithelial characteristics in wounded epithelia (Landén et al., 2016; Sindrilaru & Scharffetter-Kochanek, 2013; Sorg et al., 2017). Namely, the loss of apico-basal polarity, cell-cell adhesions, and the induction of shape changes and migratory behaviors(Nieto et al., 2016). When these M2 like macrophages form in the tumor environment they promote metastasis presumably through similar molecular programs as in wound healing. The current diagnostic approach to combat both primary tumors and metastasis are chemotherapeutics and surgical removal. However, recent investigations have revealed a subpopulation of cancer cells that help tumors to escape treatments (Jiao et al., 2024).

Polyploid giant cancer cells (PGCC) have been observed in tumors for at least 180 years, however, only recently has their role in tumor survival been appreciated (Amend et al., 2019; Casotti et al., 2023; Kasperski, 2022; Mukherjee et al., 2022; Niculescu, 2022). PGCC's can be induced by chemotherapy, antimitotic drugs, radiotherapy, hypoxia, and deficiencies in the tumor microenvironment (D. Zhang et al., 2014). They form via their own cell cycle, the giant cell cycle. The giant cell cycle starts with the initiation phase, where following an immense stressor a subset of diploid cells in G2 at the time of the stressor become decoupled from the mitotic cell cycle, and its cell cycle checkpoints, and enter a tetraploid or polyploid state. From this polyploid state they enter the self-renewal phase where they have many directions to go in and can execute them in multiple combinations. They can become endomitotic duplicating and dividing the genome creating a multinucleated PGCC and they can continue endoreplication to create a larger single nucleus. During the termination phase they can undergo reductive division by nuclear budding, nuclear fragmentation, or nuclear fission to create diploid daughter cells. These daughter cells enter the stability phase where due to mutations and genomic reorganizations they have acquired a new genome, with mitotic competency and a stable karyotype (Liu, 2020; Niu et al., 2016).

Through the giant cell cycle, PGCC's are able to survive the genotoxic stresses of our current cancer treatments like chemotherapy by escaping from premature senescence in a polyploid state (Bharadwaj & Mandal, 2020; Bharadwaj et al., 2018; Mirzayans et al., 2018; Mirzayans & Murray, 2020a, 2020b). As they are often aneuploid, they have a high degree of genetic diversity, which is thought to

promote tumor microenvironment evolution (Pienta et al., 2022). This evolution allows daughter cells of PGCC's to have a higher degree of therapy resistance (Amend & Pienta, 2015; Amend et al., 2019) and PGCC associated tumor regrowth has been observed in response to radiation therapy (Erenpreisa et al., 2008; Erenpreisa et al., 2000), chemotherapy (Puig et al., 2008; Rohnalter et al., 2015; Sundaram et al., 2004; S. Zhang, I. Mercado-Uribe, et al., 2014; S. Zhang, I. Mercado-Uribe, et al., 2014) and *RAS* oncogene activation (Leikam et al., 2015). PGCC's have also been implicated in tumor metastasis (Zhang Weihua et al., 2011), and form their own tumors when implanted into mice (Fujiwara et al., 2005). Thus, PGCC's are induced by the very treatments meant to eliminate tumors and allow them to survive, reproliferating and metastasizing after the removal of the treatments. Understanding exactly how PGCC's form, and the molecular mechanism they use to evade genotoxic stress will be critical for developing more effective chemotherapeutics. One way to understand how polyploidy becomes dysregulated in cancer, is to understand how tissues are able to induce and control it during wound healing.

*Wound induced polyploidy.*

The occurrence of polyploid cells following injury has been noted for some time, however, we have only just begun to elucidate its roles, and decipher in what contexts it aids or impedes repair (Bailey et al., 2021; Gjelsvik et al., 2019; Lang & Schnittger, 2020; Øvrebø & Edgar, 2018). One organ where this dichotomy is most stark is the heart. In mammalian systems cardiomyocytes are diploid during development (Porrello et al., 2011) but become polyploid either through endomitosis in the murine heart (Liu et al., 2010; Soonpaa et al., 1996) or endoreplication in human hearts (Mollova et al., 2013). Interestingly, neonatal mammalian hearts have a high regenerative capacity (Porrello et al., 2011), whereas adult hearts have a poor regenerative capacity exhibiting increased scarring (Ebert & Pfitzer, 1977; Senyo et al., 2013; Soonpaa & Field, 1997). Further, mouse strains with a greater proportion of diploid cardiomyocytes to polyploid showed a higher regenerative capacity to those with a higher number of polyploid cardiomyocytes (Patterson et al., 2017). Thus, it has been inferred that polyploidy is likely induced in the mammalian heart as an adaptive response to achieve repair in a tissue that has lost its capacity to mitotically regenerate. Consistent with this, the cardiomyocytes of the adult zebrafish heart show a high degree of regenerative capacity, but they are diploid not polyploid and retain their proliferative capacity (Jopling et al., 2010; Kikuchi et al., 2010). Inducing ectopic polyploidy in the cardiomyocytes of the zebrafish limit their regenerative capacity (González-Rosa et al., 2018). However, polyploidy is induced in the mitotically capable zebrafish epicardium by mechanical tension. These endomitotic and endoreplicating cells form a wavefront of repair leading diploid cells to encompass the zebrafish heart and if this polyploid wavefront is ablated a new polyploid wavefront is formed. Once the heart is re-encompassed the polyploid cells then undergo apoptosis leaving a diploid tissue behind (Cao et al., 2017). Additionally, new studies are highlighting that polyploidy in the mammalian heart does have a beneficial role (Bradley et al., 2021; Chakraborty et al., 2023). Further studies will be required to elucidate the exact contexts in which polyploidy is beneficial or harmful during heart regeneration (Derks & Bergmann, 2020).

Another organ with well characterized and conserved injury induced polyploidy is the liver (Carriere, 1969; Matsumoto, 2022; Wheatley, 1972). Similar to the heart, mammalian hepatocytes are diploid at birth and become polyploid with age (Celton-Morizur et al., 2009; Duncan et al., 2012; Guidotti

et al., 2003; Hsu et al., 2016; Kudryavtsev et al., 1993; Matsumoto et al., 2021; Severin et al., 1984; Toyoda et al., 2005a). It has been hypothesized that increased ploidy of hepatocytes allows for increased metabolic activity, and some metabolic genes are differentially expressed between diploid and polyploid hepatocytes (Richter et al., 2021). However, blocking hepatocyte polyploidy did not have an impact on liver differentiation, zonation, or metabolism in one study (Pandit et al., 2012). Despite this, many types of liver injury increase hepatocyte ploidy (Gentric et al., 2015; Madra et al., 1995; Muramatsu et al., 2000; Sigal et al., 1999; Toyoda et al., 2005a; Wilkinson et al., 2019). Interestingly, polyploidization of hepatocytes does not block them from dividing (Duncan et al., 2009). In fact, they are able to undergo multipolar reductive mitosis (Duncan et al., 2010) and transplantation of labeled polyploid hepatocytes into recipient livers resulted in the formation of labeled diploid cells (Duncan et al., 2010). It has also been noted the diploid progeny of polyploid hepatocytes can undergo re-polyploidization (Matsumoto et al., 2020). Further studies will be required to understand the benefits of hepatocyte ploidy, some studies have suggested that highly polyploid livers function normally (Lin et al., 2020; Sladky et al., 2020) and suppress tumor formation (Zhang et al., 2018), whereas others see enhancements in disease like states (Dewhurst et al., 2020; Ow et al., 2020).

Studies have also characterized other tissues which increase ploidy after injury, but less is known about these examples. The kidney induces polyploidy and this increased ploidy helps to maintain kidney function during injury (De Chiara et al., 2022; Lazzeri et al., 2018). Injured urothelial cells of the bladder induce polyploidy and the increase in genomic material in the absence of division is hypothesized to preserve the integrity of the uroepithelial barrier during repair (Jia Wang et al., 2018). Injury to the alveolar epithelium of the lung induces polyploidy and is a mechanism to maintain barrier function without excessive cell numbers (Leach & Morrisey, 2018; Weng et al., 2022; Zemans, 2022). Multiple tissues within *Drosophila* induce polyploidy in response to injury: the hindgut pylorus endoreplicates in response to apoptotic damage (Cohen et al., 2018; Losick et al., 2013; Xiang et al., 2017). There has also been significant work exploring the induction of polyploidy in the epidermis of *Drosophila*.

Polyploidy was first observed in the *Drosophila* larval epidermis (Galko & Krasnow, 2004) and then in the adult epidermis after puncture wounding (Losick et al., 2013). Adult epidermis polyploidy has been well characterized by Dr. Vicki Losick, first through her work in the Spradling lab and then through the work of her own independent laboratory. She first demonstrated that following wounding nuclei re-enter the cell cycle but do not divide and cells also fuse with neighbors to form syncytia. Nuclear polyploidy was dependent on Yorkie (the *Drosophila* homologue of Yap/Taz) and Cyclin E, whereas cell-cell fusion was dependent on the Rac GTPase (Losick et al., 2013). In a later study she was able to determine that the Yki tunes the degree of endoreplication downstream of the hippo pathway. The JNK component AP-1 was found to inhibit Yki activity to control the degree of post-wound endoreplication. She then showed the conservation of this process in a mouse model of Fuchs dystrophy where corneal cell loss was compensated for by endoreplication in a Hippo / JNK dependent manner (Losick et al., 2016). They were able to further characterize that Yki induced endoreplication through its downstream effectors Myc and E2f1, and Myc alone was sufficient to induce endoreplication in even unwound tissue (Grendler et al., 2019). They then forced nuclei in the wounded epithelium to enter the mitotic cell cycle via overexpression of *String* and concomitant knockdown of *fizzy-related*, which had been previously shown in the literature (Schaeffer et al., 2004). Forcing the wounded epithelium to undergo mitosis instead of endoreplication resulted in gaps in the epithelium, partial wound closure failure, and thinner epithelial membranes. Additionally, mitotic errors were observed such as chromatin bridging between

nuclei and micronuclei. In the presence of additional UV damage, polyploid capable epithelia were able to successfully repair, whereas forced mitotic epithelia could not (Grendler et al., 2019). Previous studies had shown that Hippo-Yap signaling was regulated by focal adhesion proteins (Elbediwy et al., 2016; Kim & Gumbiner, 2015). Thus, the Losick group explored the expression and localization of focal adhesion proteins and found that Integrin, Talin, and Focal Adhesion Kinase were all required for endoreplication. Inhibition of focal adhesion proteins reduced the activity of Yki downstream targets and also reduced the degree of cell-cell fusions leading to smaller syncytia around wounds (Besen-McNally et al., 2021). Most recently, they characterized that in the unwounded epithelium syncytia form via cell-cell fusion in an age-dependent process, not linked to apoptosis. Interestingly, age related polyploidy correlated with reduced mechanical function which could be rescued by inhibiting cell-cell fusion. Given the connection to mechanical function they explored the role of the adherens junction associated mechanosensory protein α-catenin in flies and mice and found that α-catenin suppresses cell-cell fusion. They also found that inhibiting the *Drosophila* epithelial cadherin *shotgun* increased the degree of cell-cell fusion by ~10-fold (Dehn et al., 2023). Thus, through a decade of work, Losick *et al*. robustly characterized the induction of endoreplication and cell-cell fusion in a Yki- and Rac-dependent manner revealing some of the key upstream and downstream regulators of this process and connecting it to the mechanics of the tissue.

When I started my thesis work in the Page-McCaw lab, the available literature suggested polyploidy was likely a wound induced behavior relegated to quiescent and post-mitotic tissues. Thus, I set out to explore how wounds induced mitosis by assaying a mitotic tissue, specifically the mitotically capable pupal notum. This tissue is easily accessible with a simple dissection and is stationary facilitating long-term microscopy (O'Connor et al., 2022). Additionally, during development the notum undergoes sequential round of mitosis over the first 28 hours after puparium formation (Guirao et al., 2015). As the future chapters will detail, when I performed wounding experiments 12-16 hours after puparium formation, I did not observe wound induced mitosis. Instead, the pupal notum induced individual nuclear polyploidy and cell-cell fusions resulting in syncytia which invaded the wound site and repaired the epithelium. These results indicate that even mitotically capable tissues opt for polyploidy during repair. Given the frequent occurrence of wound induced polyploidy throughout the animal kingdom and in human organs, future experiments should robustly explore the factors governing their induction and regulation. This would not only lead to the potential for translational benefits during wound repair but elucidate how the process of polyploidy is utilized in the tumor microenvironment to escape therapeutic treatments, expand tumor cell populations, and induce metastasis.

## CHAPTER 2: DISSECTING, FIXING, AND VISUALIZING THE *DROSOPHILA* PUPAL NOTUM

### AUTHORS AND AFFILIATIONS:

This chapter is adapted from White, J., Hodge, K., Page-McCaw, A., Dissecting, Fixing, and Visualizing the Drosophila Pupal Notum. *J Vis Exp. 2022 Apr 6;(182):10.3791/63682. doi: 10.3791/63682.* My contributions to this publication were conceptualization, formal analysis, investigation, writing – original draft, and visualizations.

### ABSTRACT:

The pupae of *Drosophila melanogaster* are immobile for several days during metamorphosis, during which they develop a new body with a thin transparent adult integument. Their immobility and transparency make them ideal for *in vivo* live imaging experiments. Many studies have focused on the dorsal epithelial monolayer of the pupal notum because of its accessibility and relatively large size. In addition to the studies of epithelial mechanics and development, the notum has been an ideal tissue to study wound healing. After an injury, the entire epithelial repair process can be captured by live imaging over 6–12 h. Despite the popularity of the notum for live imaging, very few published studies have utilized fixed notum samples. Fixation and staining are common approaches for nearly all other *Drosophila* tissues, taking advantage of the large repertoire of simple cellular stains and antibodies. However, the pupal notum is fragile and prone to curling and distortion after removal from the body, making it challenging to complement live imaging. This protocol offers a straightforward method for fixing and staining the pupal notum, both intact and after laser-wounding. With this technique, the ventral side of the pupa is glued down to a coverslip to immobilize the pupa, and the notum is carefully removed, fixed, and stained. The notum epithelium is mounted on a slide or between two coverslips to facilitate imaging from the tissue's dorsal or ventral side.

### INTRODUCTION:

The pupal notum of *Drosophila melanogaster* has been increasingly used for live imaging studies in the last decade because the animal is both immobile and has a transparent cuticle at this stage(Besson et al., 2015; Couturier et al., 2017; Couturier et al., 2019; Fujisawa et al., 2020; Koto et al., 2011; R. Levayer et al., 2016; Valon et al., 2021). However, the pupal notum is challenging to dissect and fix, making it difficult to complement live imaging studies with antibody and cell staining. The overall goal of this work is to create a reproducible protocol for dissecting and fixing the pupal notum for antibody and cell staining on new or previously live-imaged samples.

As larvae begin metamorphosis, the epidermis pulls away from the larval cuticle, forming a hard pupal case(Bainbridge & Bownes, 1981). The larval body plan is broken down, and the new adult body plan is developed. During this time, pupae are immobile, making them ideal for live imaging. One commonly imaged tissue is the pupal notum, an adult monolayer epithelium that forms in the dorsal thorax. The notum is visually accessible; after a simple dissection to remove the pupal case(Moreira et al., 2011). The whole animal can then be mounted, and the notum can be live imaged for hours or days, making it an ideal tissue to study epithelial cell behaviors during development, homeostasis, and following wounding(Bellaïche et al., 2001; Cristo et al., 2018; Guirao et al., 2015; O'Connor et al., 2021; E. K. Shannon et al., 2017). However, the notum is challenging to dissect and fix because it is fragile and covered with a thin transparent adult cuticle that is hydrophobic. This hydrophobic cuticle makes it prone to curling in aqueous solutions when removed from the rest of the body. Thus, notum dissection and fixation has been reported only rarely and the dissection is often not described(Hartenstein & Posakony, 1989; Kawamori et al., 2012; Loubéry et al., 2014; Yeh et al., 2000). Without a detailed protocol in the literature, it is prohibitively difficult for a *Drosophila* researcher to complement live imaging with staining of pupae.

This technique aims to reproducibly dissect and fix samples that have been previously live-imaged, including those that have been laser-wounded. Because live imaging requires removal of the pupal case, this dissection technique begins by removing the anterior pupal case, unlike previous protocols that pin down or bisect pupae within the pupal case(Au - Wang & Au - Yoder, 2011; Couturier et al., 2019; Couturier & Schweisguth, 2014). The notum is a fragile tissue, and wounding may exacerbate its fragility. Thus, to support this delicate tissue, the integument (the epithelium and attached transparent adult cuticle) of the notum and part of the head and abdomen are dissected away from the rest of the pupa while always submerged in an aqueous environment. This method reduces the likelihood of the tissue curling and being unusable. This technique has successfully stained wounded notum tissue as early as 30 min post wounding (Chapter 2, Figure 1E–H) and at 3 h post wounding (Chapter 2, Figure 1I–L). This protocol is expected to be effective for the duration of notum development or wound repair. The current technique will be helpful for researchers wishing to unite the live-imaging capabilities of the pupal notum with the abundance of available immunohistochemistry reagents.

**PROTOCOL:**

*Drosophila melanogaster* (fruit flies) were maintained at 25 °C on a standard cornmeal-molasses medium. The studies were conducted on EGFP-tagged histone H2A pupae. The flies were obtained from a public stock center (see Chapter 2, Table of Materials).

## 1. Pupae immobilization

1.1. Apply a 2" strip of double-sided tape to a microscope slide.

1.2. Identify white pupae in vials raised at 25 °C, and use a marker to indicate their location outside the vial. Return the vials to 25 °C.

NOTE: White prepupae are characterized by their immobility, white color, and everted spiracles. These form 0–1 h after puparium formation (APF), or stage P1[(Bainbridge & Bownes, 1981)].

1.3. 12-15hr later carefully remove 3–4 of the indicated pupae (without popping them) using a dissection scope and collect them on the microscope slide next to the tape.

NOTE: Pupae will now be stage P5 with an everted head sac visible at the pupae's anterior end (Bainbridge & Bownes, 1981).

1.4. Place the pupae at least one pupa width apart onto the tape with their ventral sides down.

1.5. Place a drop of adhesive glue on a paraffin film (see Chapter 2, Table of Materials) or in a centrifuge tube lid. Dip the end of a 0.1–10 µL pipette tip (no pipette) in the drop of adhesive glue. Tap the pipette tip twice on a 24 mm x 60 mm (1.5 thickness) coverslip, 1 cm x 1 cm away from a corner, creating a line of adhesive glue ~1/2 the length of the pupa.

1.6. Preset a 0.2–2 µL (P2) pipette to 2 µL, and a 200 µL (P200) pipette to 200 µL, and fit them with tips so they are ready to be filled with 1x PBS + 0.1 mM $Ca^{2+,}$ which will rapidly solidify the adhesive glue on contact.

1.7. Insert forceps (see Chapter 2, Table of Materials) near the side of the head and gently remove the case from the anterior to posterior (Moreira et al., 2011). Remove as much of the case as possible. Grasp the pupa's developing legs with a pair of blunt forceps and carefully pull the pupa from its case.

NOTE: A small rupture on the ventral portion of the pupae will not be detrimental to this procedure.

1.8. Lay the pupa in the corner of the coverslip.

1.9. Grasp the pupa at the posterior abdomen or the developing wing with blunt forceps, lift, and place the ventral side of the pupae down into the line of adhesive glue.

1.10. Quickly fill the P2 pipette with 2 µL of 1x PBS + 0.1 mM of $Ca^{2+,}$ and holding it in the air, expel just enough to form a small bubble at the tip (0.25–0.5 µL).

1.11. Touch the small bubble of the solution to one side of the pupae at the base of the thorax, then repeat on the other side.

NOTE: This will solidify a small amount of the adhesive glue to hold the pupa in place. Generally, all the solution will not be used.

1.12. Fill the P200 pipette with 200 µL of 1x PBS + 0.1 mM of $Ca^{2+}$, then place the pipette's tip over the thorax and expel the contents to submerge the pupae completely. The remainder of the adhesive glue will solidify immediately.

1.13. Remove ~100 µL of the PBS solution, so the pupa is barely submerged before proceeding immediately to the next step.

NOTE: For unwounded samples, start from step 1.1. For wounded partially dissected samples, start at step 1.5. Wounding *via* laser ablation has been described previously (Kiehart et al., 2006; O'Connor et al., 2021). Immobilization, dissection, and mounting steps need to be performed using a dissection microscope.

**2. Dissecting the notum**

2.1. Grasp a pair of microdissection scissors bracing one side of the handle against the dominant hand's index finger and middle finger, so the thumb of the dominant hand applies the cutting force (Chapter 2, Figure 2A,B).

2.2. Stabilize the neck of the scissors against the middle finger of the non-dominant hand while bracing the coverslip with the ring finger of the non-dominant hand.

2.3. Snip at the middle of the dorsal abdomen to create a small hole, ~0.2–0.5 mm. Some hemolymph will usually spill out and is a good indicator of the breach.

2.4. Make small 0.5–0.75 mm cuts through the integument from the posterior to anterior, encircling the dorsal tissue to isolate it. To create a tissue as flat as possible, avoid cutting too ventrally; only the dorsal 'dome' of the thorax should be removed along with small sections of the head and abdomen.

2.5. Repeat posterior to anterior cuts on the other side of the pupa.

2.6. Rotate the dissection stage to allow for a clean cut through the head if necessary.

NOTE: At this stage, the dorsal integument, or notum, will be separated from the rest of the pupa. If it appears separated but is not easily moved, a few cuts below the notum can help dislodge it.

2.7. Add ~200 µL of 1x PBS to the center of the coverslip and make a channel connecting it to the original dissection droplet by gently dragging the pipette tip across the cover glass from the new droplet to the original.

2.8. Using a pair of blunt forceps, gently push or drag the isolated notum to the center of the coverslip and rotate, so the interior side faces upward. Never remove the tissue from the droplet.

NOTE: It is essential to move the notum away from the original dissection site to avoid any remnants of the adhesive glue occluding the sample during later imaging.

2.9. Hold the notum down with the blunt forceps by pressing into the abdominal or head sections. Using a pair of sharp forceps and/or gentle expulsions of 1x PBS from a 200 µL pipette, remove any remaining fat body, muscle bands, or hemolymph (if present) to fully expose the monolayer epithelium and make the eventual staining more even. The dissected notum should appear as in Chapter 2, Figure 3A.

2.10. Once the tissue is clean, use a 200 µL pipette to remove as much of the PBS solution as possible (along with debris and the ventral part of the pupae), monitoring with a dissection scope to avoid aspirating the notum.

2.11. Once most of the liquid has been removed, use an absorbent tissue to carefully wipe away the rest of the adhesive glue and pupa, as well as any other debris that lingers on the coverslip.

NOTE: If some adhesive glue remains on the coverslip, it will not cause an issue so long as it is thinner than the dorsal tissue itself.

2.12. Add 150–200 µL of 4% PFA (in 1x PBS) and fix for 20 min at room temp. Depending on the dissection speed, 1 or more pupae can be dissected during the first pupa's fixation.

2.13. Remove the PFA and replace it with 1x PBS to wash the notum once for 30 s.

2.14. If proceeding with antibody staining, perform 5 min washes (3 times) in 1x PBS or 1x PBST (Chapter 2, Supplementary File 1) to permeabilize the tissue if the antigen is intracellular.

2.15. Store the sample in 1x PBS + 0.02% $NaN_3$ overnight in a humidified chamber, or if planning to stain the tissue, incubate overnight in Blocking solution (Chapter 2, Supplementary File 1).

**3. Staining the notum**

NOTE: For staining using antibodies or cellular stains follow the steps below. The notum must not be removed from the solution, as this will likely cause the tissue to curl. Thus, adapt staining protocols to be conducted entirely on the coverslip and keep in a humidified chamber for any steps longer than 5 min. Monitoring the samples under a dissection microscope can help to prevent accidental aspiration of the tissue during washes.

3.1. To visualize the cell borders, incubate in 200 µL of anti-FasIII primary Mouse IgG2a antibody (see Chapter 2, Table of Materials) at 1:8 concentration diluted in Blocking Buffer + 0.02% $NaN_3$ overnight at 4 °C.

3.2. Wash out excess primary antibody (3 times) with 200 µL of 1x PBS + 0.02% $NaN_3$ for 1 h

per wash at room temperature.

3.3. Perform secondary antibody incubation with 200 µL of 1:200 concentration anti-mouse IgGa2 in Cy3 in Blocking Buffer + 0.02% $NaN_3$ for 2 h at room temp.

3.4. Wash out excess secondary antibody (3 times) with 200 µL of 1x PBS + 0.02% $NaN_3$ for 1 h per wash at room temperature.

3.5. To visualize the nuclei, incubate samples in 1 µg/mL of DAPI for 45 min to allow sufficient time for the stain to penetrate through muscle bands; fixing in a DAPI-containing mounting medium is not effective with this tissue.

3.6. Wash out excess DAPI (3 times) with 200 µL of 1x PBS + 0.02% $NaN_3$ for 5 min per wash at room temperature, then leave in 200 µL of 1x PBS + 0.02% $NaN_3$ overnight at 4 °C, or mount immediately.

**4. Mounting and visualizing the notum**

4.1. Following staining, prepare a new 24 x 60 mm coverslip (topper) with supports.

NOTE: Because the notum is dome-shaped, flattening it completely results in distorted wrinkled tissue. Creating a gap between the two coverslips allows the notum to retain its normal shape.

4.2. Create a gap of ~200 µm by using spacers made from 22 x 22 coverslips (No. 0 thickness, ~100 µm thick), adhered ~1 cm apart with nail polish in the middle of the topper.

4.3. To adhere, place the spacers on the topper and paint the distal edges of the spacers with a thin layer of nail polish. Let dry.

NOTE: Only use a nail polish that is thin and runny; thick nail polish will add unnecessary additional space between the coverslip and topper.

4.4. Remove as much of the aqueous solution as possible from the sample.

4.5. Immediately apply two drops (~100 µL) of anti-fade mounting medium (see Chapter 2, Table of Materials) to the sample.

4.6. If necessary, use clean, sharp forceps to position the notum in the center of the anti-fade mounting medium droplet.

4.7. Place the coverslip with the notum onto a ~10 x 40 mm support, such as a piece of thin foam (cut from the packing material inside coverslip boxes), to elevate the sample so it will not adhere to the work surface.

4.8. Under a dissection scope, slowly lower the topper onto the sample. Once the anti-fade mounting medium meets the topper, gently release and allow capillary action to pull the topper down.

NOTE: Within the first few seconds, minor adjustments can be made to the coverslip position without damaging the notum.

4.9. Place another piece of foam onto the topper and use a standard microscope slide as a weight to gently coax the anti-fade mounting medium between the sample coverslip, topper, and spacers.

4.10. After 5–10 min, use an absorbent tissue to wick away any excess anti-fade mounting medium by gently touching the edges of the coverslip.

4.11. Gently apply nail polish to each corner of the coverslips to adhere them together. Once dry, paint all edges of the coverslips to seal. Avoid coating all edges first, as this can often shift the coverslip and damage the dorsal tissue.

4.12. Visualize the notum under fluorescence microscopy (see Chapter 2, Table of Materials) through the dorsal and/or the ventral side.

**REPRESENTATIVE RESULTS:**

The presented technique works well on the unwounded notum (Chapter 2, Figure 1A–D), allowing for investigation of the development and homeostasis of the tissue, e.g., the formation of the polyploid mechanosensory bristle cells(Kawamori et al., 2012), or the anterior to the posterior flow of epithelial cells(Guirao et al., 2015). This protocol is also applicable to a laser-ablated notum (Chapter 2, Figure 1E–L), where the cellular response to injury can be analyzed live with endogenous fluorophores such as Histone2-EGFP (Chapter 2, Figure 1B,F,J). Post-staining with immunohistochemistry (step 3) can reveal many features, such as Fasciclin III, which labels cell borders (Chapter 2, Figure 1C,G,K). Additionally, quantitative stains such as DAPI (Chapter 2, Figure 1A,E,I) can be used to assess DNA content changes, including wound-induced polyploidy(Au - Bailey et al., 2020).

The current protocol is particularly beneficial as it can be used following long-term live imaging experiments. As pupae are immobile, they can be imaged for hours (Chapter 2, Figure 4A,B). Importantly, this protocol does not cause considerable changes to the wound epithelium's overall architecture or morphology following dissection (Chapter 2, Figure 4B,C). Thus, features within the tissue could be imaged long-term and then further investigated with immunohistochemistry or cellular stains.

Imaging deep within tissues is complex due to their opacity, and *Drosophila* are coated in a waxy cuticle(Bainbridge & Bownes, 1981) making deep imaging even more difficult. However, with this technique, a dissected notum can be placed between two coverslips allowing for imaging of the

epithelial monolayer from either side: the apical side through the cuticle (Chapter 2, Figure 5A–D) and/or the basal side of the epithelium which faces the body cavity (Chapter 2, Figure 5E–H). These diametric views are ideally suited to visualize different structures within the tissue. For instance, the apical view is ideal for visualizing epithelial cell borders and nuclei that lie just below the cuticle (Chapter 2, Figure 5A–D). With the basal view, these apical signals are less visible (Chapter 2, Figure 5E–H). However, basal structures are observed at the wound margin (Chapter 2, Figure 5J,L yellow, white arrows). These basal structures are much brighter as there is less occlusion in the basal view than in the apical view.

**CHAPTER 2 FIGURES:**

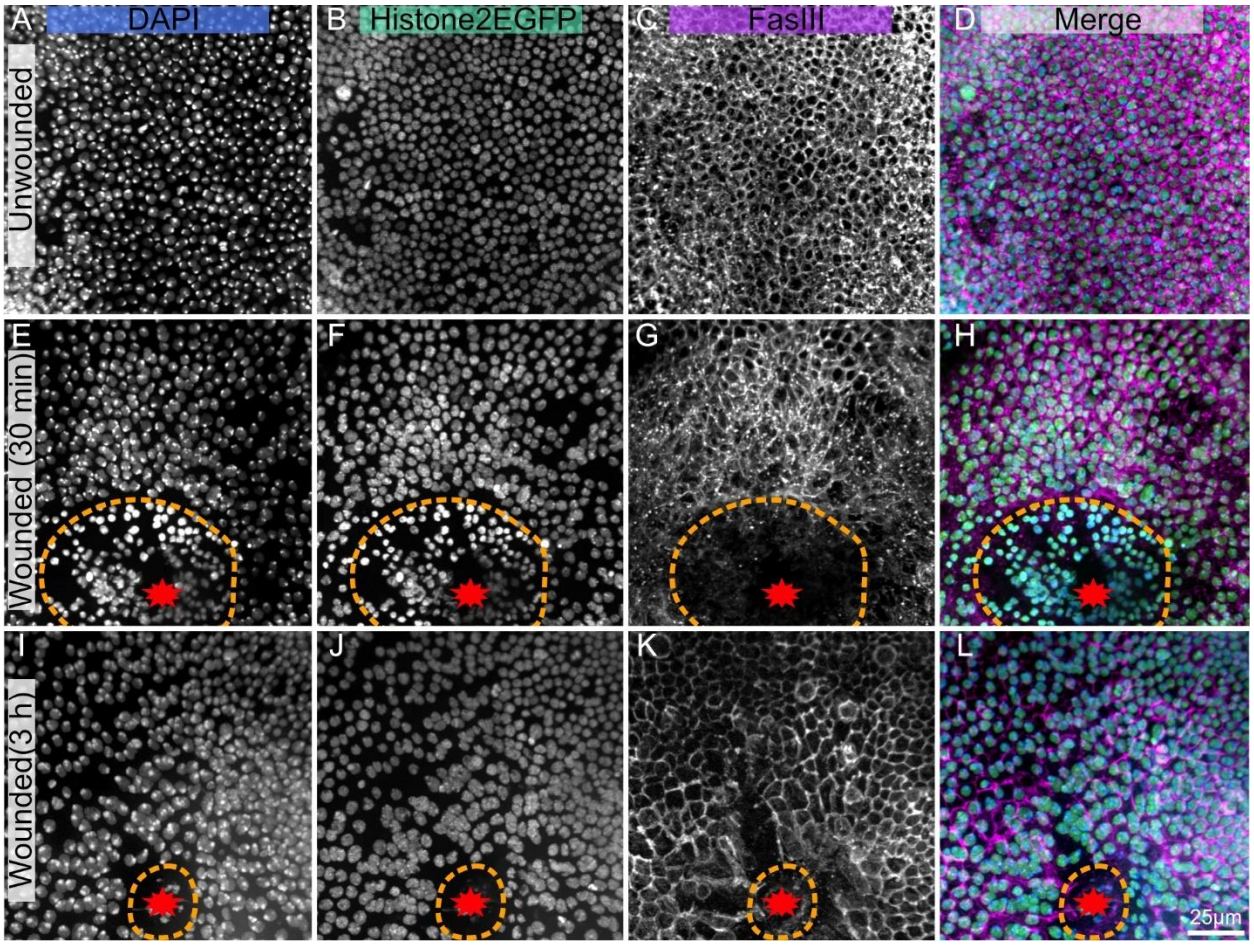


**Chapter 2, Figure 1: Dissected, fixed, and stained *Drosophila* pupal nota.** (**A–D**) Unwounded notum. (**E–H**), Wounded notum 30 min after laser ablation. (**I–L**) Wounded notum 3 h after laser ablation. (**A,E,I**) DAPI stain shows nuclei. (**B,F,J**) Transgenic Histone2-EGFP, used in live imaging, is visible after fixing and staining. (**C,G,K**) The anti-FasIII antibody shows that antibody stains work well on the fixed notum. (**D,H,L**) Merged image. The images are captured with 40x objective using spinning disc microscopy, maximum intensity projections of Z-stacks are shown with 0.3 µm Z-slices. A–D represents 263 Z-slices.

E–H represents 195 slices. I–L represents 53 Z-slices. The orange dashed line denotes wound margin. Scale bar in L is 25 µm, applicable to A–L.

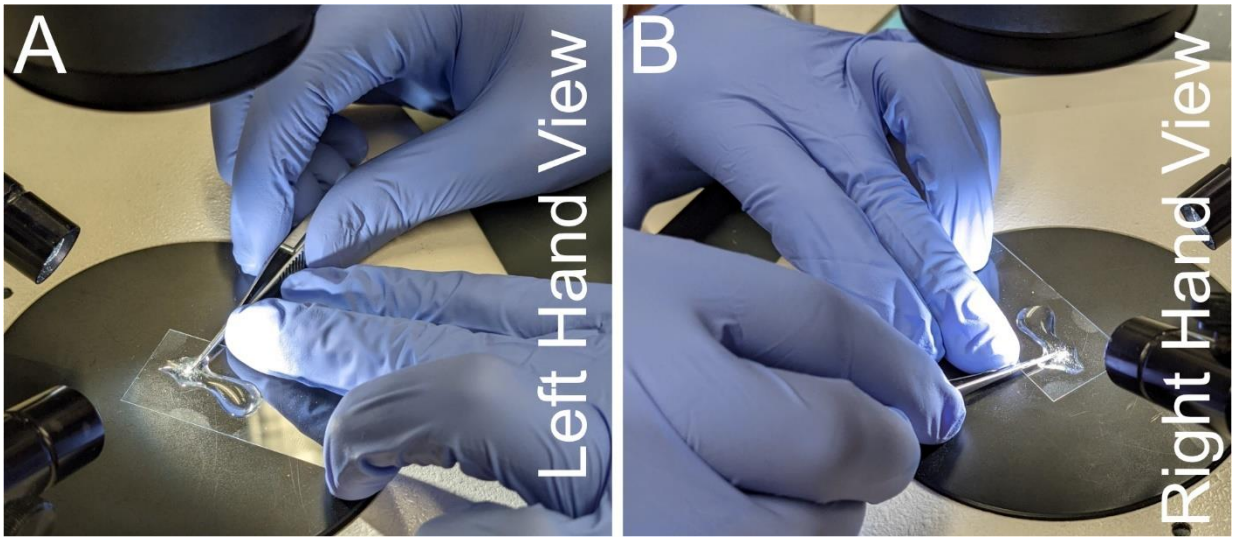


**Chapter 2, Figure 2: Hand placement for notum dissection**. (**A–B**) Left and right views of hand placement for holding the microdissection scissors. To prevent hand shaking, the neck of the scissors is placed against the middle finger of the non-dominant hand. Scissors need to be parallel to the microscope slide to avoid the warping of the notum tissue.

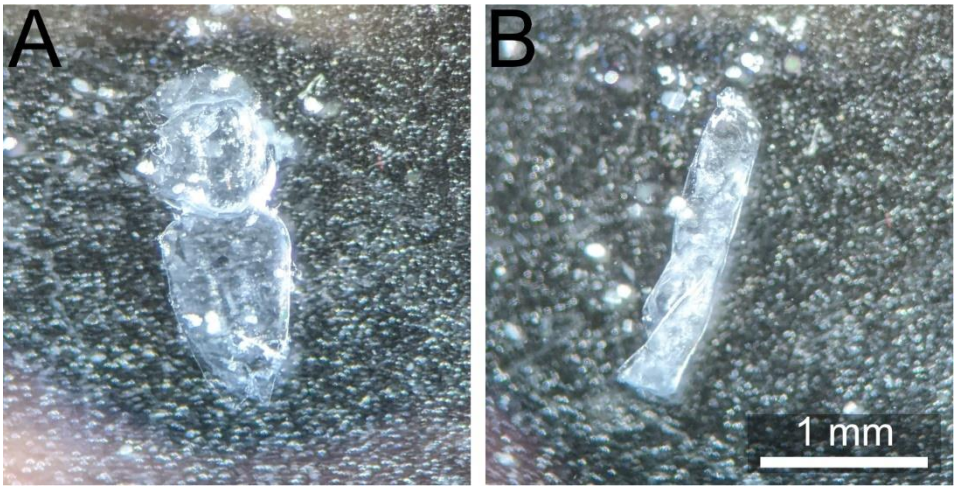


**Chapter 2, Figure 3: Correctly dissected notum *vs*. curled notum**. (**A**) Pupal notum post dissection and cleaning uncurled and ready for fixation. (**B**) Pupal notum curled on itself after being removed from 1x PBS, thus rendering it unusable.

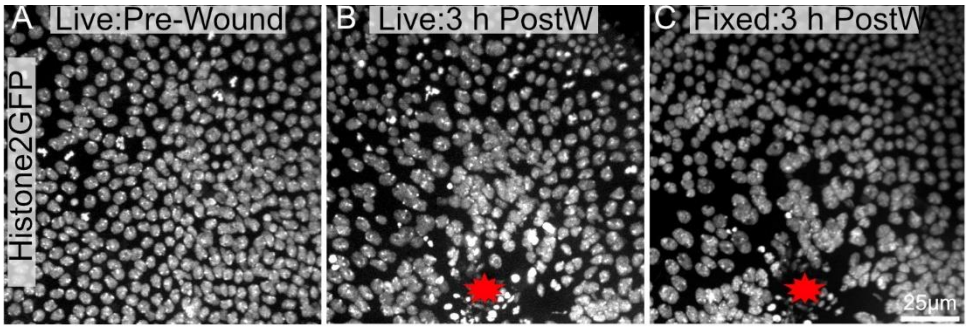


**Chapter 2, Figure 4: Pre and post-fixed images are largely similar.** A pupal notum expressing Histone2-EGFP in the nuclei was imaged (**A**) live before ablation and (**B**) 3 h after laser-ablation. (**C**) The notum was retrieved, dissected, and fixed as mentioned in the protocol and re-imaged after fixing. The wound site is labeled with a red star. The images were captured with 40x objective using spinning disc microscopy, Z-slices were taken every 0.3 µm. Maximum intensity projections of 34 Z-slices pre-wounding (A), 48 Z-slices 3 h after wounding (B), and 103 Z-slices post dissection, fixation, and staining (C) are shown. Scale bar in C is 25 µm, applicable to A–C.

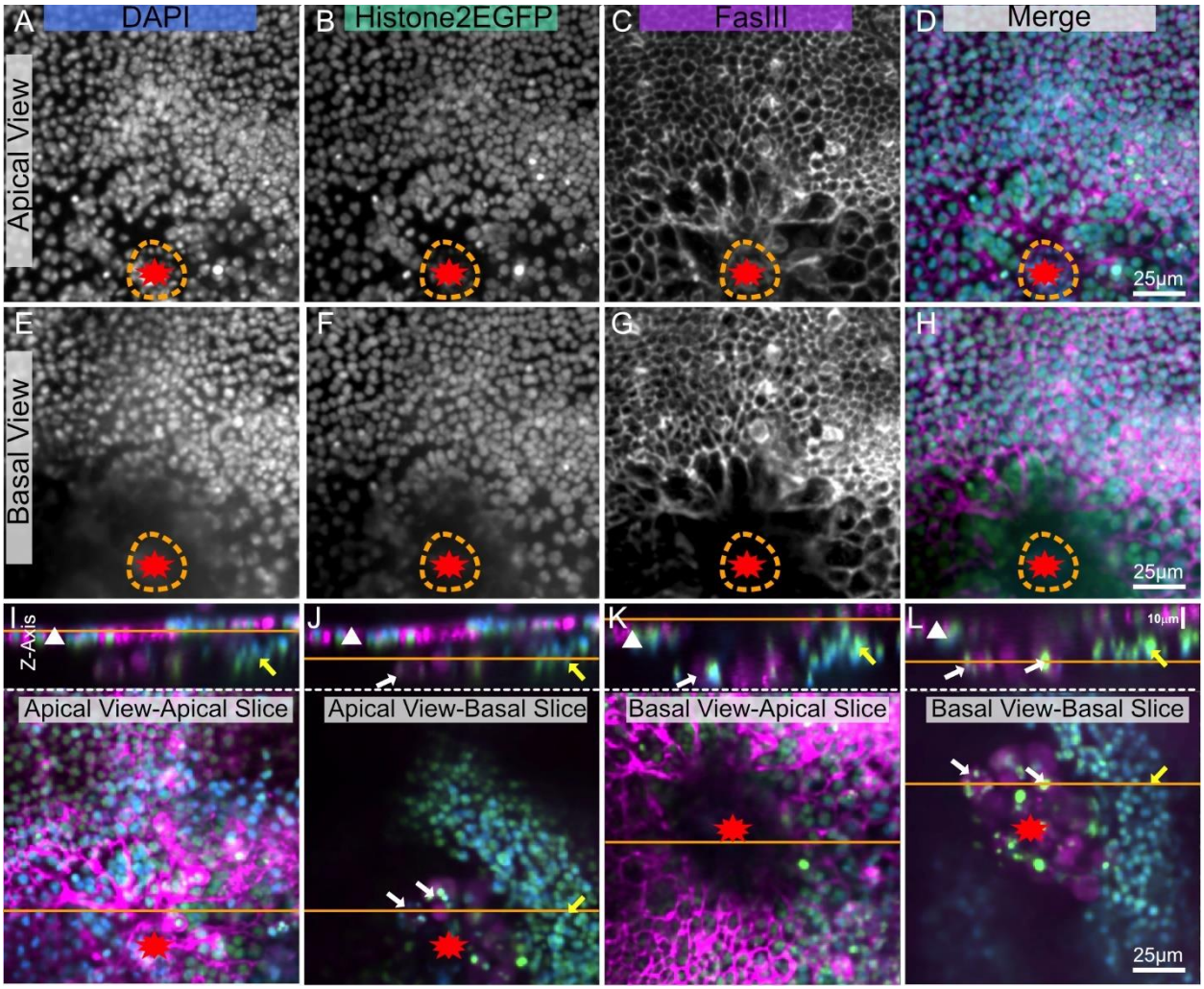

**Chapter 2, Figure 5: Imaging apical and basal sides of a wounded notum.** The same wounded pupal notum is shown in all panels. The wound is marked with a red star. The orange dotted line indicates the wound margin. (**A–D**) The notum is imaged from the apical side, through the cuticle. (**E–H**) The notum is imaged from the basal interior side. (**I–L**) The top panels show an X-Z image of the notum, apical side up, with the epithelial sheet designated by a white triangle. The orange line denotes the apical-basal plane of the X-Y slice, shown in the lower panels. Within the lower panels, the orange line shows the plane of the above X-Z image. (**I**) Apically imaged notum – apical slice. The top X-Z view shows precise imaging of the apical epithelial sheet (white triangle). This view is equivalent to a live imaging view. (**J**) Apically imaged notum – basal slice, partially obstructed by apical tissue. Other tissues denoted by yellow arrow (possible muscle band) and white arrows (possible blood cells) are visible on the basal side. (**K**) Basally imaged notum - apical slice, partially obstructed by basal tissue and wound scab (dark central area). (**L**) Basally imaged notum – basal slice. This view best shows the basal tissues denoted with yellow and white arrows. A,E: DAPI stain, B,F: Histone-EGFP, C,G: FasIII staining. The images were captured with 20x objective with spinning disc microscopy. Z-slices were taken every 0.9 µm. A–D shows the maximum intensity projection of 19 slices. E–H represents the maximum intensity projection of 17 slices. 25 µm scale bars in D,H,L apply to A–D, E–H, I–L, respectively.

**DISCUSSION:**

**Critical steps**

Optimizing three steps will dramatically increase the success of this protocol. First, in step 1.5, be sparing with the adhesive glue applied to the coverslip. If too much adhesive glue is added, the pupae can become entombed in a thick layer of solidified adhesive glue, which will make dissection impossible, and if it covers the notum itself, the adhesive glue will occlude the light from the sample. Second, during steps 2.3–2.6, ensure to remove only the top dome of the notum, excluding as much of the lateral tissue as possible. If included, the lateral tissue will become compressed during mounting and cause the middle of the notum to buckle inward, often placing it outside of the working distance of high numerical aperture objectives. Third, during the cleaning step 2.9, extreme care must be taken not to damage the monolayer epithelium. If the tissue has large portions missing or no signal can be detected, this step is likely to blame.

**Troubleshooting**

Issue 1: Following mounting, the pupa comes away from the double-sided tape during dissection. This is a common issue, especially for beginners. The best remedy is to ensure that the outside of the pupae case is completely dry/free of food debris. Removing food with a pair of blunt forceps and allowing the case to air dry for 10–15 min will help adhere to the tape. Alternatively, use the non-dominant hand and a pair of blunt forceps to hold the pupae down against the tape during

dissection. If the problem persists, applying a small, 5–10 µL drop of nail polish to the base of the posterior end of the case and allowing it to harden generally provides enough adhesion for even the unruliest of pupae.

Issue 2: Notum collapses during step 2.3, or the initial breach through the integument is not smooth. If the integument is difficult to breach, there may be too much adhesive glue from the immobilization steps. Placing the dissected pupae into less adhesive glue will improve this issue. Further, ensure that the microdissection scissors are sharp. Blunt scissors will not be able to cut into the integument and tend to cause it to collapse inwards. Once hemolymph spills out of the pupae, ensure one of the cutting blades can enter the pupa without causing the notum to deform. If the notum collapses and the blade does not enter the pupa, continue snipping until a blade enters the pupae.

Issue 3: During step 2.4, scissors catch or drag the integument. If the scissors begin to catch or drag the integument, it often helps to switch to the opposite side of the pupae and proceed to 'loosen' the integument. Further blunt microdissection scissors will make it difficult to achieve clean cuts through the integument, and sharpened scissors must be used.

Issue 4: The sample is accidentally aspirated during staining (steps 3.1–3.6). The dissected notum is challenging to see because it is transparent. It can be helpful to place a dark blue or black sheet below the coverslip to provide contrast (an old pipette tip holder rack works well.) Additionally, all solution changes can be performed under a dissection microscope.

Issue 5: No signal is detected/patchy signal is detected. After ruling out stain-specific problems, if no signal is detected or it is patchy, step 2.9 (cleaning) is likely the culprit. An absent or patchy signal can originate from damage and removal of the epithelial tissue during cleaning. Conversely, a poor signal can be caused by occlusion from the muscle bands/fat body cells if they are not removed, as they can limit the diffusion of stains and antibodies into the notum relative to the surrounding tissue. If the tissue is damaged, being gentler during cleaning is the best solution. If, instead, the stain is visible but patchy, increasing the vigor/time dedicated to the cleaning step is recommended to remove as much of the muscle and fat body as possible. Further, increasing the stain duration can help resolve this problem with better cleaning.

Issue 6: The notum tissue has a warped/wrinkled appearance during imaging. Warping and wrinkling of the tissue come from two sources. First, compressing the notum during mounting will cause it to buckle and warp. The best solution is to remove as much of the lateral tissues as possible so the dome is as short as possible and can fit between the coverslip spacers. Second, if the notum is bent during dissection, this bend will not straighten out during mounting, so extra care must be taken not to warp the notum during dissection. Accidental bending of the notum is most common when cutting the integument away from the rest of the pupae. It is tempting to have the dissection scissors at an angle relative to the pupae instead of keeping them in the sample plane as the pupae. However, angled scissors cause the integument to buckle upwards when cut instead of remaining flat.

**Existing methods, limitations, and future applications**

Wang et al.[20] reported a comparable dissection protocol for the isolation of pupal epithelium. This technique requires that the pupa remains within its case and be rapidly bisected with a scalpel. This protocol is incompatible with previously live-imaged samples, as live imaging requires removing a large section of the pupal case. Because pupae lack rigidity, pupal bisection outside of the case mangled the tissue, inspiring the creation of this protocol. The technique detailed here allows for isolation and fixation of the notum, and it could be used as the first step for a wide array of other methods such as cryosectioning, *in situ* hybridization, or electron microscopy.

This technique has some limitations. First, dissecting, fixing, and staining the notum is more time-consuming than live-imaging fluorescently tagged proteins in the notum, which requires only a simple dissection to remove the pupal case(James T. O'Connor, In revision at STAR Protocols; Moreira et al., 2011). Secondly, compared to dissections of other *Drosophila* tissues, this dissection is more difficult because of the thin, fragile tissue and hydrophobic cuticle. For simply visualizing proteins in *Drosophila* epithelia, immunohistochemistry on fixed embryos, larval wing discs, or ovaries is easier. However, this technique allows the power of live imaging to be paired with fixation and staining, making it a powerful tool once mastered.

A dissection/fixation technique has some advantages over live imaging. Basal (interior) structures can be better resolved with a basal view (Chapter 2, Figure 5 L,J). Most importantly, live imaging is limited to fluorophores that must be genetically supplied, often requiring lengthy genetic crossing schemes. In contrast, the present protocol allows the application of stains, immunohistochemistry, and other techniques which require dissection and fixation. This dramatically increases the number of signals probed in the tissue while potentially decreasing the time to experimental results.

## CHAPTER 3: WOUNDING INCREASES NUCLEAR PLOIDY IN WOUND-PROIXIMAL EPIDERMAL CELLS OF THE *DROSOPHILA* PUPAL NOTUM

This chapter is adapted from White, J., Hutson, MS., Page-McCaw, A., Wounding increased nuclear ploidy in wound-proximal epidermal cells of the *Drosophila* pupal notum. microPublication (in review) My contributions to this publication were conceptualization, formal analysis, investigation, writing – original draft, and visualizations.

**ABSTRACT:**

After injury, tissues must replace cell mass and genome copy number. The mitotic cycle is one mechanism for replacement, but non-mitotic strategies have been observed in quiescent tissues to restore tissue ploidy after wounding. Here we report that nuclei of the mitotically capable *Drosophila* pupal notum enlarged following laser ablation. Measuring DNA content, we determined that nuclei within 100 µm of a laser-wound increased their ploidy to ~8C, consistent with one extra S-phase. These data indicate non-mitotic repair strategies are not exclusively utilized by quiescent tissues and may be an underexplored wound repair strategy in mitotic tissues.

**DESCRIPTION:**

Epithelia maintain barriers to the outside environment, but after epithelial injury the loss of barrier integrity allows pathogens to invade. To re-establish the barrier and restore homeostasis, cells must cover the wound area. The mitotic cell cycle replaces cell mass as well as genetic material, and mitosis is observed in epithelial cells near a wound in mouse skin (Park et al., 2017). In the adult fly epidermis, however, epithelial cells are post-mitotic, and there is no stem cell pool to contribute new cells to close wounds. Previous studies have determined that in response to a wound, adult fly epidermal cells utilize endoreplication, which includes both growth (G) phases and S-phases but omits mitosis, resulting in larger cells with increased nuclear ploidy that close the wound (Losick et al., 2013; Losick et al., 2016). These large polyploid cells not only endocycle but also fuse with each other to form syncytia (Besen-McNally et al., 2021; Grendler et al., 2019; Losick et al., 2013; Losick et al., 2016). Similar non-mitotic repair strategies have been observed in other tissues (Cao et al., 2017; Edgar & Orr-Weaver, 2001; Gentric et al., 2015; González-Rosa et al., 2018; Lee et al., 2009; Orr-Weaver, 2015; Sigal et al., 1999; J. Wang et al., 2018; Q. Wang et al., 2013; Wilkinson et al., 2019).

We have previously investigated wound responses in the *Drosophila* pupal notum (O'Connor et al., 2021; Erica K Shannon et al., 2017). Although this tissue is mitotic, we previously reported that epithelial cells near laser wounds fuse with their neighbors to form giant syncytia (White et al, 2023). Here, to investigate the cell-cycle response to wounds, we laser-ablated *Drosophila* pupae expressing the Fluorescent Ubiquitination-based Cell Cycle Indicator (FUCCI). FUCCI is designed to provide a live readout

of cell-cycle state where green fluorescence from GFP-E2F1 corresponds to a cell in G1, red fluorescence from CycB-RFP corresponds to a cell in S-phase, and both fluorophores are present in G2/M. The epithelial cells of the unwounded pupal notum undergo waves of mitosis (Guirao et al., 2015); we wounded at 12-15h APF, when most cells were in G2 (yellow), some are in M (fluorophores lost after nuclear envelope breakdown) and G1 (green), with very few in S phase (red) (Fig. 1A$^{i}$). Post-wounding, wound-proximal nuclei did not progress through the cell cycle but rather maintained both fluorophores over the course of wound closure (Fig. 1 A$^{ii}$,A$^{iii}$). Interestingly, at 6 h post wound, nuclei had an increased nuclear volume compared to immediately after wounding (Fig. 1B), suggesting these nuclei may be polyploid. To assess the ploidy of nuclei post-wound, we fixed and DAPI-stained the notum epithelium using a protocol we developed (White et al., 2022), normalizing to haploid spermatids that were fixed and DAPI-stained along with the dissected notum (Fig.1 D$^{i}$-D$^{ii}$). Within 3 h after wounding, nuclei within 100 µm from the wound averaged ~8C, consistent with one extra S-phase (Fig. 1C). In contrast, most nuclei further from the wound had ploidy levels within the diploid range, comparable to unwounded controls (Fig. 1C). Thus, even though the pupal notum epithelium is mitotic (Guirao et al., 2015; White et al., 2023), laser ablation induces nuclear polyploidy as well as cell fusion.

Previous studies investigating developmental polyploid cells using the FUCCI system observed green (G1) or red (S) nuclei, as expected for endoreplication (Burbridge et al., 2021; Wang et al., 2021); thus, it is noteworthy that we observed a different signature of both fluorophores together. However, these previous studies analyzed unwounded tissues. In the context of injury, a previous study using FUCCI indicated G2 stalling followed injury in the diploid cells of the *Drosophila* wing imaginal disc (Cosolo et al., 2019). It may be relevant that in our laser-ablation system, wound-proximal nuclei undergo significant damage after laser ablation (O'Connor et al., 2021). Most of these nuclei were in G2 when damaged, and they may not be able to execute mitosis in their damaged state, perhaps because they fail the G2/M checkpoint, or perhaps because the mechanical environment around the wound is not suited to mitosis (Han et al., 2023). Thus, these cells may enter S-phase directly, resulting in a different FUCCI signature than developmental polyploid cells. We note that the G1 (green) marker is based on E2F1, usually destroyed during S phase; but in mammals DNA damage activates and stabilizes E2F1 (Lin et al., 2001; Wang et al., 2004; Zhang et al., 2009), recruiting E2F1 to DNA damage sites (Choi & Kim, 2019). The role of E2F1 in the DNA damage response of *Drosophila*, however, has not been explored.

Our results indicate that even a mitotically active tissue can induce nuclear polyploidy in response to damage. Why would a mitotic tissue do this? Note that these wounds are healed rapidly, within 3-6 hours, and we speculate that polyploidization may increase both cell mass and the amount of genetic material faster than the available mitotic cell cycle in a damage context.

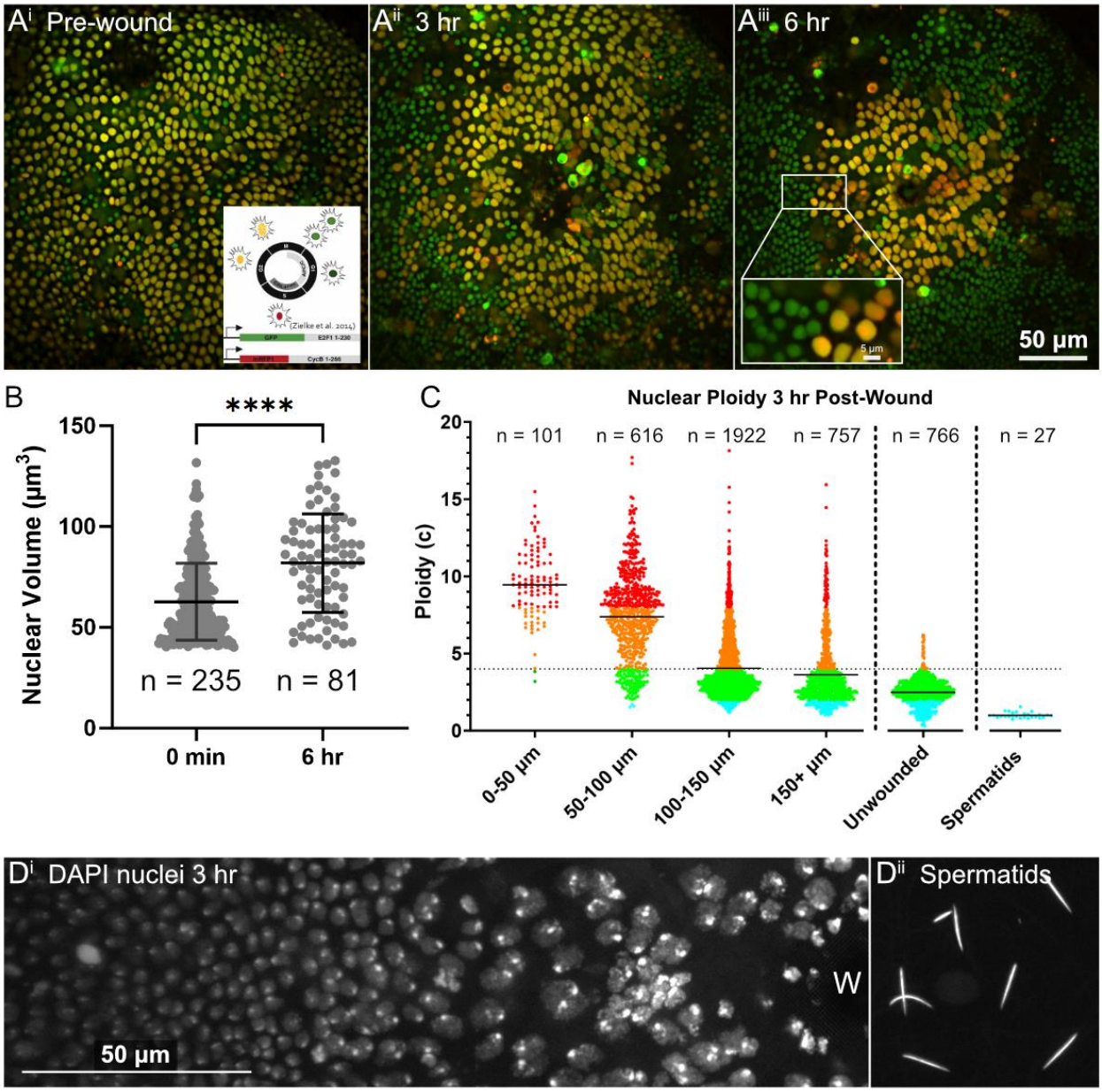


**Chapter 3, Figure 1: Wounding affects the cell-cycle and ploidy in the *Drosophila* pupal notum.**

**A:** FUCCI fly indicating cell cycle state pre-wound, 3 hr, and 6 hr post wound in the *Drosophila* pupal notum (green nuclei = G1, red = S-phase, yellow = G2/M) Most nuclei are in G2 before wounding. Bar is 50 µm; inset bar in $A^{iii}$ is 5 µm. **B:** Nuclear volume of G2 (yellow) FUCCI nuclei segmented in 3D using NIS elements from 3 independent samples. Mean and standard deviation shown (black bars), Mann-Whitney test indicates $p < 0.0001$ (****) between 0 min and 6 hr post wounding. **C:** DNA content of nuclei at 3 h after wounding. DAPI intensity was measured in 3D-segmented nuclei then normalized to DAPI intensity in haploid spermatids. Each dot represents a nucleus, and data from 4 biological replicates (wounded nota) are combined. Results are binned into 50 µm distances from wound center with *n* total nuclei within each bin shown. For reference, ploidy was measured in an unwounded control sample. Solid lines indicate the mean of each category, dotted line indicated 4C cutoff. A one-way ANOVA with multiple

comparisons comparing the unwounded control to distance bins resulted in $p < 0.0001$ to each bin. **D**: Nuclei increase in DNA content and size closer to the wound. **D$^{i}$** shows DAPI-stained nuclei 3 hr post-wounding. W=wound center. **D$^{ii}$** shows DAPI-stained spermatids used to normalize DNA content. Both Images are max intensity projections, preprocessed with rolling ball correction before projection, 19 Z-slices in D$^{i}$ and 24 Z-slices in D$^{ii}$. Bar is 50 µm.

**Methods:**

Flies:

Figure 1 A,B: *w$^{1118}$; Kr$^{If-1}$/CyO, P{ry$^{+t7.2}$=en1}wg$^{en11}$; P{w$^{+mC}$=Ubi-GFP.E2f1.1-230}5 P{w$^{+mC}$=Ubi-mRFP1.NLS.CycB.1-266}12/TM6B, Tb$^{1}$* (Bloomington stock 55124)

Figure 1 C: *P{Ubi-p63E-shg.GFP}5 / CyO ; pnr-Gal4, UAS-mCherry.NLS, tubP-Gal80$^{ts}$ / TM3* (Flybase unique identifiers: FBti0004011, FBti0151829, FBti0147460, FBti0027797)

Wounding:

Flies were mounted and wounded as described previously (O'Connor et al., 2022; White et al., 2023).

Live imaging the cell cycle:

Cell cycles were visualized with the Fluorescent Ubiquitination-based Cell Cycle Indicator (FUCCI) fly (Zielke et al., 2014). Images were captured pre-wounding, immediately post-wound, and every ten minutes on a Nikon Ti2 Eclipse with X-light V2 spinning disc (Nikon, Tokyo, Japan) using a 60x oil-immersion objective.

Volume of FUCCI nuclei:

FUCCI nuclei with both E2F1-GFP and CycB-RFP were segmented in 3D using NIS Elements GA3. Brightspots segmentations were made for both E2F1-GFP and CycB-RFP and only nuclei that contained both fluorophores were analyzed to exclude the smaller G1 green-only nuclei. Volume measurements were performed both immediately after wounding and 6 h post-wound, exported to excel, and graphs were generated using GraphPad Prism 10.

DAPI staining and measurement:

*ShgGFP / CyO ; PnrGal4, Gal80$^{ts}$, UAS-nuc-mCherry / TM3* pupae were mounted, wounded, and allowed to recover for 3 h. Spermatids were dissected from healthy unwounded male flies and allowed to dry on a 24x60 mm coverslip. Two wounded pupae were isolated on the coverslip with dried spermatids, then dissected and fixed as previously described (O'Connor et al., 2022; White et al., 2022). Pelts and spermatids were incubated with 1 µg/ml DAPI for 45 min to allow the stain to completely penetrate the tissue, then washed and mounted as described previously (White et al., 2022).

DAPI intensity was assessed by creating an NIS elements macro to segment epithelial nuclei in a 3D volume. To create the segmentation macro, we used NIS elements General Analysis 3. Nuclei were segmented in 3D based on a nuclear-localizing mCherry fluorophore. mCherry signal was enhanced with the Local Contrast preprocessing and then segmented with Brightspots detection. Single voxel Brightspots were grown to fill the whole mCherry labeled nucleus. Nuclear segmentations were then filtered based on volume to exclude erroneously small and large objects, as well as sphericity to remove erroneously fused objects. Subtle variance in mCherry signal intensity across nuclei meant a single Brightspots setting would miss many nuclei. So, three Brightspots detections were run in parallel each with subtly different thresholding parameters to capture most nuclei. Outputs of the three Brightspots segmentations were merged into one binary image which was used to obtain DAPI intensity within nuclei. Some areas of DAPI stain were contaminated by an underlying bright muscle band signal. So, the DAPI channel was thresholded by eye for each sample so only nuclei within uncontaminated areas were included. Basal immune and blood cell nuclei are not entirely removed during dissection. To exclude these nuclei, only nuclei near the apical epithelial border marker E-cadherin GFP (ShgGFP) were analyzed. E-Cad GFP signal was refined with rolling ball and local contrast pre-processing and then thresholded to create a binary E-Cad sheet. The threshold was filtered by volume to remove small artifacts not connected to the E-Cad tissue sheet. The E-Cad Sheet was then dilated and only nuclei that fell within the dilated E-Cad sheet were analyzed. Nuclei were then assigned a distance from the wound bed by thresholding the dim E-Cad signal within the wound bed, which was refined by erosion and filtering by volume to leave only a single wound bed object. All nuclei were then assigned a distance from the center of the wound bed object. Finally, the sum intensity of the DAPI signal was determined for all nuclei collated with the distance from the wound and then output to a CSV file.

A 1C (haploid) standard was created by imaging spermatids on the slide with the same conditions as the pupae. Spermatids were thresholded and filtered by volume and elongation to remove erroneous objects. Sum DAPI intensity was taken for all filtered spermatids and exported as a CSV. Within the CSV, the average intensity of spermatids was determined, corresponding to a haploid genome or 1C. All nuclei intensity values were divided by the average spermatid value resulting in the ploidy in C for nuclei and their distance from the wound. Within the CSV nuclei were sorted by distance from the wound and exported to prism.

## CHAPTER 4: WOUND-INDUCED SYNCYTIA OUTPACE MONONUCLEATE NEIGHBORS DURING DROSOPHILA WOUND REPAIR

This chapter is adapted from White, JS., Su, JJ., Ruark, EM., Hua, J., Hutson, MS., Page-McCaw, A., Wound-Induced Syncytia Outpace Mononucleate Neighbors during Drosophila Wound Repair. *eLife* (in review) My contributions to this publication were conceptualization, formal analysis, investigation, writing – original draft, and visualizations.


### ABSTRACT:

All organisms have evolved to respond to injury. Cell behaviors like proliferation, migration, and invasion replace missing cells and close wounds. However, the role of other wound-induced cell behaviors is not understood, including the formation of syncytia (multinucleated cells). Wound-induced epithelial syncytia were first reported around puncture wounds in post-mitotic *Drosophila* epidermal tissues, but have more recently been reported in mitotically competent tissues such as the *Drosophila* pupal epidermis and zebrafish epicardium. The presence of wound-induced syncytia in mitotically active tissues suggests that syncytia offer adaptive benefits, but it is unknown what those benefits are. Here, we use *in vivo* live imaging to analyze wound-induced syncytia in mitotically competent *Drosophila* pupae. We find that almost half the epithelial cells near a wound fuse to form large syncytia. These syncytia use several routes to speed wound repair: they outpace diploid cells to complete wound closure; they reduce cell intercalation during wound closure; and they pool the resources of their component cells to concentrate them toward the wound. In addition to wound healing, these properties of syncytia are likely to contribute to their roles in development and pathology.


### INTRODUCTION

Injury is a constant reality of life, and survival requires all organisms to repair wounds. Wound-induced cell behaviors like proliferation, migration, and invasion replace missing cells and close wounds (Cao et al., 2017; Park et al., 2017). Other cell behaviors are induced around wounds, but their contribution to wound healing is not well understood, *e.g.*, the fusion of cells into syncytia. Syncytia are one type of polyploid cell, and it is generally appreciated that increases in ploidy – number of genomes per cell – is a common response of post-mitotic tissues and cells to injury (Losick et al., 2013; Nandakumar et al., 2020; Tamori & Deng, 2013). Wound-induced epithelial syncytia were first observed around epidermal puncture wounds in *Drosophila* larvae and adults (Galko & Krasnow, 2004; Losick et al., 2013), consistent with the idea of polyploidy induction in non-proliferative cells. However, recent studies have observed syncytia around wounds in mitotically competent tissues: around laser-ablation wounds in *Drosophila* pupal epidermis (Wang et al., 2015) and in zebrafish epicardium damaged by endotoxin, microdissection, or laser ablation (Cao et al., 2017). Further, injury associated with the surgical implantation of biomaterials can cause immune cells to fuse into multinucleated giant cells, which are associated with rejection (S. Al-Maawi et al., 2017). Similarly, injury induces bone marrow-derived cells to fuse with various somatic cells to promote repair (Alvarez-Dolado et al., 2003; Corbel et al., 2003; Davies et al., 2009; Nygren et al., 2004). The many instances of syncytia being induced by

wounds raise the possibility that syncytia offer an adaptive benefit. It is not clear, however, what that benefit is.

Syncytia can form either by endomitosis – mitosis without cytokinesis – or by cell-cell fusion. Such fusion is widely observed throughout development in both vertebrates and invertebrates: for example myoblasts fuse into muscles (Kim, Jin, et al., 2015; Lehka & Rędowicz, 2020), and fusions occur in the lineages of the *C. elegans* hypodermis (Podbilewicz & White, 1994) as well as vertebrate trophoblast (Renaud & Jeyarajah, 2022), myoblast, and osteoclast (Søe, 2020). Cell fusions are also observed in disease: pathogen-induced epithelial fusion allows spreading of many viruses including human respiratory syncytial virus and SARS-CoV-2 (Leroy et al., 2020); and the fusion of cancer cells with bone-marrow derived cells is implicated in metastasis (Pawelek & Chakraborty, 2008).

Here, we use live imaging and clonal analysis to understand the behavior of syncytia following wounding in the *Drosophila* pupal notum. The unwounded notum is a monolayer epithelium composed of mononuclear diploid cells that are mitotically competent. Nonetheless, during the first several hours after wounding, many of the surrounding cells fuse to form giant syncytia. Some fusions are obvious with apical borders breaking down, while others appear only as shrinking of a cell's apical surface. Altogether, fusion is a common fate of cells near wounds: about half the cells fuse to form syncytia within 70 µm of a wound with 30 µm radius. Compared to their mononuclear neighbors, syncytia have dramatically improved wound-repair abilities: they outpace smaller mononuclear cells to the leading edge, they limit the need to negotiate cell intercalations as the wound closes, and they mobilize and transport actin from distal cells to reinforce the wound margin.

**RESULTS:**

*A mitotic tissue utilizes cell-cell fusions during wound repair.*

The pupal notum is a monolayer columnar epithelium composed of diploid cells that undergo regular mitotic cycles (Guirao et al., 2015) (Chapter 4, Figure S1A-C). To analyze cell behaviors around wounds, we live-imaged after laser ablation. Epithelial cell borders were labeled by the adherens junction protein p120ctnRFP (Ogura et al., 2018) and nuclei were labeled with histone His2GFP. Two hours after wounding, we observed prominent syncytial cells around the wound (Chapter 4, Figure 1A, Chapter 4, Movie S1). Some syncytia appeared to contain over a dozen nuclei within epithelial borders. For both syncytial and mononuclear cells, it was difficult to assign nuclei precisely to cell borders because notum epithelial cells are not rectangular and are not arranged at right angles with respect to the surface; in 2-D projections, a nucleus was frequently observed outside the cell's apical border (Chapter 4, Figure S1D). Accordingly, using apical area and nuclear density, we estimated the number of nuclei within the 3 largest syncytia in different wounds. The number of nuclei in these syncytia increased over time: at 1 h after wounding the three largest syncytia contained an average 3-13 nuclei, and 2 h after wounding they nearly doubled to 6-20 nuclei (Chapter 4, Figure 1B). Interestingly, larger wounds generated syncytia with larger apical areas and more nuclei, proportional to wound size, suggesting syncytium formation is a dynamic and scalable response to injury (Chapter 4, Figure 1C-E).

Live imaging of cells after wounding revealed the gradual loss of p120ctn between some epithelial cells followed by syncytial rounding (Chapter 4, Figure 1F), suggesting epithelial cell fusion. As

p120ctn was lost, the epithelial cadherin E-cadherin was also lost (Chapter 4, Figure S1E-H) indicating the disassembly of adherens junctions between the cells. We called this phenomenon “border breakdown”. Border breakdowns were found spatially clustered in the first three to four rows of cells, 30-50 µm from the wound center, and they occurred primarily within the first hour after wounding, some within 10 minutes after wounding (Chapter 4, Figure 1G,H). To test whether border breakdowns represented cell fusions, and not loss of adherens junctions caused by epithelial to mesenchymal transitions, we analyzed cytoplasmic mixing. Individual GFP-labeled cells were generated at random locations using the flip-out Gal4 technique (Pignoni & Zipursky, 1997). Before wounding, the level of cytoplasmic GFP fluorescence was stable yet exhibited cell-to-cell variability, allowing some differentiation of cells by intensity. Minutes after a nearby laser ablation, GFP was observed to diffuse from labeled cells into neighboring unlabeled cells. GFP mixing between two cells was followed by the eventual loss of their shared p120ctn-labeled cell border, confirming that border breakdown is indeed cell fusion, but that cytoplasmic mixing occurs more than 10 minutes before the border breakdown is first observed to start (Chapter 4, Figure 1I, Chapter 4, Movie S2). Border breakdowns between labeled and unlabeled cells were always preceded by GFP mixing (n=11). Thus, epithelial fusion is a rapid local response to wounding.

*Cell shrinking is a second form of cell-cell fusion occurring later during wound closure.*

Because border breakdowns occurred mostly within 1 h after wounding, it was unclear how syncytia grew between 1-2 h after wounding. However, an unexpected cell behavior was frequently observed during this time: the apical area of diploid epithelial cells shrank until they disappeared, which we termed “shrinking cells” (Chapter 4, Figure 2A). Although we first expected that shrinking cells were extruding, when we tracked the nuclei of shrinking cells, we were surprised that all nuclei moved laterally to join neighboring syncytia (n=7, Chapter 4, Figure 2B)), suggesting that shrinking cells are fusing cells. To better understand this behavior, we analyzed individual GFP-labeled cells. Like with border breakdowns, GFP mixing preceded the initiation of cell shrinking, although by a longer interval of one or more hours (Chapter 4, Figure 2C, Chapter 4, Movie S3). Additionally, X-Z projections through GFP labeled shrinking cells are consistent with cytoplasm moving into neighboring syncytia (Chapter 4, Figure 2D). Shrinking cells were distributed similarly around wounds as border breakdowns but occurred later and were more numerous (Chapter 4, Figure 2E,F). Thus, both border breakdown and cell shrinking are indicative of cell fusion.

To determine what percentage of cells around a wound will fuse, we analyzed over 100 randomly-labeled single GFP cells within the radius of observed fusion (80 µm), tracking them for 6.5 h to assess their fate (Chapter 4, Figure 3A,B): a full quarter of the cells fused (25%), sharing GFP before breaking down borders or shrinking; 67% persisted as diploid cells, most with stable GFP, but infrequently (n=3) with GFP mixing and no subsequent cell fusion; the remaining 7% could not be tracked (Chapter 4, Figure S2A). Fusing cells were strongly skewed toward the center of the wound: within 70 µm, about half the cells (47%) underwent fusion (Chapter 4, Figure 3A, right). Fusion continued for over 300 min after wounding (Chapter 4, Figure S2B,C) whereas border breakdown is concentrated in the first hour after wounding (Chapter 4, Figure 1H, Chapter 4, Figure S2C). Shrinking accounts for more than half of all fusing cells (Chapter 4, Figure 3C), and the spatial distribution of fusing cells that shrank vs. lost borders was similar (compare Chapter 4, Figure 1G and 2E). However, shrinking began later than border breakdowns, continued for several hours after wounding (Chapter 4, Figure 2F, S2C), and took longer to complete (Chapter 4, Figure S2D). Thus, shrinking fusion accounted for continuing syncytial

growth after border breakdowns subsided. Further, cell fusion is a persistent behavior over the course of wound closure.

*Syncytia outcompete mononucleate cells at the leading edge of repair.*

Because about half the cells fused to form syncytia around wounds, we were able to compare the behavior of syncytial to non-syncytial cells. Comparing cell behaviors within the same wound provided a well-controlled environment for assessing how syncytia contribute to wound closure. Using live imaging, we observed that syncytia frequently overtook unfused cells as they moved toward the wound. Chapter 4, Figure 4A shows the fusion of seven cells, with non-fusing GFP-labeled cells both distal and proximal to the fusing cells (panel 4A$^{ii}$, cells 1 and 4 respectively). Later the syncytium advanced beyond both unfused cells toward the wound; it even reached around and past wound-proximal cell 4 to extend the leading edge toward the wound (Chapter 4, Figure 4A$^{iii}$). This behavior was evident even without GFP labeling: Chapter 4, Figure 4B-C show a group of cells at the leading edge of the wound, recognized by the lack of p120ctn. At 90 min after wounding, this area of the leading edge is composed of three mononuclear cells (the middle one outlined in orange and white) flanked on either side by syncytia (outlined in yellow). In panel 4B$^{iii}$, both syncytia have pushed out the mononuclear cells from the leading edge. Thus, it appeared that syncytia were able to outpace mononuclear cells toward the leading edge.

Further, we noticed that by several hours after wounding, the leading edge of the wound was occupied primarily by syncytia. To investigate how syncytia came to occupy this position at the front lines of wound healing, we expressed MyoIIGFP/Zip-GFP, which along with actin forms the contractile purse string and makes the leading edge visible, along with p120ctnRFP to label cell borders. We analyzed the persistence of all mononuclear and syncytia cells at the leading edge over the course of closure for three wounds, starting when the leading edge was first visible (Chapter 4, Figure 4D-F). As soon as the leading edge formed 30 min after wounding, about 75% of the perimeter was occupied by syncytia (Chapter 4, Figure 4G); the rest of the perimeter was occupied by 10-13 small cells (Chapter 4, Figure 4D). As the wound closed, the syncytia became larger and displaced all the small cells, with the last small cell removed from the leading edge well before closure, which occurred 20-160 min after removal of the last small cell (Chapter 4, Figure 4D,F). No small cell persisted at the leading edge through wound closure, indicating that syncytia are better able to close wounds than unfused cells.

*Syncytia reduce intercalations and move actin to the wound.*

Why are syncytia better at closing wounds? To address this question, we considered the geometry of fusion. We observed that fusions sometimes occur between two adjacent cells equidistant from the wound, as diagramed in the top panel of Chapter 4, Figure 5A and exemplified in Chapter 4, Figure 1I$^{iii}$-I$^{iv}$ (cells 1,2) We call this type radial border breakdown, and it produces a syncytium elongated along the wound edge. Alternatively, fusion may occur between adjacent cells at different distances from the wound, as drawn in the lower panel of Chapter 4, Figure 5A and exemplified in Chapter 4, Figure 1F (cells 3,4). We call this type tangential border breakdown, and it produces a spoke-like syncytium pointing into the wound. To analyze the frequency and timing of these two different axes of fusion, we

calculated the angles of all lost borders for all border breakdowns in four wounds, binning them into radial and tangential fusions. (The angle of the axis of fusion can be determined for border breakdowns; the axis of fusion for shrinking cells is difficult to analyze, although the geometry of the starting cells must be similar.) In four wounds, 235 border breakdowns were identified: fewer radial borders broke down than tangential borders (39 vs 196), and radial borders broke down a bit later (Chapter 4, Figure 5B). However, the two types were similarly distributed around the wounds (Chapter 4, Figure S3A).

These fusion orientations provide different benefits for wound repair. Radial border fusions reduce the requirement for cell intercalation: as a wound closes, fewer cells can occupy the leading edge, necessitating a rearrangement of cell adhesions to allow cell intercalation, as depicted in the top of Chapter 4, Figure 5C. Indeed, intercalation is known to be a rate-limiting step of wound repair (Tetley et al., 2019). However, fusion of radial borders remove the need for intercalation, as shown in the bottom of Chapter 4, Figure 5C. To consider the contribution of radial border fusions to wound closure, we analyzed the three wounds from Chapter 4, Figure 4D-G and asked how many leading-edge cells fused radially vs. intercalated: 16-41% of cells removed from the leading edge were removed through fusion, reducing the burden of intercalation substantially (Chapter 4, Figure 5D). Interestingly, the larger the percentage of cells that fused rather than intercalated, the faster the wound closed (Chapter 4, Figure 5D). Thus, one mechanism syncytia use to promote wound closure is radial fusion.

In contrast, tangential border fusions might provide a way for cellular resources that would be trapped in distal cells to move toward the wound to contribute to closure. To test this hypothesis, we generated small flip-out clones expressing actin-GFP and wounded such that unlabeled cells intervened between the labeled cell and the leading edge (Chapter 4, Figure 6). We envisioned that, upon fusion, actin would equilibrate throughout the newly fused cells, pooling their resources, and indeed we did observe actin-GFP to equilibrate between cells soon after fusing. For syncytia that did not have access to the leading edge (n =2), actin-GFP levels remained uniform (Chapter 4, Figure 6A,B). In contrast, syncytia with access to the leading edge (n = 10) first uniformly distributed actin (Chapter 4, Figure 6C$^{ij}$), but once the leading edge was contacted, they redistributed actin-GFP to it (Chapter 4, Figure 6C-D). Kymographs of actin-GFP confirm that regardless of location, actin equilibrates between fusing cells within 5 minutes (Chapter 4, Figure 6B$^{iii}$, D$^{iv}$); however, nearly all actin that originated in the distal cell is redistributed to the leading edge in a syncytium positioned there (Chapter 4, Figure 6D$^{iv}$). In one striking instance, actin-GFP appeared to travel through three cells to arrive at the leading edge from its initial location three rows back (Chapter 4, Figure 6E-G, Movie S4). Importantly, although actin is labeled from only one of the fusing cells, it likely represents the total actin from all fusing cells, explaining why syncytia are better able to occupy the leading edge. We envision that other resources would also be concentrated as needed by syncytia. We conclude that syncytia formed by cell fusion are able to outcompete their mononuclear neighbors by reducing intercalation and by concentrating the collected resources of many cells.

**DISCUSSION:**

Previous work established that polyploid cells – both cells with multiple nuclei and cells with single enlarged nuclei – are important for closing epithelial wounds in post-mitotic tissues (Losick et al., 2013). Here we report that in a mitotic tissue, the epithelial monolayer of the pupal notum, syncytia form around wounds by cell fusion at a remarkably high rate, with almost half the epithelial cells within 5 cells of the wound fusing with neighbors over the course of hours. Syncytial size increases with wound size, indicating syncytia formation is a dynamic and scalable response to wounding. Syncytia form via two temporally distinct processes, a rapid breakdown of epithelial borders within 40 min of wounding, and later cell shrinking which persists 30 min to 2 h after wounding. We confirmed that both border breakdown and cell shrinking are cell fusion events, rather than epithelial to mesenchymal transitions or extrusions, by generating small clones of cells labeled with cytoplasmic GFP and observing the diffusion of GFP from a source cell into neighboring cells after wounding, indicating cell fusion. Strikingly, although the resulting syncytia are fewer in number than persisting diploid cells, they completely displace unfused cells at the leading edge of the wound such that wounds are closed entirely by syncytia.

We identified several factors that endow syncytia with wound closing abilities. Live imaging indicated that syncytia are faster than smaller cells at extending toward the wound, and once there, they maintain their positions at the leading edge, forcing out smaller cells. Epithelial wounds close by the cinching of an actin cable, sometimes called the purse string (Abreu-Blanco et al., 2012; Bement et al., 1993b; Martin & Lewis, 1992; Masako Tamada et al., 2007); as the cable tightens and shortens, the leading edge becomes smaller, with room for fewer and fewer cells. Cells are removed from the leading edge by intercalation, a process that requires them to remodel their adhesions. A previous study found that intercalation is the rate-limiting step of wound closure; further, the greater the tension in cellular adhesions, the slower the wound closure, a finding both predicted by computational modeling and verified experimentally. Thus, fluidity promotes closure (Tetley et al., 2019). By fusing, cells reduce the need for adhesion remodeling and intercalation as the leading edge becomes smaller. Moreover, the resulting larger cell has significantly more fluidity and less epithelial tension than the diploid progenitors, as recently demonstrated in syncytia formed by age-induced epidermal cell fusion (Dehn et al., 2023).

In addition to promoting wound closure by reducing the burden of intercalation, syncytia can redirect toward the wound cellular resources that would be trapped in individual diploid cells. We demonstrated this ability by visualizing labeled actin from one cell as it fused with an unlabeled cell. As expected after fusion, labeled actin diffuses and equilibrates throughout the new large cell. Remarkably however, when the syncytium is in contact with the leading edge, labeled actin from the distal cell is concentrated at the leading edge, even if the original cell is several cells away from the leading edge. This result suggests that syncytia can apply up to N times more actin to the leading edge, where N represents the number of cells that fused; considering that we observed syncytia with dozens of nuclei, this could represent a significant enhancement of actin at the leading edge. Increased actin can explain the ability of syncytia to outcompete diploid cells at the leading edge. In addition to the actin purse-string, actin also forms filopodia and lamellipodia important for migration, offering an explanation for how syncytia extend more quickly than diploid neighbors toward the wound, and these structures also participate in closing the wound (Abreu-Blanco et al., 2012; Farooqui & Fenteany, 2005). Presumably, other resources such as mitochondria and ribosomes could also be pooled and concentrated by syncytia at cellular locations where they promote wound healing. It is known that mitochondrial fragmentation promotes the repair of single-cell wounds, with more fragmentation correlated with faster repair (Fu et al., 2020). Further, fragmentation is localized to the site of cellular injury (Horn et al., 2020), raising the

possibility that syncytia may increase the local concentration of fragmented mitochondria. Ribosomes have been observed to be localized in wounded tissue, accumulating at the tips of severed neurons (Noma et al., 2017), and it is possible that syncytia may increase the localized pool of ribosomes in epidermal wounds. By pooling the cellular resources of component cells, syncytia may also allow lethally damaged cells to survive by providing them with needed survival factors originating in cells further from the wound. Thus, the concept of resource sharing that we demonstrate with actin may have ramifications for many resources.

We observed two cellular behaviors that attended fusion, border breakdowns and cell shrinking. Border breakdowns occurred sooner after wounding than shrinking and appeared to be a faster process, as shrinking lasted for hours. These differences in appearance and timing suggest that the mechanisms behind these fusions may be somewhat independent. For shrinking cells, we envision that the original site of cytoplasmic fusion, the fusion pore, occurs in the basolateral membrane, whereas border-breakdown fusion pores are nearer the apical adherens junctions observed to break down. The adherens junctions would be under more tension than the basolateral membranes, and this may explain why fusion proceeds more quickly there; we recently found that although epithelial tension drops after laser wounding, it is restored within about 10 min (Han et al., 2023) , consistent with the timing of apical border breakdown.

It is unclear what triggers either type of wound-induced epithelial fusion. Many developmentally programmed cell fusions are mediated by fusogens, cell surface proteins that bring opposing membranes into close contact with each other, as in the *C. elegans* hypodermis (Chernomordik & Kozlov, 2008; Iosilevskii & Podbilewicz, 2021; Markvoort & Marrink, 2011; Mohler et al., 2002; Podbilewicz et al., 2006; Sapir et al., 2007; Shemer et al., 2004). For other cell fusions, the fusogen is elusive and may not exist, for example in *Drosophila* myoblast fusions, which occur when a fusion competent myoblast generates actin-rich podosome-like membrane protrusions that invade a founder cell (Kim, Ren, et al., 2015; Lee & Chen, 2019; Petrany & Millay, 2019; Rushton et al., 1995; K. L. Sens et al., 2010), but we did not observe these structures in fusing epidermal cells. Wound-induced fusion may be a response to the plasma membrane damage that occurs around wounds; indeed, plasma membrane damage has been documented around both laser wounds and puncture wounds (McNeil & Steinhardt, 2003; O'Connor et al., 2021; E. K. Shannon et al., 2017).

Polyploidy as a wound response has begun to get increased recognition. In adult *Drosophila,* epithelial puncture wounds are repaired by both endoreplication and syncytia formation (Au - Bailey et al., 2020; Besen-McNally et al., 2021; Grendler et al., 2019; Losick, 2016; Losick et al., 2013; Losick et al., 2016). In the zebrafish epicardium, genetic ablation is repaired by a wavefront of multinucleated polyploid cells formed by endomitosis, and these lead diploid cells to encompass the heart (Cao et al., 2017). In adult mammalian cardiomyocytes, polyploidy may be an adaptive response to maintain growth after the cardiomyocytes lose their ability to complete mitosis. Mouse cornea endothelial cells endoreplicate to increase polyploidy to restore tissue ploidy following genetic ablation (Losick et al., 2016). Mammalian hepatocytes are known to become increasingly polyploid with age (Carriere, 1969; Wheatley, 2008) and in response to various types of injury and disease (Gentric et al., 2015; Madra et al., 1995; Muramatsu et al., 2000; Sigal et al., 1999; Toyoda et al., 2005b; Wilkinson et al., 2019). All mechanisms that promote polyploidy – fusion, endomitosis, endoreplication – result in larger cells with the potential to localize more resources; of these, fusion would act the fastest after wounding because there is no need for DNA replication. Interestingly, in *Drosophila* embryos, wounds induce the surrounding cells to become larger by increasing their volume alone and not their ploidy (Scepanovic et al., 2021), suggesting that simply an increase in size is important. Although many examples of wound-induced polyploidy exist, it is still likely to be an underreported phenomenon, as endpoint analysis might

miss a transient polyploid response to injury; live imaging is the surest way to identify a polyploid wounding response.

Another polyploid response to injury can occur after surgical implantation of biomaterials for the purpose of guiding regeneration, as reviewed previously (S. Al-Maawi et al., 2017). In some cases, only mononuclear cells of the immune system respond to the implant, and in these cases the biomaterial is integrated into the body; in other cases, the implant triggers the fusion of immune cells into multinucleated giant cells, and in these cases the material is degraded and rejected. These multinucleated giant cells seem to share properties with the syncytia of the pupal notum, as they are formed by fusion in response to an environmental trigger and they have an aggressive ability to protect the animal in response to wounding. As these studies highlight, understanding the formation, maintenance, and regulation of polyploid cells may improve our ability to successfully implant biomaterials to aid tissue regeneration.

It is often noted that wound responses are similar to cancer cell behaviors. This similarity extends to wound-induced syncytia and their counterparts, polyploid giant cancer cells, as both cell types are highly aggressive and invasive. Chemotherapeutics induce the formation of polyploid giant cancer cells (Illidge et al., 2000; Mosieniak et al., 2015; Ogden et al., 2015; Y. Wang et al., 2013), and some studies indicate that they can form through cell-cell fusion in tumors (Melzer et al., 2018; Noubissi et al., 2015; A. E. Powell et al., 2011; Song et al., 2021; Zhang et al., 2021). Once formed polyploid giant cancer cells are hypothesized to escape further chemotherapy treatments due to increased resistance to genotoxic stress (Z. Weihua et al., 2011). These polyploid giant cancer cells and their progeny also exhibit increased migration and invasion potential (Qu et al., 2013; Zhao et al., 2021). The parallels between the behaviors of polyploid giant cancer cells and the wound-induced syncytia of the pupal notum highlight the importance of understanding wound induced syncytia formation in a highly reproducible system, as a basic understanding of how these cells form in the *Drosophila* notum could inform how they become dysregulated in cancer.

**METHODS:**

**Key Resources Table**

| Reagent type (species) or resource | Designation | Source or reference | Identifiers | Additional information |
|---|---|---|---|---|
| Fly line (*Drosophila melanogaster*) | "HistoneGFP" | BDSC: | 24163 | w[*]; P{w[+mC]=His2Av-EGFP.C}2/SM6a |
| Fly line (*Drosophila melanogaster*) | "p120ctnRFP" | (obtained as a gift from Shigeo | | y; ubiP-p120ctn-TagRFP |

| | | | | |
|---|---|---|---|---|
| | | Hayashi(Ogura et al., 2018)) | | |
| Fly line (*Drosophila melanogaster*) | "AyGal4" | BDSC: | 3953 | w[1118]; P{w[+mC]=AyGAL4}25/CyO |
| Fly line (*Drosophila melanogaster*) | "hsFLP" | BDSC: | 55813 | w[1118]; P{y[+t7.7] w[+mC]=hs-FLPD5}attP2 |
| Fly line (*Drosophila melanogaster*) | "GFP" | BDSC: | 1521 | w[*]; P{w[+mC]=UAS-GFP.S65T}eg[T10] |
| Fly line (*Drosophila melanogaster*) | "Actin-GFP" | BDSC: | 7310 | w[1118]; P{w[+mC]=UASp-Act5C.T:GFP}2; l(3)*[*]/TM6C, Sb[1] Tb[1] |
| Fly line (*Drosophila melanogaster*) | "MyosinII-GFP" | BDSC: | 51564 | w[*]; P{w[+mC]=PTT-GC}zip[CC01626]/SM6a |
| Fly line (*Drosophila melanogaster*) | "HistoneRFP" | BDSC: | 23651 | yw; His2AvRFP / (CyO) |
| Software | FIJI | Schindelin et al., 2012 | RRID: SCR_002285 | |
| Software | NIS Elements | Nikon Instruments Inc. | RRID: SCR_002285 | |
| Software | Microsoft Excel | Microsoft | https://www.microsoft.com/en-us/microsoft-365/excel | |
| Software | GraphPad Prism 9 | GraphPad | https://www.graphpad.com/scientific-software/prism/ | |

| | | | | |
|---|---|---|---|---|
| Software | Affinity Designer | Affinity Serif | https://affinity.serif.com/en-us/designer/ | |

**Resource availability:**

**Lead contact**

Requests for fly lines, reagents, and additional questions should be directed to Dr. Andrea Page-McCaw (andrea.page-mccaw@vanderbilt.edu)

**Materials availability**

Fly lines generated in this study are available from the Bloomington *Drosophila* Stock Center or from the lead contact.

**Data availability**

All microscopy movies have been stored on Dropbox and can be made available for download upon request.

**Experimental model and subject details**

***Drosophila melanogaster***

*Drosophila* lines used in this study are in Table S1. All *Drosophila* lines were maintained on standard cornmeal-molasses media supplemented with dry yeast. All flies, except those used in heat-shock flip clonal analysis, were raised at room temperature. For clonal analysis experiments flies were raised at 18 degrees Celsius until the 3$^{rd}$ instar stage when they were heat shocked in a circulating water bath at 37 degrees Celsius for 3 minutes. They were then allowed to develop at room temperature to 15-18hr after puparium formation (APF) before wounding experiments (described below) were conducted.

**Method details**

**Pupal mounting**

At room temperature, white prepupae were identified and marked within plastic food vials. Pupae were allowed to age until the 15-18 APF stage. 15-18 APF pupae were then removed from the vial onto a piece of double-sided tape (Scotch brand, catalogue #665) applied to a microscope slide. Using fine forceps, the anterior pupal case was removed exposing the head and notum of all pupae applied to the tape, as previously described in (James T. O'Connor, In revision at STAR Protocols; E. K. Shannon et al., 2017). The tape was carefully removed from the microscope slide and inverted onto a pre-prepared cover glass (Corning 2980-246, 24 mm x 64 mm) (O'Connor et al., 2022). The pupae were carefully pressed down onto the cover glass by adhering the section of tape above the pupal head. Once the notum was visibly pressed onto the cover glass an oxygen permeable membrane (YSI, standard membrane kit, cat#1329882) was applied to prevent the pupae from drying out during imaging.

**Pupal survival**

Following imaging, pupae were kept mounted as described above and allowed to continue to develop and eclose for 3-4 days. Pupae that continued developing until they were able to crawl out of the partially dissected case were classified as 'survived' and their data acquired form these samples were used for analysis. If a pupae did not survive to eclosion, the associated datasets were not used in the study.

**Live imaging**

Images were collected using a Nikon Ti2 Eclipse with X-light V2 spinning disc (Nikon, Tokyo, Japan) with a 40X 1.3 NA oil-immersion objective or 60X 1.4 NA oil-immersion objective. Unless otherwise noted samples were imaged pre-wounding, immediately after wounding, every 2 min for 30 min, and then every 10 min for 6 h. Images were pre-processed in NIS-Elements using combinations of background subtraction, rolling ball correction, local contrast, and Denoise a.i. Assembly of figure panels was done using Affinity Designer and frames were centered on the entity in focus, compensating for frame shift due to wounding.

**Laser ablation**

A single pulse of a 3rd harmonic (355 nm) Q-switched Nd:YAG laser (5 ns pulse-width, Continuum Minilite II, Santa Clara, CA) was used for laser ablation. Laser pulse energies were kept to 1.9 µJ +/- 0.1 µJ, increased from our previously report (O'Connor et al., 2021) to keep the wound size similar between old and new ablation rig.

**Border breakdown and tangential vs radial assignment analysis**

Individual border breakdown events were manually observed using FIJI by identifying syncytia late in the movie and back-tracking to determine which borders broke down to form them. Each border that was broken down was traced back to the first frame after wounding to develop the map on Fig 1G. For each border breakdown, distance from the center of the wound and time after wounding were recorded in Microsoft excel. Border breakdown events were categorized as tangential or radial based on the orientation of the border relative to a vector pointing outward from the center of the wound. Specifically, the line tool in FIJI was used to measure both the angle of the border with respect to the horizon, theta, and the angle of the line from the center of the wound to the center of the border with respect to the horizon, alpha. If cos(alpha-theta) was less than cos(45 degrees), then the border was classified as tangential. Otherwise, the border was classified as radial.

**Shrinking cell initiation / duration analysis**

Shrinking cells were identified in live microscopy movies by beginning at the end of the movie and playing backwards in FIJI. Backwards, a shrinking cell appears to bloom from the epithelial layer, characterized by the expansion of a bright puncta of p120ctnRFP. Each cell that underwent this behavior was marked on a single frame of the movie, then the distance from the center of the wound when shrinking started was denoted as well as the time that the shrinking started and completed. All cells that shrank were then manually traced back to the first frame after wounding to develop the map of shrinking cells (Fig 2C).

**Approximating nuclei per syncytia**

Nuclei and cell borders do not align in Z-projections of the pupal notum as the cells are non-prismatic. To estimate the number of nuclei per syncytium, the pre-wounding density of nuclei per unit area was determined for the circular region where syncytia form after wounding. Next, the apical area of the three largest syncytia/cells around a wound was measured at 0h, 1 h and 2 h post wounding. The area of each syncytia was multiplied by the nuclear density to yield the approximate number of nuclei per syncytia. The number of nuclei in each of the three syncytia was averaged to give a value for each of three samples in Fig. 1B.

**Measuring apical area of syncytia across varied wound sizes**

The three largest syncytia were determined by eye in FIJI for six samples, three ablated at 1.5 µJ and three ablated at 3 µJ ablation. The apical area of syncytia was measured 3 h post wounding using the p120ctnRFP signal. Initial wound size was calculated by measuring Myosin II marked leading edge when it became apparent 30-160 min post wounding.

**Unfused cells at leading edge: count and percent analysis**

Unfused cells at the leading edge were identified using FIJI by a lack of border breakdowns. Each unfused cell was manually observed over the duration of wound closure and the time at which it departed from the leading edge was noted. A count of unfused cells at the leading edge was created in Excel and formal graphs were generated using Prism 9. To measure percent of the leading edge comprised of unfused vs. syncytial cells, each unfused cell's leading edge contact was measured in FIJI using the polygon line tool. The total circumference of the wound was measured using the polygon line tool and unfused cell measurements were subtracted from the total to infer the syncytial occupancy at the leading edge. Formal histograms were generated using Prism 9.

**Analyzing GFP labeled cells**

107 individually labeled GFP cells were analyzed across 5 wounds over 6.5 h. The position of the ablation was optimized to place as many individually labeled cells within 40-80um from the center of the wound as possible. After wounding it was possible to identify a mixing event by the decrease in intensity from the source cell with a corresponding increase in intensity of a previously unlabeled neighbor. Intensity differences made it possible to distinguish instances where two source cells were adjacent to each other but only one had a mixing event. However, large patches of source cells were not evaluated because inter-patch mixing was not distinguishable. To evaluate if border breakdowns were preceded by mixing, the 11 individually labeled cells that had border breakdowns were tracked back to the start of the movie and confirmed to have a mixing event. There was never an instance where a labeled source cell had a border breakdown without a prior mixing event occurring.

**Wound Closure Analysis**

A pigmented scar forms at the site of laser ablation making identifying the exact moment a wound is closed difficult. Since the scar is approximately the same size in each sample, the time point at which the Myosin II signal disappeared below the scar was used as a proxy for closure.

**Calculating Intercalation**

The change in the number of cells when the leading edge forms at 30 min ($N_{start}$) to when the wound is closed ($N_{end)}$ is equal to the number of intercalations plus the number of radial fusion events. Thus, (intercalations = ΔN – radial fusions). For the same three samples used in Fig 3D, we determined ΔN from $N_{start}$ at 30 min and $N_{end}$ when the wound had closed. Radial fusions were tallied by manually observing border breakdown events between the leading-edge cells and intercalations were calculated. Each radial fusion was counted as one prevented intercalation event.

**Kymograph and plot profile analysis**

Actin-GFP intensity was analyzed using the kymograph tool in FIJI after drawing a 11-pixel line through the middle of the syncytia. Profile plot values were exported from NIS elements to Excel and graphs were generated using Prism.

**CHAPTER 4 FIGURES:**

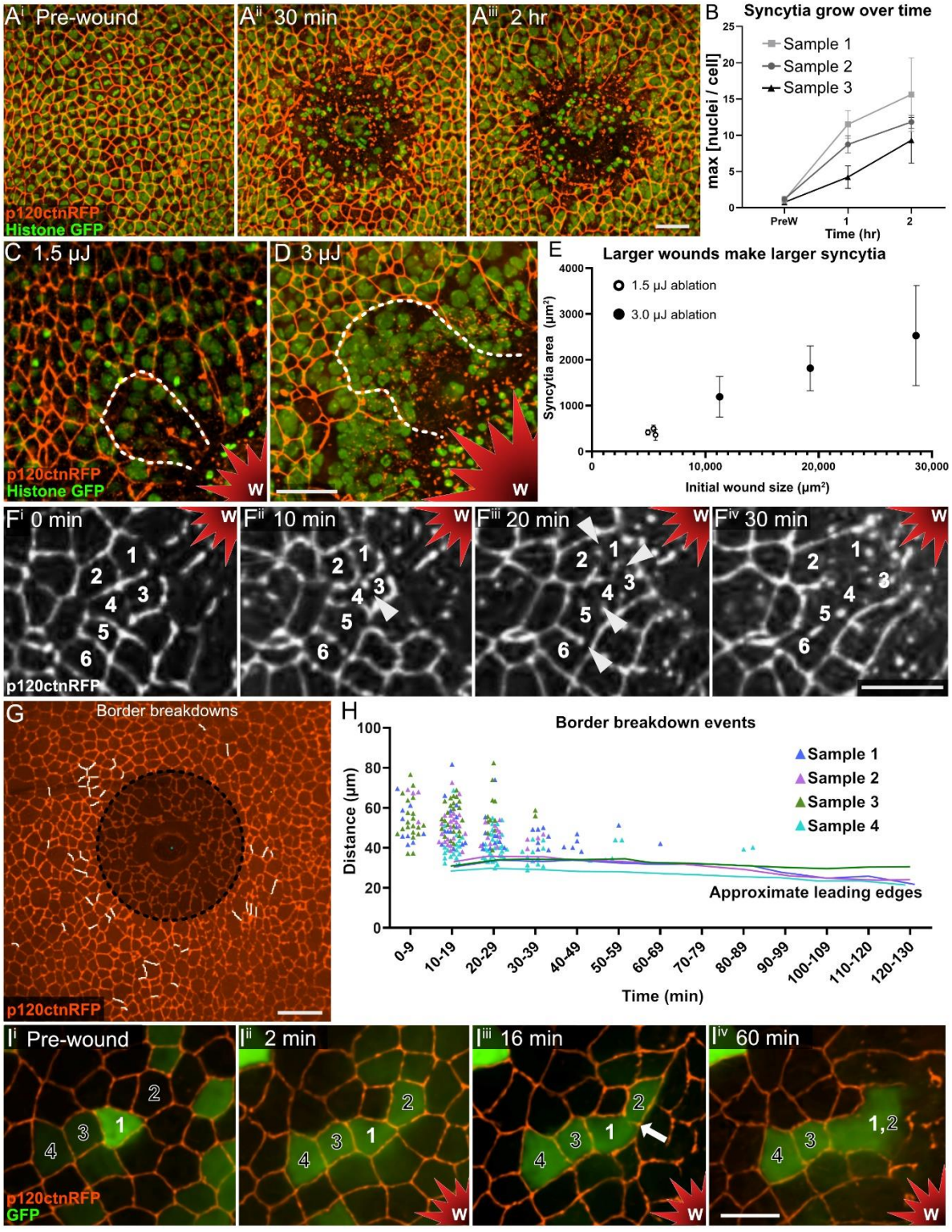

**Chapter 4, Figure 1. Wounds induce epithelial syncytia via cell fusion.**

**A)** Syncytia form within 2 h post wounding, evident by the clustering of multiple nuclei within cell borders. **B)** The number of nuclei per syncytia increases over time after wounding. Number of nuclei was estimated based on area and nuclear density (see text) for the 3 largest syncytia of 3 different wounds, mean and SD. **C-D)** Larger wounds generate larger syncytia. Images are at 3 h post wounding, single syncytium outlined. **E)** Apical area of three largest syncytia is proportional to initial wound size, mean and SD. **F)** A time course of six cells fusing within 30 min after wounding. Apical borders are lost (white arrowhead) as syncytia form. Original cells are numbered. **G)** All borders lost to cell fusion (white) mapped to cells in the first frame after wounding. The leading edge of wound closure will form at dashed line; cells within the shaded area were damaged by the wound and will be dismantled. **H)** Distance from the wound center vs time for all border breakdowns in 3 wounds. Each symbol represents a cell border. Leading-edge locations indicated by solid lines. **I)** Cytoplasmic GFP is expressed in cell 1 before wounding and mixes with neighboring cells 2-4 by 2 min after wounding. Cytoplasmic sharing is followed by the lagging fusion indicator of visible border breakdown (white arrow). The fates of cells 3 and 4 are shown at later times in Chapter 4, Figure 2D. Maximum intensity projections in A, C-D, G; single Z slices in F, I. Scales: A-D,G = 20 µm, F,I = 10 µm. W and red star indicate wound. This work was conducted by James White and Jasmine Su.

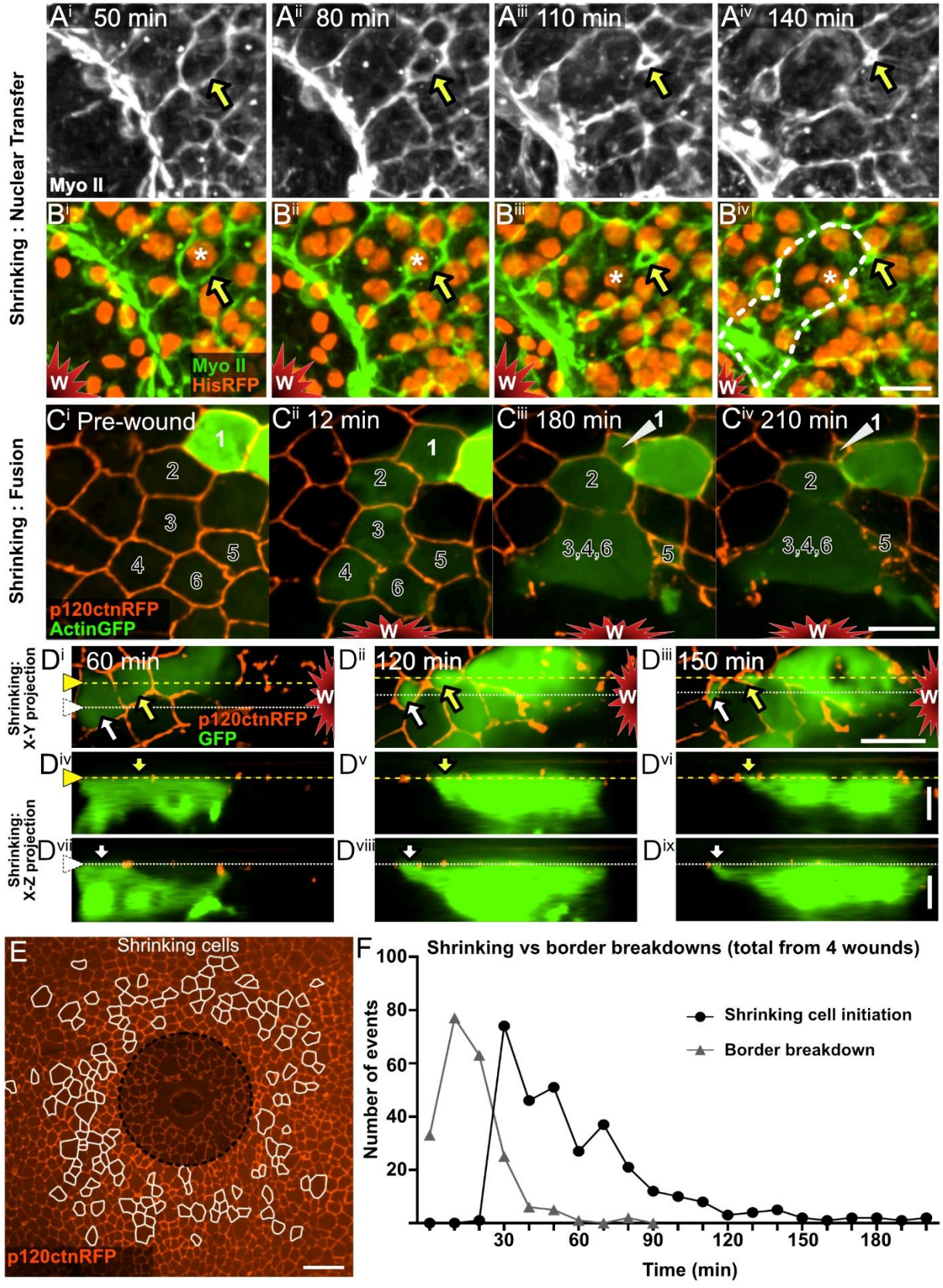
Shrinking : Nuclear Transfer
Shrinking : Fusion
Shrinking: X-Y projection
Shrinking: X-Z projection
Myo II
Myo II HisRFP
p120ctnRFP ActinGFP
p120ctnRFP GFP
50 min
80 min
110 min
140 min
Pre-wound
12 min
180 min
210 min
60 min
120 min
150 min
Shrinking cells
p120ctnRFP
Shrinking vs border breakdowns (total from 4 wounds)
Shrinking cell initiation
Border breakdown
Number of events
Time (min)

**Chapter 4, Figure 2: Cell fusion often appears as cell shrinking.**

**A)** An epithelial cell (yellow arrow) shrinks in the epithelial plane after wounding. **(B)** Same sample as A, showing the shrinking cell's nucleus (asterisk) entering a neighboring syncytium, outlined in $B^{iv}$. **C)** Cell 1 expresses actin-GFP before wounding. After wounding, cell 1 fuses with cells 2-6 evidenced by GFP sharing, then cell 1 shrinks. **D)** Two cells shrink in the X-Y plane (white and yellow arrows in $D^{i}$-$D^{iii}$). X-Z projections are shown for each ($D^{iv}$-$D^{vi}$ for the top yellow line; $D^{vii}$-$D^{ix}$ for the lower white line). Rather than extrude, the shrinking cells' cytoplasm moves to the right, to join with the neighboring wound-proximal syncytium, via basal connections. These frames are a continuation of the sample shown in Chapter 4, Figure 1I. **E)** All shrinking cells mapped to first frame after wounding. **F)** All shrinking cells and border breakdowns were tracked in 4 wounds. Border breakdown fusions happen sooner after wounding than shrinking fusions. A, B, C, $D^{i-iii}$, E show maximum intensity projections. $D^{iv-ix}$ show X-Z projections. Scales: A, B, C, $D^{i-iii}$, E = 10 µm; $D^{iv-ix}$ = 5 µm. This work was conducted by James White, Elizabeth Ruark, and Jasmine Su.

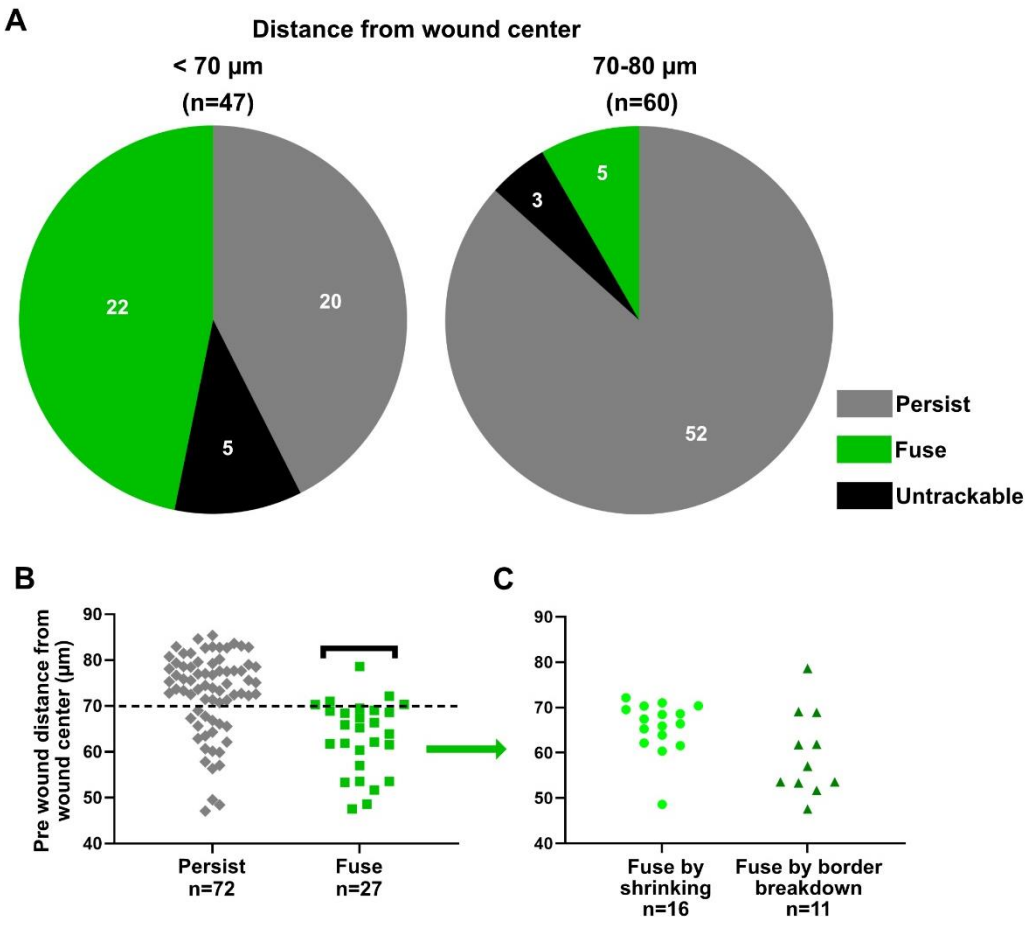


**Chapter 4, Figure 3: Half the cells near the wound fuse to form syncytia, demonstrated by tracking individual cell fates.**

**A)** All GFP labeled cells in the region of fusion (80 µm) were tracked in 5 wounds over 6.5 h after wounding to determine frequency of fusion (GFP mixing) or persistence (no GFP mixing). Untrackable cells lost GFP, see Chapter 4, Figure S2A. **B)** Fusion is common within 70 µm. **C)** Shrinking-fusion and border-breakdown fusion occur at similar distances from the wound.

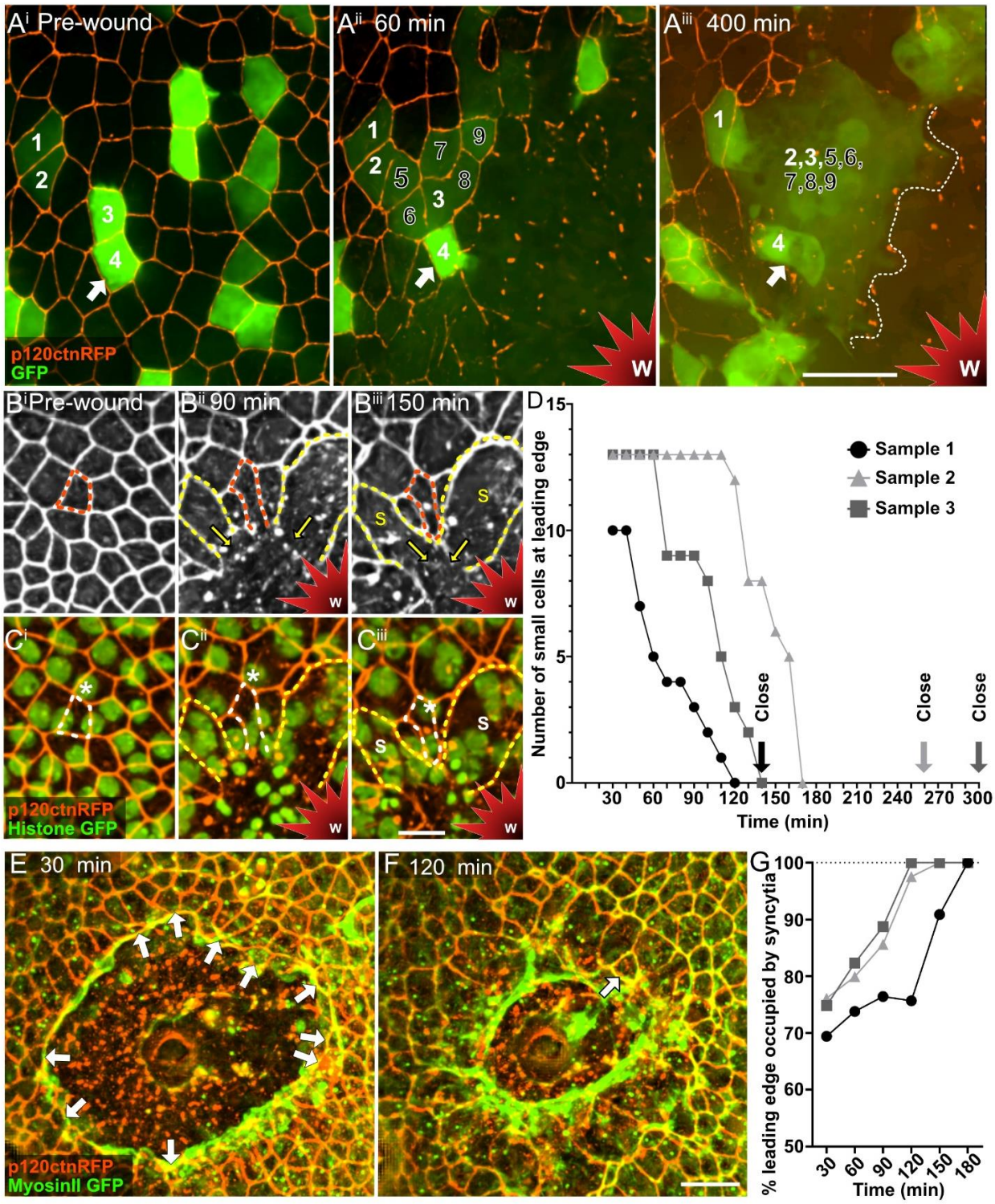
Ai Pre-wound
Aii 60 min
Aiii 400 min
1
2
3
4
5
6
7
8
9
2,3,5,6,
7,8,9
p120ctnRFP
GFP
W
Bi Pre-wound
Bii 90 min
Biii 150 min
S
w
Ci
Cii
Ciii
*
p120ctnRFP
Histone GFP
D
Number of small cells at leading edge
Sample 1
Sample 2
Sample 3
Close
Time (min)
E 30 min
F 120 min
p120ctnRFP
MyosinII GFP
G
% leading edge occupied by syncytia
Time (min)

**Chapter 4, Figure 4: Syncytia outpace smaller cells.**

**A)** Before wounding, two clusters of cells are labeled with GFP, 1-2 and 3-4 (white numbers). After wounding, cells 2 and 3 fuse with neighbors 5-9 to form a syncytium (dashed leading edge in Aiii), which advances toward the wound, passing unfused cell 4 (arrow). **B-C)** Unfused cell (outlined in orange and white) with corresponding nucleus (asterisk in C) is replaced at leading edge by neighboring syncytia (S and yellow outline, yellow arrows). **D)** All small cells are excluded from leading edge by syncytia well before the wound closes 20-160 min later. **E,F)** Images of sample 1 from the graph D. Unfused cells (arrows) were tracked over the course of wound closure and mapped back to the 30 min timepoint. At 120 min, the last unfused cell is ejected from leading edge (arrow). The wound closed at 140 min. **G)** Percent of leading-edge perimeter occupied by syncytia increases to 100%. Images are single Z slices in $A^{i}$-$A^{ii}$ and maximum intensity projections in $A^{iii}$-F. Scale: A,E-F = 20 µm, B-C = 10 µm.

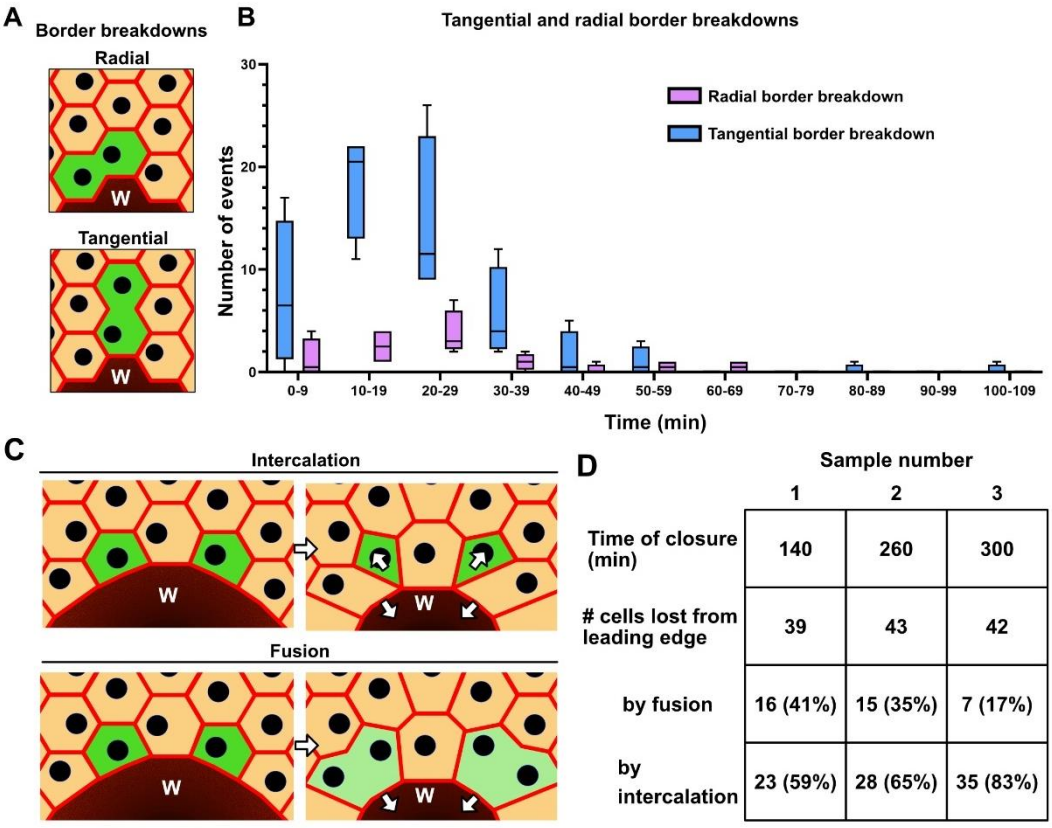


**Chapter 4, Figure 5: Radial border fusions reduce the number of wound proximal intercalations**.

**A)** Illustration of tangential vs radial border breakdown. **B)** More tangential than radial borders break down after wounding. **C)** Radial border fusions reduce intercalation at a wound. **D)** Quantification of intercalations and fusions around the wounds of Chapter 4, Figure 4D,G. This work was conducted by James White and Jasmine Su.

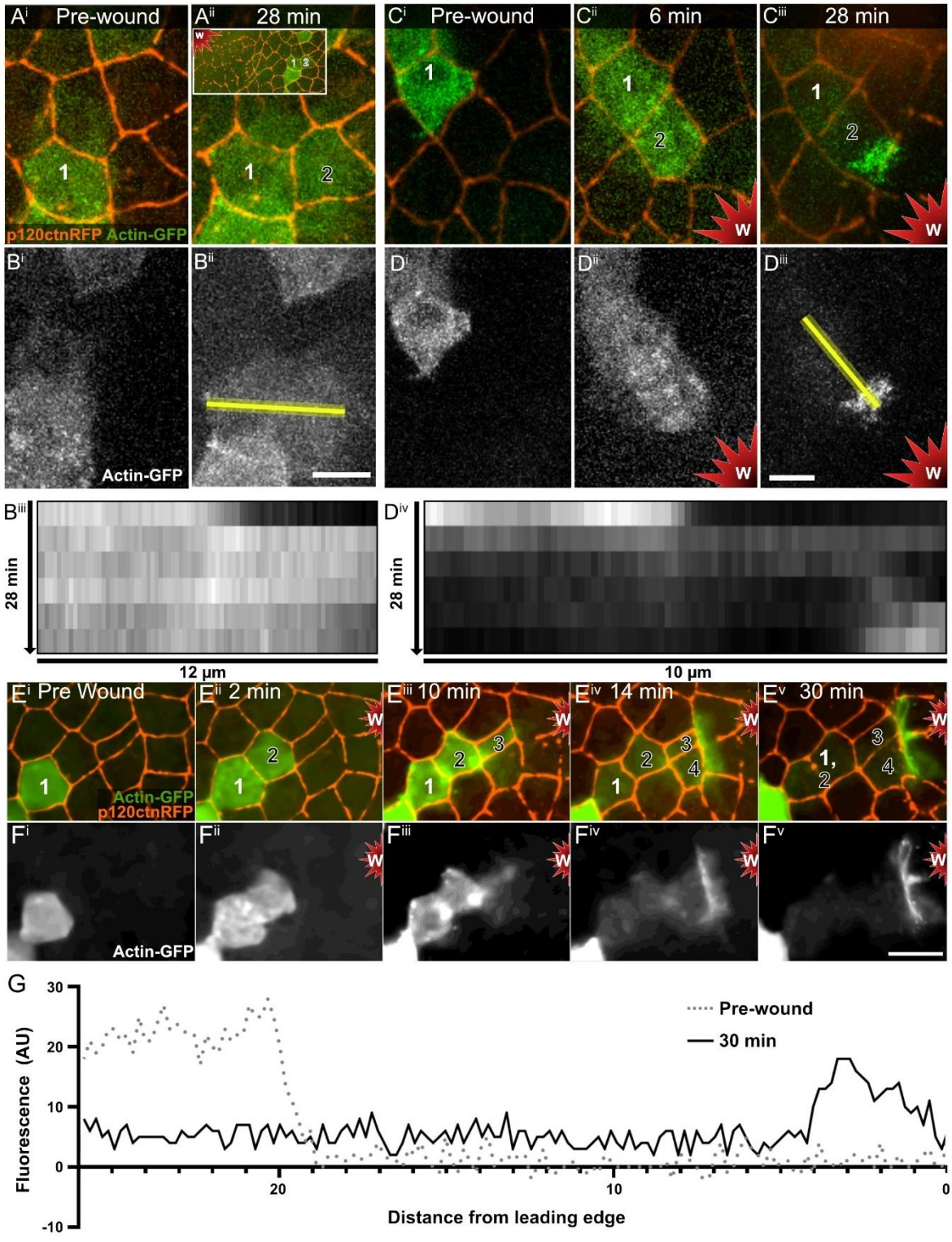
A^i Pre-wound
A^ii 28 min
C^i Pre-wound
C^ii 6 min
C^iii 28 min
p120ctnRFP Actin-GFP
B^i
B^ii
D^i
D^ii
D^iii
Actin-GFP
B^iii
D^iv
28 min
12 µm
10 µm
E^i Pre Wound
E^ii 2 min
E^iii 10 min
E^iv 14 min
E^v 30 min
Actin-GFP
p120ctnRFP
F^i
F^ii
F^iii
F^iv
F^v
G
Pre-wound
30 min
Fluorescence (AU)
Distance from leading edge

**Chapter 4, Figure 6: Syncytia concentrate pooled resources at the leading edge.**

Random scattered cells expressing Actin-GFP were generated by heat-shock mediated flip-out expression of Gal4. **A-B)** Labeled actin is expressed in cell 1 before wounding ($A^{i}$). Actin-GFP rapidly equilibrates between cells 1 and 2 by 28 minutes after wounding, demonstrating cytoplasmic fusion. At 180 min, cell 2 shrunk into cell 1. The resulting syncytium has no access to the leading edge, and actin remains equilibrated, as shown in the kymograph ($B^{iii}$) generated from actin-GFP intensity over time at the yellow line in $B^{ii}$. **C-D)** Labeled actin is expressed in cell 1 before wounding ($C^{i}$) and equilibrates between cells 1 and 2 by 6 minutes after wounding, demonstrating cytoplasmic fusion ($C^{ii}$). The resulting syncytium contacts the leading edge, and by 28 min after wounding actin from cell 1 is redistributed to the wound margin by 28 min after wounding, as shown in the kymograph ($D^{iv}$) of actin intensity over time at the yellow line in $D^{iii}$. At 55 min after wounding, cell 1 shrunk into cell 2. **E-F)** Before wounding, actin-GFP in cell 1 is three cells away from the future leading edge. After wounding, fusion of cells 1-4 allows actin-GFP to move to and accumulate at the leading-edge actin cable. Border breakdown occurs between cells 1-2 ($E^{v}$) which later shrink into cells 3,4 (see Movie S4). **G)** Mean profile plot of actin-GFP comparing the syncytia in $F^{v}$ at 30 min after wounding (dark line) with the cells in $F^{i}$ before wounding (dotted line) demonstrating that nearly all actin-GFP has been redistributed to the leading edge from its starting position 20-30 µm away. Single Z slices for $E^{i-ii}$, $F^{i-ii}$; maximum intensity projections for A-D, $E^{iii-v}$, $F^{iii-v}$. Scale A-$B^{ii}$, $C^{i}$-$D^{iii}$ = 5 µm, E-F = 10 µm.

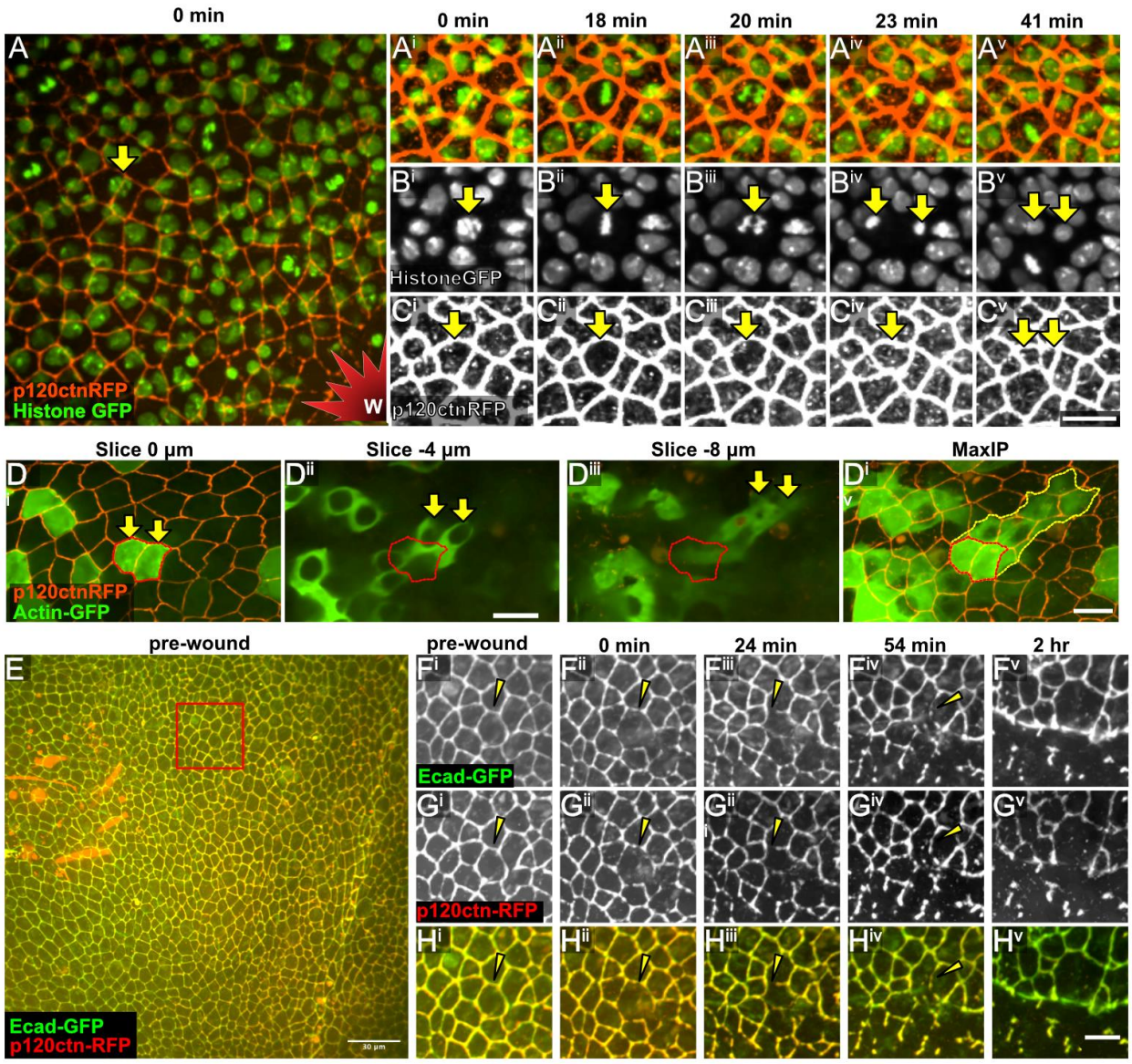


**Chapter 4, Supplemental Figure 1: Characteristics of the pupal notum epithelium.**

A-C) An example of mitosis occurring ~80 µm from the wound. D) Z-slices at different depths of GFP-labeled cells reveal that the apical area (red outline) does not reflect the position of cells at basal slices (yellow arrows). E-H) Ecad-GFP and p120ctnRFP colocalize and behave similarly during border breakdown. Arrowheads in F-H points to borders breaking down in first hour after wounding. This work was conducted by James White and Junmin Hua.

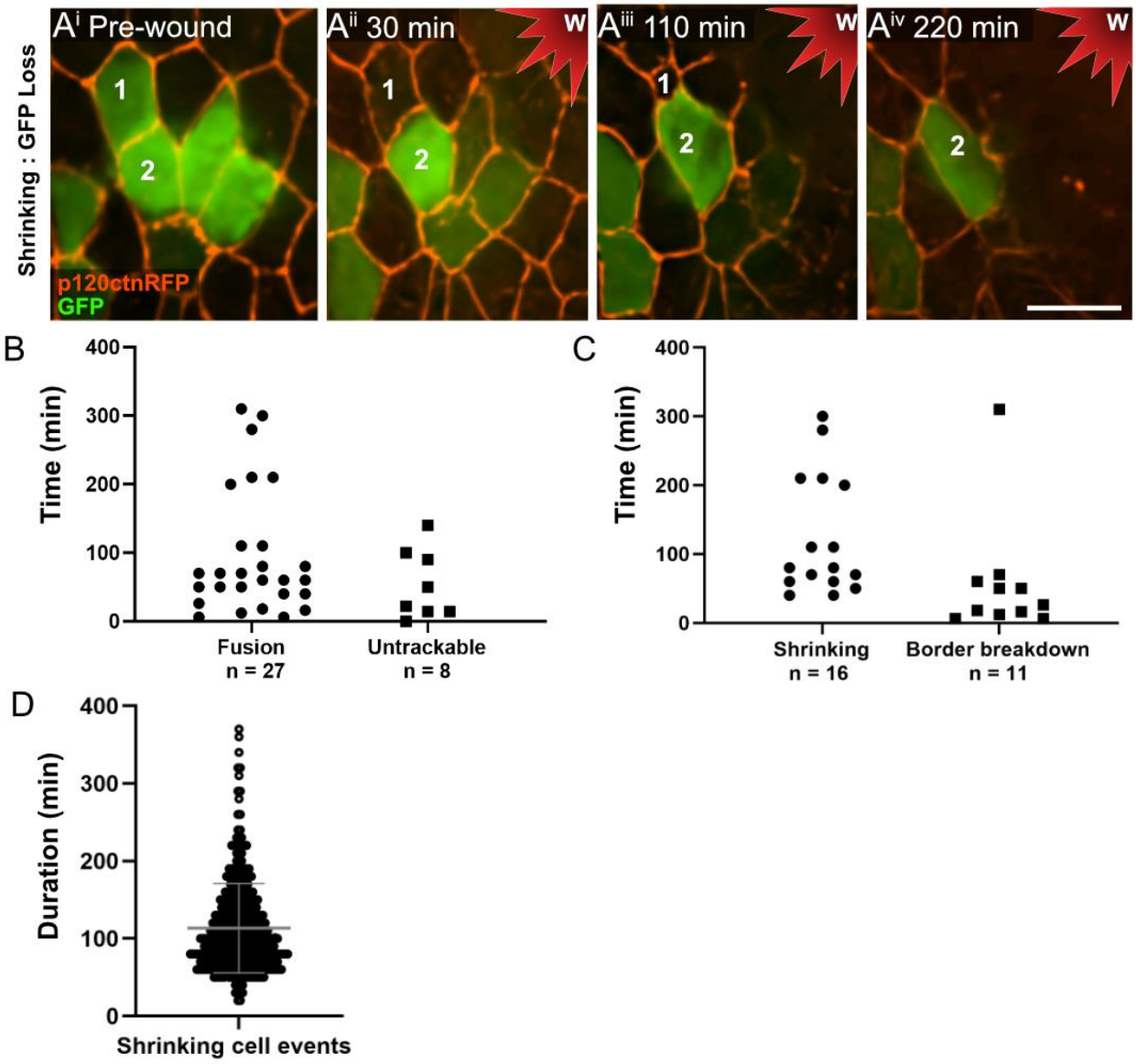


**Chapter 4, Supplemental Figure 2: Temporal analysis of fusion events.**

A) An example of an untrackable cell is shown. After wounding, cell 1 loses cytoplasmic GFP, but there is no obvious recipient cell. Cell 1 then shrinks. B) Cells individually labeled with GFP reveal the timing and frequency of fusion or GFP loss (untrackable). C) Fusion cells from panel B were divided into two types of fusion events, shrinking cells and border breakdowns, to compare the temporal onset of each type of fusion. D) Cell shrinking was a lengthy and variable process, lasting hundreds of minutes. Shrinking cells were identified by p120ctnRFP.

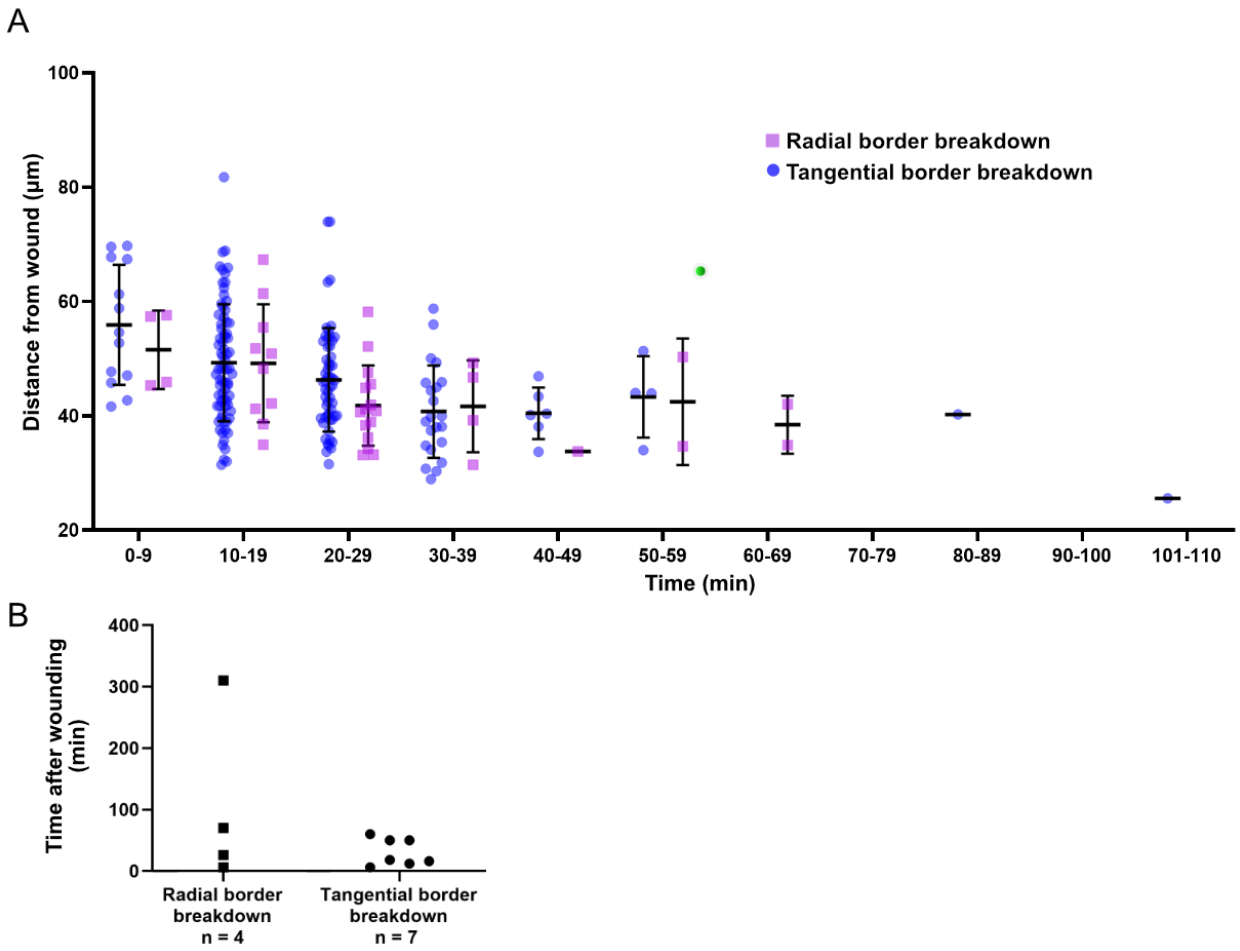


**Chapter 4, Supplemental Figure 3: Comparisons of tangential and radial border breakdowns.** A) The distance of tangential and radial border breakdown events from the wound, compared over time binned into 10 min intervals. Border breakdown events were identified by p120ctn. B) The timing of tangential vs radial border breakdown fusion events observed in single GFP-labeled cells. This work was conducted by James White and Jasmine Su.

**Chapter 4, Supplemental Movie 1: Syncytial cells form after wounding in the *Drosophila* pupal notum.** Epithelial cell borders in red (p120ctnRFP) and nuclei in green (HistoneGFP). White box on first frame denotes field of view in Chapter 4, Figure 1A. Movie begins before wounding and extends to 2 h after wounding.

**Chapter 4, Supplemental Movie 2: GFP mixing precedes border breakdown after wounding.** Arrow in first frame points to cell border between cells that will fuse after wounding. GFP diffusion into the unlabeled cell precedes visible border breakdown. w, wound region. Cell borders are labeled with p120ctnRFP. Movie begins before wounding and extends to 2 h 50 min after wounding. Same cells as Chapter 4, Figure 1I and 2D.

**Chapter 4, Supplemental Movie 3: Shrinking cells contribute to syncytia.** Arrow in first frame points to an individual cell labeled with Actin-GFP that fuses by shrinking after wounding. This cell contributes its actin-GFP to neighboring cells minutes after wounding then shrinks much later; shrinking is first evident about 1.5 h after wounding and is nearly complete by 3.5 h after wounding. w, wound region. Cell borders are labeled with p120ctnRFP. Same cells as Chapter 4, Figure 2C.

**Chapter 4, Supplemental Movie 4: Syncytia pool actin and concentrate it at the leading edge of repair.** An individual cell labeled with actin-GFP fuses with wound proximal cells and contributes its actin to the leading edge of the syncytium. w, wound region. The original source cell and its immediate neighbor go on to shrink into wound proximal cells. Cell borders are labeled with p120ctnRFP. Same cells as Chapter 4, Figure 6E,F.

**CHAPTER 5: DISCUSSION**

*A mitotic tissue utilizes polyploidy to heal*

When I began my thesis work it was generally though that polyploidy was induced in tissues with poor regenerative capacity and that by studying polyploidy we could uncover new therapeutic strategies for these tissues (Øvrebø & Edgar, 2018). However, my thesis work has shown that the mitotically capable *Drosophila* pupal notum induces both nuclear polyploidy and cell-cell fusion derived syncytia after laser ablation. Further, long-term imaging of the wounded notum reveals that as the wound heals, and after the wound has closed, some of the syncytia and the polyploid nuclei within them are removed from the epithelium (Appendix D). Transient wound induced polyploid cells are also observed in the zebrafish epicardium after injury (Cao et al., 2017). This leads to the question of how often other tissues induce a transient population of polyploid cells to compensate for injury or disease? Could there be a yet undiscovered population of polyploid cells induced in wounded mammalian tissues? This is not entirely unlikely as, if they are transient, they may not have been observed in tissues that cannot be live imaged such as *in vivo* human skin. Future studies should be conducted probing these tissues to determine if polyploidy occurs during mammalian epidermal wound healing as this would present new therapeutic approaches to wound care.

*Wound induced nuclear polyploidy, pathways for future investigation*

Initial experiments sought to characterize wound induced divisions in the pupal notum, to test the hypothesis that a mitotically capable tissue would deploy division to compensate for lost cells. Thus, I wounded and live imaged the fluorescent cell cycle indicator fly (FUCCI) to live image entrance into, and the progression of wound proximal cells through mitosis. However, we did not observe mitosis, instead both fluorophores of the FUCCI system were maintained within enlarged intact nuclei near the wound (Chapter 3, Figure 1A$^{i}$ - A$^{iii}$). This surprising result suggested that the wounded notum may be inducing nuclear polyploidy similar to the larval and adult tissues (Besen-McNally et al., 2021; Galko & Krasnow, 2004; Grendler et al., 2019; Losick et al., 2013; Losick et al., 2016; Wang et al., 2015) despite having access to mitosis (Guirao et al., 2015). To study this further we needed to DAPI stain the wounded notum, however, the pupa is encased in an impermeable waxy cuticle and due to its small size and the breakdown of the larval body plan, it is not easy to dissect. Thus, we developed a dissection and fixation protocol to access this tissue described in Chapter 2 (White et al., 2022) and were able to probe nuclear ploidy around the wounds described in Chapter 3 (White et al., in review). We determined that, indeed, wound-proximal nuclei become polyploid and based on the comparison of DAPI intensity with 1C spermatid controls we estimate that the majority of nuclei within 100 µm of the wound are undergoing at least one additional genome replication to become 8C (Chapter 3, Figure 1C).These results are significant given that this is a mitotically capable tissue and further studies will be required to determine how exactly this nuclear polyploidy is induced.

Individual nuclear polyploidy can be achieved by arresting the cell cycle before nuclear envelope breakdown during mitosis. Different terms have been introduced for polyploid nuclei depending on exactly where in the cell cycle the nucleus deviated. In 2015 Dr. Terry Orr-Weaver sought to align the

polyploidy field and introduce standard nomenclature (Orr-Weaver, 2015). Based on this precedent, the nuclei we observe around wounded nota are becoming polyploid by either endocycling (also called endoreduplication which is interchangeable with endoreplication (Zielke et al., 2013)) or an early endomitosis (Orr-Weaver, 2015). Endocycles are a shortened cell cycle comprised of a concurrent Gap and S-phase's without entering Mitosis. In most cells that enter the endocycle, they first stall in G2 and then through a variety of mechanisms in different tissues they block mitosis entry and re-initiate S-phase, which will be discussed in greater detail below. Endomitosis refers to a cell that has entered mitosis but arrests at some point before completing cytokinesis. This means that an endomitotic cell could have two nuclei within one cytoplasm if it is arrested after anaphase but before cytokinesis. However, if mitosis was arrested after prophase and before anaphase the endomitotic cell would have a single nucleus. It follows that there are important distinctions between an endocycling vs. endomitotic nucleus and at present, my data cannot distinguish between the two. I propose the following future directions to remedy this.

*Distinguishing endocycling*

Initiation of endocycling has been elucidated in the *Drosophila* ovarian follicle cells which become polyploid to support the germline cyst (Chapter 5, Fig.1). It begins with the expression of the Delta ligand by the oocytes triggering the Notch receptor on the follicle cells (Deng et al., 2001; López-Schier & Johnston, 2001). Notch signaling inhibits String/Cdc25-dependent liberation of CDK1, thus inhibiting CycA and CycB activation. Without CycA / CycB activation the follicle cells cannot enter mitosis (Schaeffer et al., 2004; Shcherbata et al., 2004). Mitosis inhibition is reinforced by up-regulation of Fzr which associates with the APC complex to degrade CycA and CycB. With mitosis blocked the follicle cells arrest in a G2 like state. Notch also suppresses the CDK inhibitor Dacapo which allows CycE/Cdk2 to accumulate and initiate S-phase entry (Zielke et al., 2013). Once the first endocycle has been initiated sequential endocycles are regulated by a set of "core oscillators" which have been uncovered by studying the *Drosophila* salivary gland. During G phase E2F1 activates CycE allowing S-phase entry (Zielke et al., 2011). Once replication forks are active and have active PCNA, a PCNA-interacting protein activates the CRL4·Cdt2 ubiquitin ligase which subsequently flags E2F1

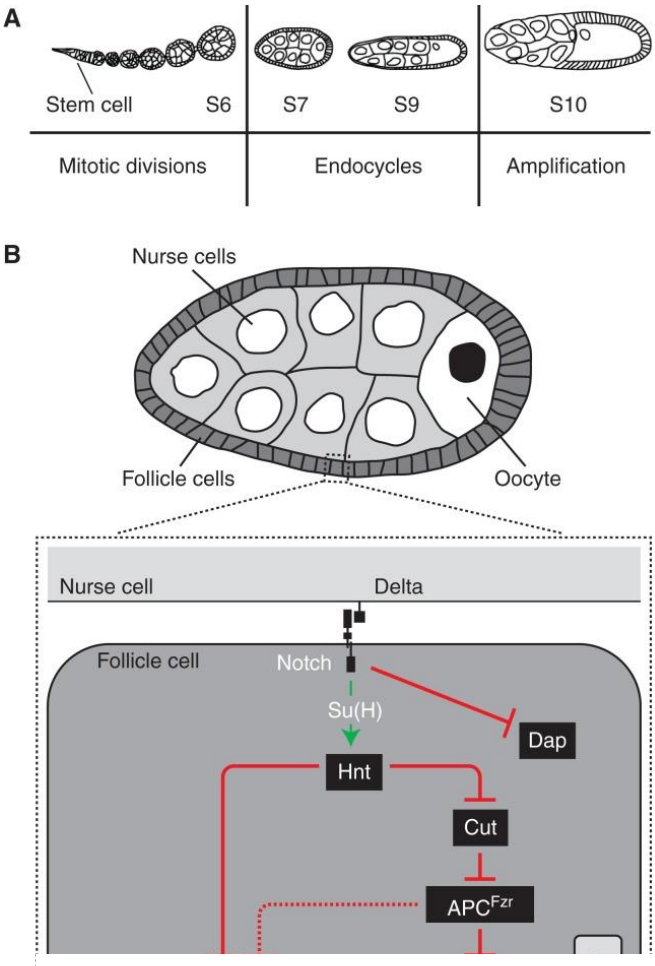


**Chapter 5, Figure 1: Endocycling in *Drosophila* follicle cells.** From (Zielke et al., 2013)

for degradation (Arias & Walter, 2006; Havens & Walter, 2009; Shibutani et al., 2008). Low levels of E2F1 cause the loss of CycE, allowing for the accumulation of the APC·Fzr complex which degrades Geminin and allows for the assembly of preRC's (Zielke et al., 2013). Thus, endocycles are maintained by E2F1 / CycE oscillations after Notch-Delta initiation.

The Notch-Delta signaling pathway is also utilized within the pupal notum during the patterning of the mechanosensory bristle lineage at the stage our experiments are conducted. The stereotyped placement of the bristles is organized by basal filopodia protrusions that allow lateral inhibition to occur over 2-4 cell distances between precursor cells (Cohen et al., 2010). It is also appreciated that the proteolytic activation of the Notch receptor requires mechanical force to expose a cryptic cleavage site on the Notch receptor (Gordon et al., 2015; Mack et al., 2017). This is a promising future direction for determining how endocycles are initiated in the pupal notum after wounding. I would hypothesize that the Notch receptor could be activated by the rapid relaxation of the pupal notum after wounding (Han et al., 2023; O'Connor et al., 2021) or by the reorganization of the actin cytoskeleton during the actomyosin wave movement through the tissue (Antunes et al., 2013). Ectopic Notch activation while the epithelial cells of the notum are in G2, as they appear in Chapter 3 Figure 1A[i], could trigger the same endocycling initiation pathway outlined in follicle cells in the previous paragraph. To test this hypothesis, I would suggest the following specific experiments.

To determine if Notch signaling is ectopically activated following wounding, one could live image a transcriptional reporter of Notch (E(spl)mα-GFP (Castro et al., 2005)) within the pupal notum every 10 minutes for 3 hours after wounding. I would expect that the GFP transcriptional reporter should appear following wounding in the pupal notum. To elucidate if Notch-dependent transcriptional activation is required for endocycling one would need to inhibit notch activity with *UAS-Mastermind* D/N. This dominant negative form of the Notch intracellular domain transcriptional coactivator could be expressed in the pnr region of the pupal notum by crossing to the labs *ShgGFP ; pnrGal4, Gal80ts, UAS-mCherry.NLS / S-T* stock. Three hours after wounding the pelts could be DAPI stained (White et al., 2022) and assessed for DAPI intensity. Nuclei which received the knockdown would also be mCherry positive and could be compared to control domain nuclei which lacked mCherry. If Notch is an upstream regulator of endocycling in the pupal notum, *UAS-Mastermind* D/N will block endocycling within the pnr domain but not the control domain of the notum resulting in reduced DAPI intensity in knockdown nuclei. Finally, the downstream effectors of Notch signaling could be explored to determine if the pathway is consistent with the follicle cells. In follicle cells Notch blocks mitosis entry by inhibiting String and upregulating Fizzy-related through Hindsight allowing for preRC assembly (Sun & Deng, 2007). An enhancer trap for String (B:63867) and gene trap for fizzy-related (B:80615) could be crossed into a p120ctnRFP and *UAS-GFP.NLS* background, wounded and live imaged every 10 min for 6 hr. It would be expected that String would be downregulated after wounding whereas Fizzy-related would be upregulated in wound proximal nuclei compared to distal nuclei still undergoing mitotic division. It would also be expected that RNAi against *String* and *Fizzy-related* would block wound induced endocycling and could be tested in the same modality as the Notch D/N.

*Distinguishing Endomitosis:*

Endomitosis is an altered cell cycle that can result in either a mononucleated or bi-nucleated polyploid cell (Orr-Weaver, 2015). During development endomitosis occurs in keratinocytes (Gandarillas, 2012; Gandarillas & Freije, 2014; Zanet et al., 2010), megakaryocytes (Nagata et al., 1997; Ravid et al.,

2002; Trakala et al., 2015), cardiomyocytes (Hesse et al., 2012; Liu et al., 2010; Senyo et al., 2013), and hepatocytes (Duncan, 2013; Gentric & Desdouets, 2014; Miyaoka et al., 2012; Pandit et al., 2012; Vinogradov et al., 2001) of mammals as well as the subperineurial glia (Unhavaithaya & Orr-Weaver, 2012) of *Drosophila*. Following injury, mammalian cardiomyocytes induce endomitosis (Ebert & Pfitzer, 1977; Senyo et al., 2013). However, this increased polyploid has been associated with reduced regenerative capacity (Bersell et al., 2009; Kikuchi, 2014; Vivien et al., 2016) in mammalian hearts. Inducing endomitosis in the highly regenerative zebrafish heart by interfering with the cytokinesis driver Ect2 blocked the regenerative capacity of the cardiomyocytes. Other cytokinesis regulators have been characterized, Anln and Septin, which drive bi-nucleated endomitosis in the liver and megakaryocytes (Donne et al., 2020; Geddis et al., 2007). Very little is known about mononucleated endomitosis drivers and based on my observations while working with Histone-eGFP pupae (Chapter 4, Figure 1A$^{i}$ -A$^{iii}$, C-D, Figure 4 C$^{i}$-C$^{ii}$, Appendix C), it appears that chromosomes do not align in metaphase around wounds. So, if the nuclei are endomitotic they must be arresting in prophase or prometaphase. To characterize this, I would propose the following preliminary experiments.

Probing for early mitotic markers such as active CycA, CycB by adapting existing FRET Cyc – Cdk1 technologies into *Drosophila* would be an ideal starting point *(Gavet & Pines, 2010; Zhang et al., 2001)*. After wounding, these tools would resolve whether CycA / CycB are becoming activated signaling mitotic entry and suggesting that wound proximal nuclei are utilizing endomitosis. Next, although chromosomes do not appear to align in metaphase, it may be possible to detect chromatin condensation during prophase. During prophase, the chromatin condenses in preparation of chromosome alignment in metaphase, imaging the Histone-GFP at a higher resolution (e.g. super resolution) should reveal if wound proximal nuclei are condensing their chromatin compared to distal diploid cells. A positive control for this process would be to assess the chromatin compaction of distal mitotically capable cells as they pass through prophase.

*Elucidating the role of increased nuclear ploidy in the wounded pupal notum:*

Chapter 3 characterized the induction of nuclear polyploidy, and I have proposed above experiments to elucidate the mechanism by which the nuclei become polyploid. However, there remains the question of what role nuclear polyploidy plays during wound closure. Studies in the mammalian liver and the hindgut pylorus of the fly indicate that polyploidy is a mechanism to restore tissue function while balancing oncogenic risk (Bailey et al., 2021). Indeed forcing the hindgut pylorus into the mitotic cell cycle by knockdown of *Fzr* sensitized the hindgut to oncogenic growth (Cohen et al., 2018). So, induction of nuclear polyploid in the pupal notum could be a mechanism to restore the ploidy of the notum tissue, while preventing potentially damaged nuclei from having full access to mitosis. This could be tested by utilizing the previously published methods of inducing mitosis either by knockdown of *Fzr* or the knockdown of *Fzr* and simultaneous overexpression of *stg (Grendler et al., 2019).* Forcing the wounded pupal notum to undergo mitotic division instead of deploying nuclear polyploidy would likely result in deleterious effects. Non-syncytial cells that attempted mitotic divisions within the migrating epithelium could result in epithelial barrier integrity issues as they rounded up in preparation of division while the surrounding tissues remained elongated towards the wound. Although, the mechanism which allow for this process to occur in unwounded migrating epithelial cells may still be effective in the turbulent environment of the repairing epithelium. Further, spindle fiber assembly and chromosomal segregation in a migrating tissue would likely result in segregation errors and either generate aneuploid daughter cells or failed division and chromatin bridging. It would be very interesting to investigate

syncytial cells in the context of forced mitosis. Given syncytia form within 30 min after injury (Chapter 4, Figure 1H) I expect that syncytia formation itself would not be linked the nuclear polyploidy and that forcing mitosis would not affect the formation of syncytia. However, the first analysis would be to determine if forced mitosis affected syncytia formation. Subsequent long-term imaging would reveal whether syncytial cells attempt to restore tissue ploidy through mitotic divisions. Attempted mitosis within a syncytial cell could prove disastrous as there are multiple sets of nuclei and likely multiple sets of centrosomes present within one syncytial cytoplasm. Multi-polar divisions within polyploid giant cancer cells result in aneuploid daughters and chromatin bridging, which would very likely compromise the epithelial barrier in the pupal notum. It is also possible that forced mitosis would result in increased levels of bi-nucleated endomitosis within the notum. Finally, it would be prudent to explore the persistence of forced mitotic syncytial cells compared to control syncytia around epithelial wounds. The number of syncytial cells decreases during wound closure in control samples (Appendix D), so an increased degree of syncytial extrusion would be a readout of reduced resilience of forced mitotic cells compared to control.

The resilience of polyploid cells to genotoxic stress has been well characterized (Baonza et al., 2022; Mehrotra et al., 2008). When the adult *Drosophila* epithelium is exposed to UV irradiation and wounded, polyploid epithelial cells are able to repair the damage but forced mitotic cells were unable to repair (Grendler et al., 2019). Similarly, follicle cells of the *Drosophila* ovary were resistant to irradiation when allowed to endocycle, but when endocycles were suppressed the mitotically cycling follicle cells underwent apoptosis when exposed to irradiation (Hassel et al., 2014). This resistance to irradiation could be conferred by the downregulation of apoptotic genes. Indeed all isoforms of p53 have been shown to be downregulated in the endocycling polyploid cells of the *Drosophila* salivary gland and fat body (B. Zhang et al., 2014). Additionally, overexpression of p53 in endocycling cells was not sufficient to induce apoptosis indicating that there are other levels of apoptotic suppression within endocycling cells (Mehrotra et al., 2008; B. Zhang et al., 2014). Apoptotic resistance is a requirement for developmentally programmed endocycling cells as underreplicated heterochromatic regions and unresolved replication forks within their genomes would normally trigger cell death (Belyaeva et al., 1998; Marchetti et al., 2003; Nordman et al., 2011; Spradling & Orr-Weaver, 1987). Thus, induction of endocycling in wound proximal nuclei could also activate anti-apoptotic pathways allowing damaged cells at the leading edge to survive under conditions that they normally could not. An interesting future direction would be to explore the regulation of *p53*, *Reaper, Head involution defective,* and *Sickle* following wounding in the pupal notum. I would expect that apoptotic programs would be suppressed in wound proximal cells and this would confer resistance to genotoxic stress of polyploidy, as well as the toxic environment that the wound itself presents, for example the high levels of ROS present in the wound bed (Dunnill et al., 2017).

*Wound induced cell-cell fusion perspectives and future directions*

Another potential mechanism for dealing with the harsh wound environment is through cell-cell fusions. One could imagine that, after injury, there would be a gradient of damage radiating out from the wound site. Cells closest to the wound would have the most damage and be at the highest risk of dying. They would likely have lost cytoplasm and organelles from ruptures in the plasma membrane and we have previously observed that the nuclear envelope is compromised following injury in wound proximal nuclei (O'Connor et al., 2021). Loss of the nuclear envelope integrity allows enzymes and proteases to attack the chromatin resulting in DNA damage (Gauthier & Comaills, 2021). Due to these stresses, cells which had originally survived the wound would die and cause the wound area to further expand.

However, by inducing cell-cell fusion with more distal and less damaged cells, leading edge cells could survive and prevent the expansion of the wound bed after injury. I acquired some preliminary data that cannot rule out this hypothesis. By exposing the notum to increased proteostatic stress through heat shocking, I was able to determine that by 60 min after wounding the wound bed was significantly larger in heat shocked samples than control (Appendix B). However, further experiments would need to be conducted to determine whether this expansion was the result of impaired proteostatic machinery in heat shocked samples. In addition to potentially promoting survival, we have determined that cell-cell fusions allow for rapid resource relocalization following wounding which will be elaborated on in the coming paragraphs. First, I would like to outline in brief the known mechanisms of cell-cell fusion in the literature.

During development cell-cell fusion plays an essential role across the animal kingdom. In sexually reproducing species, life begins with the fusion of the sperm with egg cells through mechanisms that still need to be fully elucidated (Brukman et al., 2019; Klinovska et al., 2014). During development cells of many tissues fuse into syncytia. This process has been well studied in the nematode *Caenorhabditis elegans* as they undergo a reproducible number of fusions allowing for close study (Iosilevskii & Podbilewicz, 2021; Podbilewicz & White, 1994). This has allowed for the discovery of the fusogenic proteins eff-1 (epithelial fusion failure-1) (Mohler et al., 2002) and aff-1, (anchor cell fusion failure-1) (Sapir et al., 2007). In the tissues that deploy eff-1 and aff-1 they are required for fusion, and must be displayed on the plasma membrane of both cells participating in the fusion (Mohler et al., 2002; Sapir et al., 2007). Interestingly, they are such potent drivers of fusion that they can induced fusion in cells that would otherwise not fuse (Sapir et al., 2007; Shemer et al., 2004). In *C. elegans* eff-1 and aff-1 either in concert or separately drive fusion in, but not limited to, the excretory duct (Stone et al., 2009), the interface of the pharynx and the intestine (Rasmussen et al., 2008), spike cells of the tail (Chiorazzi et al., 2013; Sulston et al., 1983), and the epidermis (Altun & Hall, 2009).

Bona-fide fusogenic proteins are rare in the animal kingdom and remain elusive in *Drosophila (Kim & Chen, 2019).* However, in Drosophila muscle cell fusion occurs between muscle founders and fusion competent myoblasts and depends upon immunoglobulin (Ig) domain-containing cell adhesion molecules (CAMs)(Ruiz-Gómez et al., 2000; Strünkelnberg et al., 2001). Similarly, myoblast fusion in zebrafish utilizes a homologous CAM to that in *Drosophila (Srinivas et al., 2007)*. Additionally, both *Drosophila* and vertebrate cell fusion requires actin cytoskeletal rearrangements to induce fusion. Most of the regulators act through the Arp2/3 complex (Berger et al., 2008; Erickson et al., 1997; Geisbrecht et al., 2008; Gildor et al., 2009; Hakeda-Suzuki et al., 2002; Jin et al., 2011; Kaipa et al., 2013; Kim, Jin, et al., 2015; Kim et al., 2007; Luo et al., 1994; Massarwa et al., 2007; Richardson et al., 2007; Rushton et al., 1995; Schäfer et al., 2007; Schröter et al., 2004). Reviewed previously (Kim & Chen, 2019), in brief the Arp2/3 complex is required for the formation of an F-actin podosome like protrusion generated by the fusion-competent myoblast (Berger et al., 2008; Chen, 2011; Richardson et al., 2007; Kristin L Sens et al., 2010). This structure extends into the muscle founder cell which produces a resisting force on its membrane (Duan & Gallagher, 2009; Duan et al., 2018; Kim, Ren, et al., 2015). The pushing and resisting forces allow the plasma membranes to come into close enough contact to initiate fusion, as this would be otherwise energetically unfavorable, see Chapter 5, Fig 2 (Kim & Chen, 2019). Cell-cell fusion is also induced in the pathological context by some viruses which not only fuse with the plasma membrane of their host cells but drive infected cells to fuse with healthy neighbors (Leroy et al., 2020). However, it is unlikely that the factors playing a role in viral fusion participate in cell-cell fusions in the pupal notum. Sterling work by another graduate student in the Page-McCaw lab, Junmin Hua, has been directed towards uncovering the mechanism by which cells fuse after injury in the pupal notum. She has made exciting progress elucidating the mechanism by which the rapid fusions characterized by p120ctnRFP loss occur, which will be expounded upon in her thesis research. However, I will propose experiments to investigate whether the second wave of fusions (which we termed “shrinking cells” (Chapter 4, Figure 2)) are the result of a similar mechanism to muscle cell fusions.

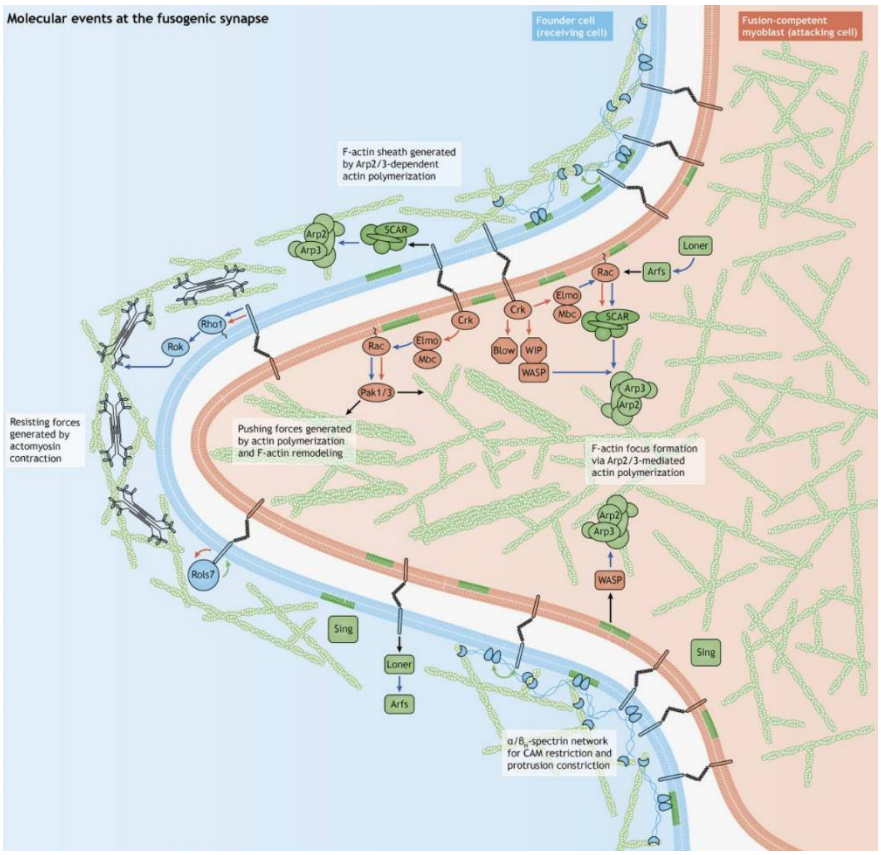


**Chapter 5, Figure 2: The *Drosophila* Fusogenic Synapse.** From (Kim & Chen, 2019)

The CAMs responsible for Drosophila muscle cell fusion are *dumfounded* and *roughest* in founder cells and *sticks and stones* and its paralog *hibris* in the fusion competent myoblast. Flybase curations indicate that both *dumfounded* and *roughest* RNA are present in the early pupae and are expressed in the epithelia of the adult making it likely that they are expressed in the pupal notum. *Sticks and stones* is weakly expressed in the pupa and adult epithelium, however, *hibris* is strongly expressed in the early pupa and epithelium of the adult(Brown et al., 2014; Li et al., 2022). Thus, it is possible that these CAMs drive shrinking cell fusion in the pupal notum after injury. To test for this, it would be interesting to quantify the frequency of shrinking cells when *dumbfounded*, *roughest*, and *hibris* were knocked down in the *pnr* region compared to the control domain where these proteins would still be produced. If shrinking cell fusion is driven by the same machinery as muscle cell fusion, there should be a significant reduction of shrinking cell fusion in the *pnr* domain compared to the control. Then, HA tagged versions of *hibris* and *dumbfounded* could be crossed into the LifeAct-RFP fly the lab has. Pupae could then be wounded and dissected and stained with an antibody specific for the HA-tag, and secondary with GFP. If these CAMs are facilitating fusion of shrinking cells, a puncta of GFP labeled Hibris or Dumbfounded would be expected to colocalize with a LifeAct protrusion from a Hibris puncta. In contrast, a LifeAct intracellular network would be expected to colocalize with a Dumbfounded-labeled puncta. These experiments would help to elucidate how the initial fusion pore is created during shrinking cell fusion. However, further experiments would need to be conducted to understand the mechanism by which the shrinking cells actually shrink.

A likely explanation is that shrinking cells are utilizing the same machinery as cell-cell extrusion. However, before initiating the contraction machinery of cell-cell extrusion, the shrinking cell would have created a fusion pore between the shrinking cell and its recipient neighbor. Then upon contraction, instead of rounding up and extruding, the contraction force would drive the cytoplasm and organelles of the shrinking cell through the fusion pore and into the recipient cell. Cell extrusion due to overcrowding is a known phenomenon in the pupal notum (Romain Levayer et al., 2016; Marinari et al., 2012) and there is evidence for extrusion selection being driven by mechanical forces (Marinari et al., 2012). The stretch activated calcium ion channel Piezo1 is required for live cell extrusion in MDCK monolayers and zebrafish epidermis (Eisenhoffer et al., 2012; Gudipaty et al., 2017). When Piezo1 is activated in the cell that will extrude the sphingosine kinase is activated to produce sphingosine-1-phosphate within the extruding cell. This lipid activates the sphingosine 1-phosphate receptor 2 and subsequently p115 RhoGEF, which drives the formation of an actomyosin ring in the cells surrounding the extruding cell (Gu et al., 2011; Rosenblatt et al., 2001; Slattum et al., 2009). To determine if this process is occurring in shrinking cells, I would recommend beginning by reanalyzing the movies the lab already has. We should have both LifeActRFP and MyosinII-GFP (separately) post-wounding movies that would include the duration of shrinking cells. So, if the shrinking cells are utilizing cell extrusion machinery the actomyosin cable should be observable around the shrinking cells. Since LifeAct and Myosin II also label the cell-cell borders it should be possible to identify shrinking cells and look for the cable in its neighbors. If the cable was present around shrinking cells, it would warrant further analysis into the knockdown of *Piezo1*, *sphingosine kinase*, and the *sphingosine 1-phosphate receptor 2* within the *pnr* domain and comparing the frequency of shrinking cells when the extrusion machinery is inhibited to the control domain. In the event that extrusion machinery is not utilized for shrinking cells, it would be interesting to explore if the contractile force is coming from the shrinking cell itself. Presumably this would have to take the form of a contraction force from the cortical actin network within the shrinking cell itself. These experiments

would be critical to further understand the mechanism by which shrinking cells contribute their resources towards the leading edge during wound closure.

In addition to sending resources to the leading edge, shrinking cells may also play a role in drawing more distal, less damaged cells towards the wound. During dorsal closure apoptotic extruding amnioserosa cells contribute a third of the mechanical force for closure to occur (Reed et al., 2004; Toyama et al., 2008). Additionally, extruding apoptotic cells at the *Drosophila* presumptive leg-joints exert a pulling force on surrounding cells causing folding and reinforces joint development (Monier et al., 2015). Thus, extrusion can provide mechanical force and shrinking cells may be using this mechanism to draw more distal cells towards the wound area. This would be beneficial as I have preliminary data indicating more distal cells from the wound are able to undergo proliferation (Appendix C). Additionally, I have observed that during wound closure some syncytia are removed from the epithelium (Appendix D) and the loss of that cell and genomic material would have to be compensated for. Thus, by drawing distal cells that retained their ability to divide closer to the wound these cells would be poised to undergo compensatory division if a syncytium was removed from the epithelium. These data would reinforce a broad hypothesis about syncytia: syncytia act as a rapid but disposable "Band-Aid" for wounds. If the wound were to be closed only by diploid healthy cells, multiple rows of damaged cells at the leading edge after wounding would be excluded from the repair process. This would result in a larger wound and increase the time it would take to close the wound. Instead, fusing damaged cells near the wound would cobble together a damaged but functional patch that can re-epithelize the wound before being removed.

Chapter 4 showed that these cell-cell fusions after wounding indeed allow for the pooling of cellular resources. By leveraging the powerful genetic tools available in *Drosophila* we first created individual GFP expressing cells within the pupal notum at a low frequency with 1-2 cells labeled with multiple unlabeled cells between them. After wounding we were able to visualize the cytoplasmic GFP from GFP labeled cells entering and filling previously unlabeled adjacent cells followed by the removal of the intervening p120ctnRFP labeled borders (Chapter 4, Figure 1I$^{i}$-I$^{iv}$). This cytoplasmic mixing was observable throughout all the individual Z-planes as well as maximum intensity projection ruling out the possibility of a protrusion of the original GFP labeled cell underneath the unlabeled cell. To understand the role that cell-cell fusion plays during wound closure, we generated individually labeled cells expressing actin-GFP, monomers of actin tagged with GFP. As actin is critical for cell migration and wound closure it would very likely be a resource pooled during wound closure. Upon wounding we observed actin-GFP from labeled cells mixing with and filling previously unlabeled neighbors. Strikingly, if the syncytial cell had access to the leading edge the actin-GFP could be seen accumulating there likely in an actomyosin purse string structure. We even observed actin that was originally three cells away from the leading edge move through two previously unlabeled cells and pool at the leading edge. It will be exciting to further elucidate this process, and this observation unlocks many interesting questions. Firstly, it would be exciting to explore what other cellular resources are pooled at the leading edge of repair, myosin II and GTPases are likely candidates as well as ribosomes or even the plasma membrane that was removed from the borders between fusing cells. Additionally, organelles could be re-localized to the leading edge like mitochondria networks and possibly the ER. Second, previous research has suggested that the rate at which actin is moved into leading edge protruding zones of rat fibroblasts could not be explained by diffusion alone (Zicha et al., 2003). Instead, they suggest that myosin II dependent cell contraction during migration causes a pressure gradient resulting in hydrodynamic flow oriented towards the negative pressure area generated by an expanding leading edge. It would be

interesting to conduct similar FRET experiments to explore the rate of actin relocalization in syncytial cells after wounding to understand whether a similar mechanism of hydrodynamic flow occurs in syncytial cells. Additionally, it would be interesting to explore how actin aggregates at the leading edge. The aggregation itself indicates that the actin is no longer passively diffusing, as that would result in a signal similar to the GFP clones. Multiple mechanisms could be at play driving the accumulation of actin at the leading edge.

It has been well documented that single cell and multicellular wounds assemble an actomyosin purse string which draws the wound closed reviewed previously (Begnaud et al., 2016). The assembly of the wound induced purse string is largely dependent on myosin II (Abreu-Blanco et al., 2012; Fernandez-Gonzalez & Zallen, 2013; W. Wood et al., 2002) and the GTPases Rho, Rac, and Cdc42 (Abreu-Blanco et al., 2011; Abreu-Blanco et al., 2014; Benink & Bement, 2005; Brock et al., 1996; Desai et al., 2004; Soto et al., 2013; William Wood et al., 2002). In single cell wounds Rho accumulates at the leading edge driving the formation of actin filaments and recruits myosin II and directs the localization of Cdc42 and Rac. Cdc42 helps to maintain actomyosin ring integrity, whereas the Rac genes are responsible for the recruitment of additional actin to the leading edge via cortical flow. Fluorescently tagged versions of each of these GTPases have been generated (Abreu-Blanco et al., 2014) so it would be interesting to determine if their localization pattern is conserved in the multicellular wounds in the pupal notum. Additionally individual cells expressing these tagged GTPases could be expressed in the pupal notum and their relocalization to the leading edge of syncytia could be assessed to reinforce the resource pooling hypothesis. It would be interesting to explore whether the kinetics of these factors are altered in syncytial vs unfused leading-edge cells. Perhaps increased turnover in syncytia contributes to their ability to outpace unfused cells (Chapter 4, Figure 4).

We were able to quantify the number of cells that did not fuse into syncytia after wounding (Chapter 4, Figure 4D). Indeed, a small percentage of cells remained unfused, which allowed us to address the relative fitness of syncytia vs unfused cells during wound closure. Strikingly, we observed that 100% of unfused cells were removed from the leading edge before closure and that only syncytia persisted at the leading edge to close wounds (Chapter 4, Figure 4B$^{i}$-G). Thus, syncytia are able to outcompete unfused cells at the leading edge; exactly how this advantage is executed remains unknown. One possibility is that unfused cells at the leading edge are highly damaged by the wound and then accumulate additional damage through exposure to factors like reactive oxygen species released from the wound (Dunnill et al., 2017). Unfused cells would have to manage the stress of wound damage and the toxic wound bed with limited resources, whereas syncytia would be able to buffer those stresses across multiple cells worth of organelles and proteins. This would mean that overall unfused cells are disadvantaged in most regards and simply cannot compete overall. Another possibility is that syncytia have the resources to produce a stronger purse string. It would be interesting to explore the tricellular junctions shared between syncytia and unfused cells space at the leading edge. In multicellular wounds the actomyosin purse string is connected between cells by cadherin-based adherens junctions (Abreu-Blanco et al., 2011; Brock et al., 1996; Campos et al., 2010; Clark et al., 2009; Danjo & Gipson, 1998; Florian et al., 2002; Hartsock & Nelson, 2008; M. Tamada et al., 2007; Tepass et al., 2001; W. Wood et al., 2002). Syncytia would have an abundance of adherens junctional components as well as the endocytic machinery to remodel those junctions. It would be interesting to explore whether syncytia first create larger actomyosin purse-strings compared to their unfused neighbors, or if this is a process unliked to the cell size. If syncytia did produce larger purse-strings, they would likely need more adherens junctions

at the plasma membrane to sustain that cable introducing discrepancies between syncytial and unfused cell interfaces. These discrepancies may trigger a feedback mechanism to identify that the unfused cells are less capable at the leading edge resulting in their intercalation. Additionally, syncytial advantage could be a product of being able to assemble larger migratory machinery.

Active migration via filapodial and lamellipodial extensions play an important role during wound closure (Rothenberg & Fernandez-Gonzalez, 2019). Indeed, Wood *et al.* showed that protrusive filipodia were required to complete the final sealing of a wound that was primarily closed via a purse string mechanism (William Wood et al., 2002). Cdc42 is a key mediator of filopodial formation (Abreu-Blanco et al., 2012) and likely plays a role during pupal notum repair. It is additionally possible that Arp2/3-dependent lamellipodia observed during mouse fibroblast migration could play a role during closure (Suraneni et al., 2012). However, previous studies knocking down Arp2/3 in the pupal notum did not affect cellular contraction and actin flow towards the wound and the researchers noted that they observed no phenotype (Antunes et al., 2013). I have observed the formation of large filipodia like structures in the pupal notum after wounding and it would be interesting to explore the role of filipodia during closure in the pupal notum. My preliminary observations indicate that syncytia can produce large filipodia like structures (Appendix F). However, future studies will be required to determine if these structures are filopodia and what role they play during pupal wound healing. It would be interesting to observe highly-expressed LifeActRFP, such that even small filipodia are labeled, then compare the size of filopodial extensions between syncytia and unfused cells. If syncytia are producing larger filopodia they would be able to reach further and pull harder than unfused cells allowing them to outcompete them at the leading edge.

Additional experiments might elucidate the contribution of cell-cell fusion during wound repair by building a fly in which endoreplication was inhibited via *UAS-Yorkie RNAi* (Losick et al., 2013) and cell-cell fusion was inhibited by the scanning ablation technique (Han et al., 2023). This would be expected to block wound closure as it does in the adult *Drosophila* (Losick et al., 2013). Then using either the LexA (Lai & Lee, 2006) or Q-system (Riabinina & Potter, 2016) drive the *C. elegans* fusogens eff-1 or aff-1 within the *pnr* domain of the pupal notum. If these fusogens are sufficient to induce cell-cell fusion within the pupal notum, they could be used as a rescue condition for cell-cell fusion. It would be exciting to explore whether restoring fusion would increase wound closure around a scanning ablation wound which lacked endoreplication. These experiments would help to elucidate the role syncytia play during wound closure. By understanding how syncytia are regulated in a highly reproducible system like *Drosophila* we can begin to understand how cell-cell fusions are regulated and the roles they have in other systems.

*Contexts for cell-cell fusion in human disease*

In humans some of the most highly regulated cell-cell fusions take place in the osteoclast lineage. Osteoclasts are the only cell type capable of resorbing bone and their aggressiveness is linked to their degree of multinucleation, which is exclusively determined by cell-cell fusion (Boissy et al., 2002; Delaisse et al., 2020; A. M. Møller et al., 2020; A. M. J. Møller et al., 2020; Pereira et al., 2020; Piper et al., 1992; Sims & Martin, 2020). Despite their ability to fuse, pre-osteoclasts which are contained in small

clusters do not spontaneously fuse (Søe, 2020; Søe et al., 2019), their physiological fusion is only permitted at the bone surface (Søe et al., 2021). However, this process becomes dysregulated during cancer metastasis into bone and can lead to ectopic multinucleation and increased aggressiveness of osteoclasts-like cells which can then destroy heathy bone resulting in sever disease states(Lhoták et al., 2000; Saltel et al., 2006; Winding et al., 2000). Similarly, there is a growing body of research that suggests cell-cell fusion between tumor cells and macrophages may confer tumor cells with enhanced migratory capabilities (Pawelek et al., 2006; Pawelek & Chakraborty, 2008; Anne E Powell et al., 2011; Shabo et al., 2015; Silk et al., 2013). Although spontaneous fusion occurs at low levels in tumors, it is suspected that damage due to radiation and inflammation can increase fusion rate (Johansson et al., 2008; Lindström et al., 2017; Nygren et al., 2008; Powell & Marrion, 2007; Anne E Powell et al., 2011). This would be interesting as injury induced cell fusion within tumors would be consistent with my thesis results. Finally, cell-cell fusions are becoming extremely relevant in the field of biomaterial implantation. This stems from the fact that when the host mounts an immune response towards an implant material and macrophages cannot successfully phagocytose the material, they fuse into multinucleated giant cells (MacLauchlan et al., 2009). Although there role is unexplored, the presence of these multinucleated giant cells is associated with implant rejection (Sarah Al-Maawi et al., 2017; Barbeck, Lorenz, Holthaus, et al., 2015; Barbeck, Lorenz, Kubesch, et al., 2015; Barbeck, Udeabor, et al., 2015; Ghanaati et al., 2013; Lorenz et al., 2015).

**Chapter 6: Future Directions and Conclusions**

*Wound induced nuclear polyploidy, distinguishing endocycling:*

1. Determine if Notch signaling is ectopically activated following wounding, live image a transcriptional reporter of Notch (E(spl)mα-GFP (Castro et al., 2005)) within the pupal notum every 10 minutes for 3 hours after wounding. Expectation: The GFP transcriptional reporter should appear following wounding in the pupal notum.
2. Elucidate if notch dependent transcriptional activation is required for endocycling by inhibiting notch activity with *UAS-Mastermind* D/N (a dominant negative form of the Notch intracellular domain transcriptional coactivator) within the *pnr* region of the pupal notum by crossing to the labs *ShgGFP ; pnrGal4, Gal80ts, UAS-mCherry.NLS / S-T* stock. Three hours after wounding DAPI stain dissected pelts (White et al., 2022) and assess DAPI intensity of knockdown mCherry positive nuclei to control domain nuclei which lack mCherry. Expectation: If Notch is the upstream regulator of endocycling in the pupal notum, *UAS-Mastermind* D/N will block endocycling within the *pnr* domain but not the control domain of the notum.
3. Explore the downstream effectors of Notch signaling. In follicle cells notch blocks mitosis entry by inhibiting *String* and upregulating *Fizzy-related* through hindsight allowing for preRC assembly (Sun & Deng, 2007). An enhancer trap for *string* (B:63867) and gene trap for *fizzy-related* (B:80615) could be crossed into a p120ctnRFP and *UAS-GFP.NLS* background wounded and live imaged every 10 min for 6 hr. Expectation: Consistent with follicle cell endocycling, I would expect a downregulation of *string* and upregulation of *fizzy-related* in wound proximal nuclei compared to distal nuclei still undergoing mitotic division.

*Wound induced nuclear polyploidy, distinguishing endomitosis:*

1. Probe for early mitotic markers such as active CycA, CycB by adapting existing FRET Cyc – Cdk1 technologies into *Drosophila (Gavet & Pines, 2010; Zhang et al., 2001)*. After wounding, these tools would resolve whether CycA / CycB are becoming activated signaling mitotic entry and suggesting that wound proximal nuclei are utilizing endomitosis.
2. Probe for the chromatin condensation during prophase. During prophase the chromatin condenses in preparation of chromosome alignment in metaphase, imaging the Histone-GFP at a higher resolution than I have previously (100x or super resolution) should reveal if wound proximal nuclei are condensing their chromatin compared to distal diploid cells.

*Elucidating the role of increased nuclear ploidy in the wounded pupal notum:*

1. Force the wounded pupal notum to induce mitosis instead of nuclear polyploidy via the knockdown of *fzr* and simultaneous overexpression of *stg (Grendler et al., 2019).* Expectation: Live imaging of p120ctnRFP and Histone-EGFP will resolve delayed closure rate, presence of micro nuclei / chromatin bridging events, and reduced cell persistence at the leading edge in the mitotic wounds compared to polyploid capable wounds.
2. Determine whether nuclear polyploidy suppresses apoptosis after wounding through the regulation of *p53*, *reaper, head involution defective,* and *sickle* in the pupal notum. Expectation: following wounding reporters of apoptosis will be reduced/ absent in wound proximal cells compared to unwounded controls.

*Wound induced cell-cell fusion, future directions:*

1. Determine the role of *Drosophila* CAMs in shrinking cell fusion. Quantify the frequency of shrinking cells when *dumbfounded*, *roughest*, and *hibris* were knocked down in the *pnr* region compared to the control domain where these proteins would still be produced. Expectation: if shrinking cell fusion is driven by the same machinery as muscle cell fusion, there should be a significant reduction of shrinking cell fusion in the *pnr* domain compared to the control.
2. Visualize CAMs during shrinking cells fusion after wounding. Cross HA tagged versions of *hibris* and *dumbfounded* could be crossed into the LifeAct-RFP fly the lab has. Wound, dissect, and stain pupae with an antibody specific for the HA-tag, and secondary with GFP. Expectation: if these CAMs are facilitating fusion of shrinking cells, a puncta of GFP labeled *hibris* or *dumbfounded* would be expected to colocalize with a LifeAct protrusion from a *hibris* puncta. In contrast, a LifeAct intracellular network would be expected to colocalize with a *dumbfounded*-labeled puncta.
3. Explore the role of cell extrusion machinery in shrinking cell fusion. Reanalyze LifeActRFP and Myosin GFP (separately) post-wounding movies over the duration of cell shrinking. Expectation:

if the shrinking cells are utilizing cell extrusion machinery the actomyosin cable should be observable around the shrinking cells. Since LifeAct and Myosin II also label the cell-cell borders it should be possible to identify shrinking cells and look for the cable in its neighbors.

4. Further explore the role of extrusion machinery around shrinking cells. Knockdown *Piezo1*, *sphingosine kinase*, and the *sphingosine 1-phosphate receptor 2* within the pnr domain and compare the frequency of shrinking cells in the *pnr* and control domains. Expectation: if extrusion machinery is involved in shrinking cells fusion, inhibition of the cell shrinking machinery would reduced the frequency of shrinking cells in the *pnr* domain compared to the control.
5. Characterize what other cellular resources are pooled at the leading edge of repair. Candidates include but are not limited to myosin II, GTPases, ribosomes, plasma membrane removed from the borders between fusing cells, organelles like mitochondria networks and the ER.
6. Characterize whether the localization of GTPases in single cell wounds are conserved in syncytial cells. The localization of myosin II, Cdc42, and Rac in single cell wounds is known and fluorescently tagged versions of each of these GTPases have been generated (Abreu-Blanco et al., 2014).
7. Analyze the size and intensity of the purse string labeled with actin-GFP and myosin II-GFP comparing syncytial cells to unfused cells at the leading edge. Additionally characterize the turnover of adherens junction proteins at the leading-edge tricellular junctions. Expectation: syncytia may outcompete unfused cells due to an abundance of endocytic machinery allowing them to remodel their adherens junctions at a faster rate that unfused cells.
8. Characterize the size of filipodia-like protrusions in syncytial vs non-syncytial cells. Expectation: preliminary data using LifeActRFP indicate syncytia produce larger filipodia-like structures.
9. Elucidate the contribution of cell-cell fusion during wound repair. Eliminate endoreplication genetically with *UAS-YorkieRNAi* (Losick et al., 2013) and cell-cell fusion using our labs scanning ablation technique (Han et al., 2023). Then drive the *C. elegans* fusogens *eff-1* or *aff-1* within the *pnr* domain of the pupal notum. Expectation: if these fusogens are sufficient to induce cell-cell fusion within the pupal notum, they could be used as a rescue condition for cell-cell fusion and measuring closure rate of the fusogen vs. non-polyploid control domains would reveal the contribution of syncytia during closure.

*Conclusion:*

Through my thesis work I have used and developed tools in *Drosophila melanogaster* to robustly characterize wound induced polyploidy within the mitotically capable pupal notum. I determined wound proximal cells induce both nuclear polyploidy as well as cell-cell fusions to become syncytia. Syncytia formation allows cellular resources otherwise trapped in distal cells to rapidly relocalize to the leading edge of repair and contribute to the wound closure process. This resource pooling is likely how syncytia outcompete unfused cells at the leading edge to exclusively execute closure. My data demonstrate polyploidy is not relegated to quiescent non-mitotic tissues and highlights the importance of conducting further studies uncovering other systems which deploy wound induced polyploidy, taking note that these polyploid populations may be transient. I eagerly await future results from the Page-McCaw and Losick labs as well as the field as a whole on the underlying mechanisms of wound induced polyploidy and its roles during wound closure. By robustly characterizing cell-cell fusions we have the opportunity

to uncover novel wound care targets, improve for bio-implantation success rates, and elucidate how polyploidy becomes dysregulated in cancer leading to chemotherapy resistance and metastasis. So, furthering our understanding of wound induced polyploidy has the potential to positively influence human health, but also expand our understanding of a truly fascinating and bizarre biological process.

**Appendix A:**

*Syncytia invade the wound margin of a scanning ablation wound.*

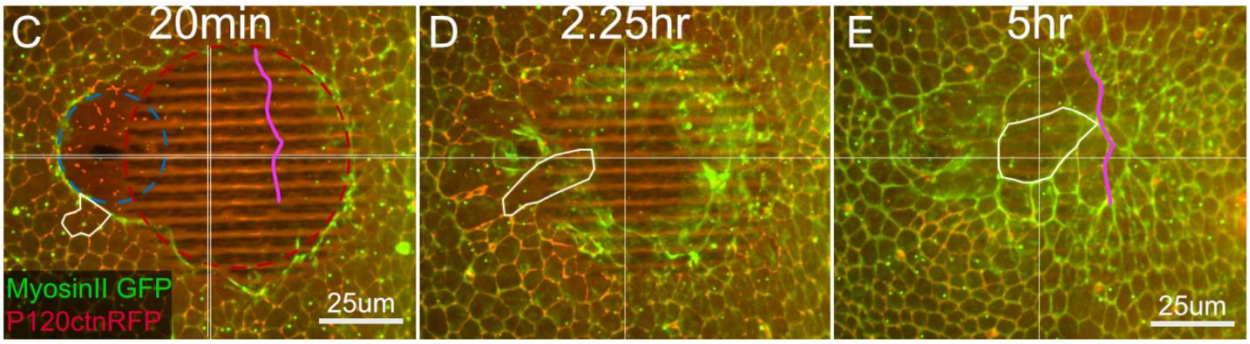


This was a very exciting set of preliminary data indicating that syncytia were more able than their unfused counterpart to close wounds. In this experiment I first generated a scanning ablation wound which lacked a large cavitation bubble and plasma membrane damage blocking syncytia formation (red circle). I then created a second wound on the left side of the original wound which did have a cavitation bubble and plasma membrane damage (blue circle) leading to the formation of syncytia on the left side of the original wound (outlined in white). The second wound naturally caused the total wound area to expand which is centered around the white crosshairs. Interestingly the syncytial side not only traversed more distance by the 2.25 hr mark, but also eventually passed the wound center and invaded the non-syncytial side of the wound eventually reaching the magenta line to re-epithelialize the tissue by 5 hr post wound. This data shows the invasive capabilities syncytia compared to unfused cells. This wounding modality could make an excellent tool for exploring the mechanistic differences between syncytial and non-syncytial cells once it is fully validated. There would also be some interesting potential experimental opportunities if it was combined with the *pnr* region split expression system, as this would provide a layer of genetic manipulation.

**Appendix B:**

*Cell-cell fusion as a mechanism to compensate for proteolytic stress.*

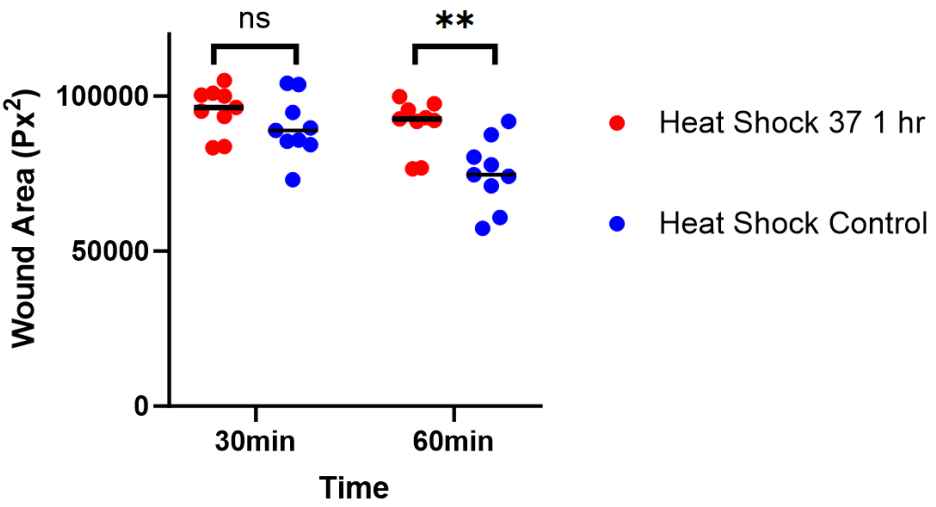


We hypothesized that after wounding the cells closer to the leading edge would be burdened with misfolded and damaged proteins. Some cells would be unsalvageable and doomed to die, however, there could be a zone where cells are on the verge of dying but could be saved if they received additional proteostatic resources from distal cells via cell-cell fusion. If this were the case, reducing the proteostatic capacity of the tissue would be expected to increase the number of cells dying and increase the wound size. To test this, I exposed 12-15 hr APF pupae to 1 hr of heat shock at 37 degrees C. This would cause an accumulation of misfolded proteins in the pupae so the proteostatic capacity would be heavily burdened before wounding. These data were a first foray into looking at whether syncytia buffer the proteolytic stress that cells at the leading-edge likely experience. I performed this experiment twice on the pupae of the cross between ♀ p120ctnRFP x ♂ ZipGFP / S-T. I had 4 pupae in each condition (heat shocked or not) on the first day, and 5 in each condition on the second. I then measured the size of the wound bed based on Myosin II signal at 30 min and 60 min after wounding and performed a student's t-test comparing the experimental and control groups with all 9 samples pooled together at each timepoint.

Heat shocked wounds were not significantly larger than control at the 30 min timepoint, however, by 60 min post wounding control wounds were significantly smaller than heat shocked wounds. Thus, these data do not rule out the hypothesis syncytia buffer proteostatic stress after wounding. Further experiments would need to be conducted to ascertain whether the impeded closure in heat shocked wounds was the result of proteostatic burden. An alternative hypothesis would be that the heat shock interfered with migration more directly. This is based off my observation that the Myosin II GFP appeared globally reduced in the heat shocked condition pre-wounding compared to the control samples. However, I did not quantify this trend and it may be due enhanced degradation of GFP under high temperatures.

**Appendix C:**

*Quantifying cell division after wounding in the pupal notum.*

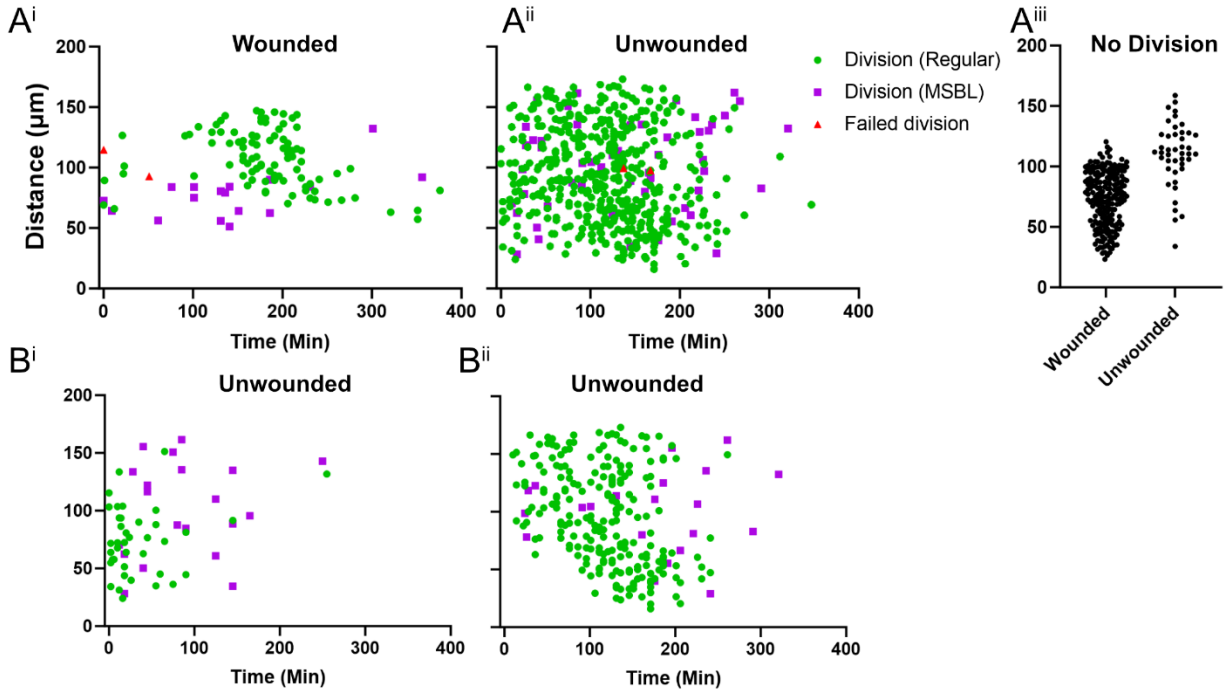


We wanted to understand how wounding affected division in the surrounding tissue as we had observed that distal cells retained their ability to divide. So, I wounded three pupae at ~12-15 hr APF and live imaged for 8 hr. Additionally I imaged three unwounded pupae within the same age range as a control dataset. These pupae had Histone2-eGFP and p120ctnRFP labeled so I could see nuclear division with GFP and assess cytokinesis based on the RFP signal. I cropped out a rectangle anterior to the wound, the width was determined by the size of the wound bed at 30 min post wounding and the height of the rectangle was determined by the where the p120 signal began to drop off due to pupal curvature (which varies sample to sample). I then annotated every nucleus within this rectangle in NIS elements and manually watched each one over the course of the 8hr long movie. If I saw the nucleus divide, I then switched to the p120 channel and assessed whether the cell underwent cytokinesis, if I observed cytokinesis that was classified as a division event. Based on the p120 signal I was also able to determine if the dividing cell was part of the mechanosensory bristle lineage due to a bright and distinct p120 puncta, this lineage undergoes endocycles so I wanted to potentially exclude those cells form analysis. Finally, I observed a very low frequency of failed divisions where the nuclei divided but cytokinesis failed. I also recorded if the nucleus did not divide.

$A^{i}$-$A^{iii}$ show aggregate data across the three wounded and unwounded samples. This was exciting as there was a striking reduction in division up to 150 min after wounding ($A^{i}$), whereas unwounded samples divided at approximately the same rate over the course of the imaging. However, when I looked at each data set individually ($B^{i}$-$B^{ii}$) there was a clear difference sample to sample in the unwounded condition indicating that the X-axis sample to sample was not consistent. Indeed a previous study had found that there are sequential waves of division within the pupal notum within the timeframe that I

had dissected and imaged my samples (Guirao et al., 2015). I believe the variance sample to sample is due to my window of selecting pupae for imaging being too tolerant. So, I had started to image the sample in $B^{i}$ close to the end of the first wave of division, whereas I started to image $B^{ii}$ at the start or shortly after the first wave of division began. I attempted to use the mechanosensory bristle lineage cells as a fiduciary mark to align the x-axes of each data set but mechanosensory bristle formation is also variable so that was unsuccessful. I expect that the trend observed in my wounded samples is real and that wounding is suppressing division within the notum after wounding, however, given the variability in the unwounded dataset that could be represented in the wounded set this data is not publication worthy. To avoid this in the future pupae would need to be dissected immediately after the pupal head is visible through the case and imaged within 30min of that developmental timepoint. All the datasets would then be properly aligned, and the wave of division would be captured across all the samples. However, I would advise that this endeavor be undertaken by someone willing to develop the tools to automate this process as manually doing this process was one of the most tedious efforts I have ever undertaken over my entire academic career.

**Appendix D:**

*Syncytial extrusion after wounding.*

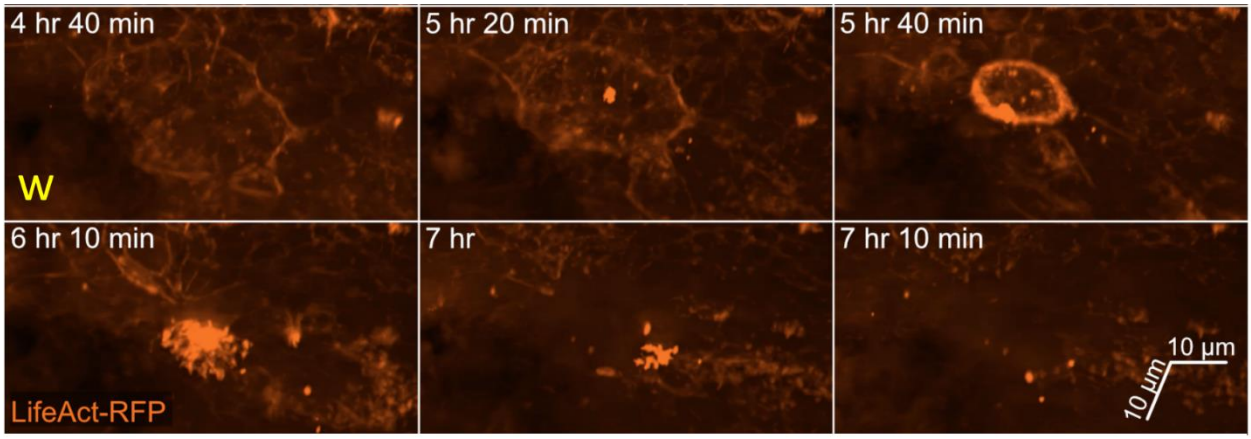


This was an interesting behavioral observation detected while imaging the actin label LifeActRFP. At approximately 5 hr and 20 min after wounding the apical domain of the syncytia began to contract and 20 min later an obvious purse string like structure was generated accompanying the syncytial extrusion out of the epithelium into the basal hemolymph. This observation has been observed with p120ctnRFP as well and is being studied by another graduate student in the lab Junmin Hua. It will be interesting to address whether this is canonical cell extrusion with the purse string being generated by surrounding neighbors. Additionally, how the syncytia is flagged for removal will be interesting to explore. Perhaps accumulation of DNA damaged with the syncytial nuclei, either from nuclear envelope rupture immediately after wounding, or the accumulation of additional damage from the toxic wound bed environment is signaling that the syncytia should be removed. This must be a finely tuned process however because if syncytia extruded too early the wound would likely not close effectively. Perhaps as the wound is drawn closed increased crowding around the leading-edge signals for the least fit syncytia to be extruded? It would also be interesting to explore the dynamics of syncytial removal and compensatory division. The data above indicates that distal nuclei maintain their capacity to divide, so syncytial extrusion could draw more distal and proliferatively capable cells in to compensate for the lost genomes. This would be exciting because it would frame syncytia as a temporary but disposable 'band-aid' that facilitates rapid wound closure and then extrude allowing for compensatory division to restore the ploidy of the tissue with diploid cells. It should be noted that most but not all syncytia are removed from the wound by 24 hr after wounding. If we can understand how the pupal notum is able to induce and then eliminate syncytia after wounding, it may shed light on how this process becomes dysregulated in the context of polyploid giant cancer cell formation.

**Appendix E:**

*HisGFP is likely not a faithful live marker of ploidy.*

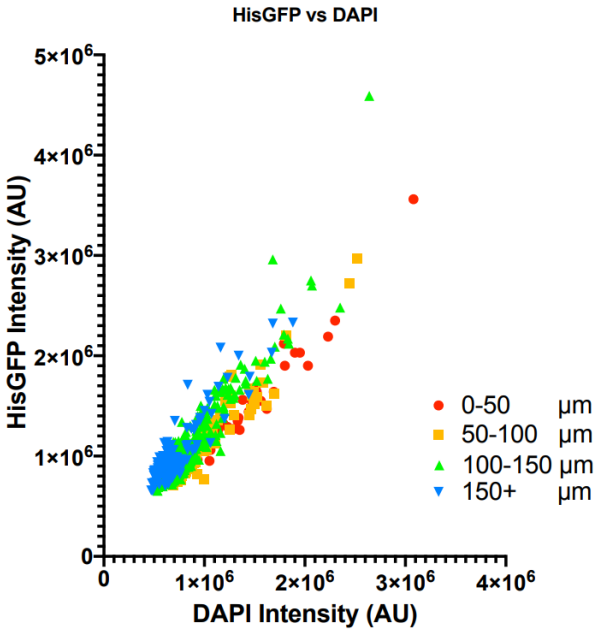


After determining that endocycling was being induced in the pupal notum by wounding I wanted to find a live marker of ploidy. So, I wounded a Histone2-eGFP fly and 3 hr post wounding dissected and stained the pupa. Nuclei were segmented in 3D and the intensity of both the DAPI and HisGFP was recorded for each nucleus as well as its distance from the wound. When we binned the nuclei according to their distance from the wound, we observed a trend where the nuclei closest to the wound had less Histone2-GFP than DAPI compared to more distal nuclei. This means that the Histone2-eGFP was under reporting the degree of ploidy following wounding and would likely not make a good live marker of ploidy. As we had recently acquired exciting data on the syncytial arm of my project I diverted attention away from these studies.

**Appendix F:**

*Syncytia produce large filopodia like structures.*

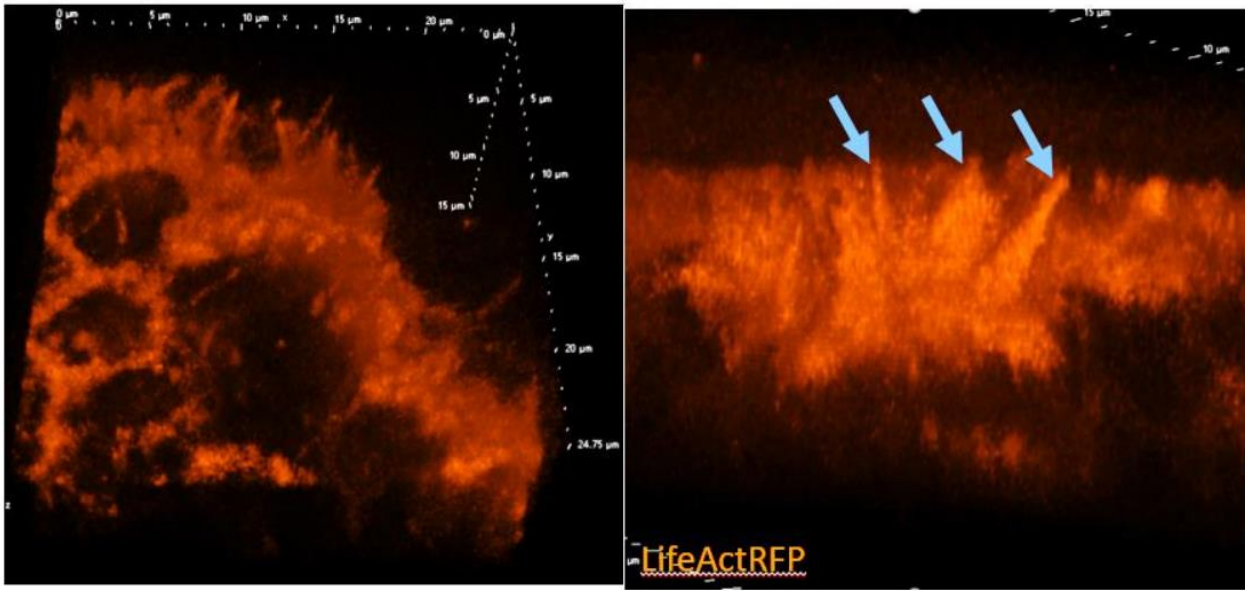


Using *UAS-LifeActRFP* being driven by *pnr>Gal4* and imaged with a 100x objective I was able to visualize filamentous actin after wounding. Here stills from a 3D visualization ~40 min after wounding revealed large filipodia like protrusions (arrows) extending from a leading-edge syncytium. The length of these syncytial protrusions is ~5 µm, which for scale is the average diameter of a diploid cell in the notum. So, syncytia are capable of generating large migratory structures which are likely to contribute to their ability to outcompete unfused neighbors at the leading edge. It would be interesting to repeat this experiment and then quantify the size of syncytial vs non-syncytial filipodia. I attempted to do this very experiment, but in an attempt to drive LifeActRFP around the entire wound I switched my driver to a pre-flipped AyGal4, which would drive LifeAct under the actin promoter. Oddly, I was not able to visualize the same large filipodia using this driver. So, if a future trainee wanted to quantify this it would be prudent to start with the *pnr>Gal4* driver. This would likely result in exciting correlational data, however, I do not believe the tools currently exist to be able to inhibit filopodia in syncytial but not unfused cells. It may be possible to engineer an optogenetic dominant negative form of Cdc42, whereby a UV pulse directed specifically at syncytia could block filipodia formation and then it would be expected that unfused neighbors would then bypass the non-migratory syncytia. That tool would likely require a PhD project to develop in and of itself though.

**Appendix G:**

*Basement membrane formation during pupal development.*

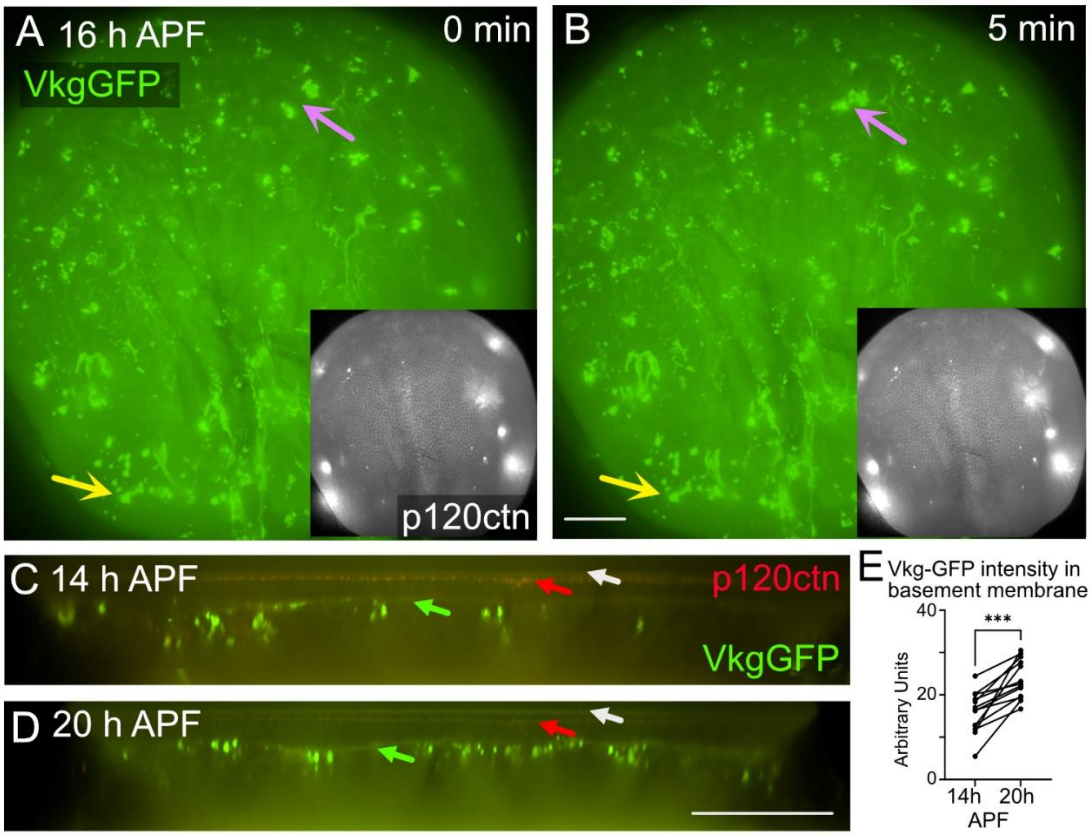


These studies were conducted by rotation students Chloe Hecht and Thomas Mehaffey in the Page-McCaw lab. Using pupae expressing p120ctnRFP and Collagen IV GFP they were able to identify mobile Collagen labeled puncta which we hypothesize are immune cells within the hemolymph. Additionally, a thin band of collagen is visible beneath the epithelial monolayer and this signal increases from 14 hr to 20 hr after puparium formation, which would be consistent with a developing basement membrane. My contribution to these experiments was in aiding with the mentorship of the rotation students and performing image processing after they had left the lab. This data opens an exciting new avenue for research as the pupa could be used to study the formation of the basement membrane in a tissue what is extremely tractable to long term imaging.

***Appendix H:***

*Final quote.*

"So long and thanks for all the fish." (Adams, 1980)

Abreu-Blanco, M. T., Verboon, J. M., Liu, R., Watts, J. J., & Parkhurst, S. M. (2012, Dec 15). Drosophila embryos close epithelial wounds using a combination of cellular protrusions and an actomyosin purse string. *J Cell Sci, 125*(Pt 24), 5984-5997. https://doi.org/10.1242/jcs.109066

Abreu-Blanco, M. T., Verboon, J. M., & Parkhurst, S. M. (2011). Cell wound repair in Drosophila occurs through three distinct phases of membrane and cytoskeletal remodeling. *Journal of Cell Biology, 193*(3), 455-464.

Abreu-Blanco, M. T., Verboon, J. M., & Parkhurst, S. M. (2014, Jan 20). Coordination of Rho family GTPase activities to orchestrate cytoskeleton responses during cell wound repair. *Curr Biol, 24*(2), 144-155. https://doi.org/10.1016/j.cub.2013.11.048

Adams, D. (1980). *The hitchhiker's guide to the galaxy*. First American edition. New York : Harmony Books, 1980. ©1979. https://search.library.wisc.edu/catalog/999547338802121

Akaishi, S., Akimoto, M., Ogawa, R., & Hyakusoku, H. (2008). The relationship between keloid growth pattern and stretching tension: visual analysis using the finite element method. *Annals of plastic surgery, 60*(4), 445-451.

Al-Maawi, S., Orlowska, A., Sader, R., James Kirkpatrick, C., & Ghanaati, S. (2017, Feb). In vivo cellular reactions to different biomaterials-Physiological and pathological aspects and their consequences. *Semin Immunol, 29*, 49-61. https://doi.org/10.1016/j.smim.2017.06.001

Al-Maawi, S., Orlowska, A., Sader, R., James Kirkpatrick, C., & Ghanaati, S. (2017, 2017/02/01/). In vivo cellular reactions to different biomaterials—Physiological and pathological aspects and their consequences. *Seminars in Immunology, 29*, 49-61. https://doi.org/https://doi.org/10.1016/j.smim.2017.06.001

Aldaz, S., Escudero, L. M., & Freeman, M. (2010). Live imaging of Drosophila imaginal disc development. *Proceedings of the National Academy of Sciences, 107*(32), 14217-14222.

Aldaz, S., Escudero, L. M., & Freeman, M. (2013). Dual role of myosin II during Drosophila imaginal disc metamorphosis. *Nature communications, 4*(1), 1761.

Altun, Z., & Hall, D. (2009). Epithelial system, hypodermis. *WormAtlas. doi, 10*.

Alvarez-Dolado, M., Pardal, R., Garcia-Verdugo, J. M., Fike, J. R., Lee, H. O., Pfeffer, K., Lois, C., Morrison, S. J., & Alvarez-Buylla, A. (2003, Oct 30). Fusion of bone-marrow-derived cells with Purkinje neurons, cardiomyocytes and hepatocytes. *Nature, 425*(6961), 968-973. https://doi.org/10.1038/nature02069

Amend, S. R., & Pienta, K. J. (2015). Ecology meets cancer biology: the cancer swamp promotes the lethal cancer phenotype. *Oncotarget, 6*(12), 9669.

Amend, S. R., Torga, G., Lin, K. C., Kostecka, L. G., de Marzo, A., Austin, R. H., & Pienta, K. J. (2019). Polyploid giant cancer cells: Unrecognized actuators of tumorigenesis, metastasis, and resistance. *The Prostate, 79*(13), 1489-1497.

Anderson, J. M., & Van Itallie, C. M. (2009, Aug). Physiology and function of the tight junction. *Cold Spring Harb Perspect Biol, 1*(2), a002584. https://doi.org/10.1101/cshperspect.a002584

Antunes, M., Pereira, T., Cordeiro, J. V., Almeida, L., & Jacinto, A. (2013). Coordinated waves of actomyosin flow and apical cell constriction immediately after wounding. *Journal of Cell Biology, 202*(2), 365-379. https://doi.org/10.1083/jcb.201211039

Arias, E. E., & Walter, J. C. (2006). PCNA functions as a molecular platform to trigger Cdt1 destruction and prevent re-replication. *Nature cell biology, 8*(1), 84-90.

Assémat, E., Bazellières, E., Pallesi-Pocachard, E., Le Bivic, A., & Massey-Harroche, D. (2008). Polarity complex proteins. *Biochimica et Biophysica Acta (BBA)-Biomembranes, 1778*(3), 614-630.

Athilingam, T., Tiwari, P., Toyama, Y., & Saunders, T. E. (2021, 2021/12/01/). Mechanics of epidermal morphogenesis in the Drosophila pupa. *Seminars in Cell & Developmental Biology, 120*, 171-180. https://doi.org/https://doi.org/10.1016/j.semcdb.2021.06.008

Au - Bailey, E. C., Au - Dehn, A. S., Au - Gjelsvik, K. J., Au - Besen-McNally, R., & Au - Losick, V. P. (2020, 2020/06/09/). A Drosophila Model to Study Wound-induced Polyploidization. *JoVE*(160), e61252. https://doi.org/doi:10.3791/61252

Au - Wang, W., & Au - Yoder, J. H. (2011, 2011/10/02/). Drosophila Pupal Abdomen Immunohistochemistry. *JoVE*(56), e3139. https://doi.org/doi:10.3791/3139

Auerbach, C. (1935). Development of the legs, wings and halteres in wild type and certain mutant strains of Drosophila melanogaster. *Annexe Thesis Digitisation Project 2017 Block 15*.

Bailey, E. C., Kobielski, S., Park, J., & Losick, V. P. (2021, Oct 1). Polyploidy in Tissue Repair and Regeneration. *Cold Spring Harb Perspect Biol, 13*(10). https://doi.org/10.1101/cshperspect.a040881

Bainbridge, P. (2013). Wound healing and the role of fibroblasts. *Journal of wound care, 22*(8).

Bainbridge, S. P., & Bownes, M. (1981, Dec). Staging the metamorphosis of Drosophila melanogaster. *J Embryol Exp Morphol, 66*, 57-80.

Baonza, A., Tur-Gracia, S., Pérez-Aguilera, M., & Estella, C. (2022). Regulation and coordination of the different DNA damage responses in Drosophila. *Front Cell Dev Biol, 10*, 993257. https://doi.org/10.3389/fcell.2022.993257

Baranwal, S., & Alahari, S. K. (2009, Jun 19). Molecular mechanisms controlling E-cadherin expression in breast cancer. *Biochem Biophys Res Commun, 384*(1), 6-11. https://doi.org/10.1016/j.bbrc.2009.04.051

Barbeck, M., Lorenz, J., Holthaus, M. G., Raetscho, N., Kubesch, A., Booms, P., Sader, R., Kirkpatrick, C. J., & Ghanaati, S. (2015). Porcine Dermis and Pericardium-Based, Non–Cross-Linked Materials Induce Multinucleated Giant Cells After Their In Vivo Implantation: A Physiological Reaction? *Journal of Oral Implantology, 41*(6), e267-e281.

Barbeck, M., Lorenz, J., Kubesch, A., Böhm, N., Booms, P., Choukroun, J., Sader, R., Kirkpatrick, C. J., & Ghanaati, S. (2015). Porcine dermis-derived collagen membranes induce implantation bed vascularization via multinucleated giant cells: a physiological reaction? *Journal of Oral Implantology, 41*(6), e238-e251.

Barbeck, M., Udeabor, S., Lorenz, J., Schlee, M., Holthaus, M. G., Raetscho, N., Choukroun, J., Sader, R., Kirkpatrick, C. J., & Ghanaati, S. (2015). High-temperature sintering of xenogeneic bone substitutes leads to increased multinucleated giant cell formation: in vivo and preliminary clinical results. *Journal of Oral Implantology, 41*(5), e212-e222.

Barbieri, J. S., Wanat, K., & Seykora, J. (2014). Skin: Basic Structure and Function. In L. M. McManus & R. N. Mitchell (Eds.), *Pathobiology of Human Disease* (pp. 1134-1144). Academic Press. https://doi.org/https://doi.org/10.1016/B978-0-12-386456-7.03501-2

Bazellières, E., Aksenova, V., Barthélémy-Requin, M., Massey-Harroche, D., & Le Bivic, A. (2018, 2018/09/01/). Role of the Crumbs proteins in ciliogenesis, cell migration and actin organization. *Seminars in Cell & Developmental Biology, 81*, 13-20. https://doi.org/https://doi.org/10.1016/j.semcdb.2017.10.018

Begnaud, S., Chen, T., Delacour, D., Mège, R. M., & Ladoux, B. (2016, Oct). Mechanics of epithelial tissues during gap closure. *Curr Opin Cell Biol, 42*, 52-62. https://doi.org/10.1016/j.ceb.2016.04.006

Bellaïche, Y., Gho, M., Kaltschmidt, J. A., Brand, A. H., & Schweisguth, F. (2001, 2001/01/01). Frizzled regulates localization of cell-fate determinants and mitotic spindle rotation during asymmetric cell division. *Nature Cell Biology, 3*(1), 50-57. https://doi.org/10.1038/35050558

Belyaeva, E. S., Zhimulev, I. F., Volkova, E. I., Alekseyenko, A. A., Moshkin, Y. M., & Koryakov, D. E. (1998). Su (UR) ES: a gene suppressing DNA underreplication in intercalary and pericentric heterochromatin of Drosophila melanogaster polytene chromosomes. *Proceedings of the National Academy of Sciences, 95*(13), 7532-7537.

Bement, W. M., Forscher, P., & Mooseker, M. S. (1993a, May). A novel cytoskeletal structure involved in purse string wound closure and cell polarity maintenance. *J Cell Biol, 121*(3), 565-578. https://doi.org/10.1083/jcb.121.3.565

Bement, W. M., Forscher, P., & Mooseker, M. S. (1993b). A novel cytoskeletal structure involved in purse string wound closure and cell polarity maintenance. *Journal of Cell Biology, 121*(3), 565-578. https://doi.org/10.1083/jcb.121.3.565

Benink, H. A., & Bement, W. M. (2005). Concentric zones of active RhoA and Cdc42 around single cell wounds. *The Journal of cell biology, 168*(3), 429-439.

Berger, S., Schäfer, G., Kesper, D. r. A., Holz, A., Eriksson, T., Palmer, R. H., Beck, L., Klämbt, C., Renkawitz-Pohl, R., & Önel, S.-F. (2008). WASP and SCAR have distinct roles in activating the Arp2/3 complex during myoblast fusion. *Journal of Cell Science, 121*(8), 1303-1313. https://doi.org/10.1242/jcs.022269

Bernardo, M. E., & Fibbe, W. E. (2013). Mesenchymal stromal cells: sensors and switchers of inflammation. *Cell stem cell, 13*(4), 392-402.

Berry, C. E., Downer, M., Jr., Morgan, A. G., Griffin, M., Liang, N. E., Kameni, L., Laufey Parker, J. B., Guo, J., Longaker, M. T., & Wan, D. C. (2023). The effects of mechanical force on fibroblast behavior in cutaneous injury. *Front Surg, 10*, 1167067. https://doi.org/10.3389/fsurg.2023.1167067

Bersell, K., Arab, S., Haring, B., & Kühn, B. (2009). Neuregulin1/ErbB4 signaling induces cardiomyocyte proliferation and repair of heart injury. *Cell, 138*(2), 257-270.

Besen-McNally, R., Gjelsvik, K. J., & Losick, V. P. (2021). Wound-induced polyploidization is dependent on Integrin-Yki signaling. *Biology Open, 10*(1), bio055996. https://doi.org/10.1242/bio.055996

Besson, C., Bernard, F., Corson, F., Rouault, H., Reynaud, E., Keder, A., Mazouni, K., & Schweisguth, F. (2015, 2015/04/20/). Planar Cell Polarity Breaks the Symmetry of PAR Protein Distribution prior to Mitosis in Drosophila Sensory Organ Precursor Cells. *Current Biology, 25*(8), 1104-1110. https://doi.org/https://doi.org/10.1016/j.cub.2015.02.073

Bharadwaj, D., & Mandal, M. (2020). Senescence in polyploid giant cancer cells: A road that leads to chemoresistance. *Cytokine & growth factor reviews, 52*, 68-75.

Bharadwaj, D., Parekh, A., Das, S., Jena, B., & Mandal, M. (2018). Polyploid giant cancer cells induce growth arrest and cytoskeletal rearrangement in breast cancer cells. *New Biotechnology, 44*, S141.

Biehler, C., Rothenberg, K. E., Jette, A., Gaude, H.-M., Fernandez-Gonzalez, R., & Laprise, P. (2021, 2021/07/02). Pak1 and PP2A antagonize aPKC function to support cortical tension induced by the Crumbs-Yurt complex. *eLife, 10*, e67999. https://doi.org/10.7554/eLife.67999

Bilder, D., Schober, M., & Perrimon, N. (2003). Integrated activity of PDZ protein complexes regulates epithelial polarity. *Nature cell biology, 5*(1), 53-58.

Bleuming, S. A., He, X. C., Kodach, L. L., Hardwick, J. C., Koopman, F. A., Ten Kate, F. J., van Deventer, S. J., Hommes, D. W., Peppelenbosch, M. P., Offerhaus, G. J., Li, L., & van den Brink, G. R. (2007, Sep 1). Bone morphogenetic protein signaling suppresses tumorigenesis at gastric epithelial transition zones in mice. *Cancer Res, 67*(17), 8149-8155. https://doi.org/10.1158/0008-5472.Can-06-4659

Boissy, P., Saltel, F., Bouniol, C., Jurdic, P., & Machuca-Gayet, I. (2002). Transcriptional activity of nuclei in multinucleated osteoclasts and its modulation by calcitonin. *Endocrinology, 143*(5), 1913-1921.

Bonche, R., Chessel, A., Boisivon, S., Smolen, P., Thérond, P., & Pizette, S. (2021). Two different sources of Perlecan cooperate for its function in the basement membrane of the Drosophila wing imaginal disc. *Developmental Dynamics, 250*(4), 542-561.

Bonello, T. T., Choi, W., & Peifer, M. (2019). Scribble and Discs-large direct initial assembly and positioning of adherens junctions during the establishment of apical-basal polarity. *Development, 146*(22). https://doi.org/10.1242/dev.180976

Böttcher, R. T., & Niehrs, C. (2005, Feb). Fibroblast growth factor signaling during early vertebrate development. *Endocr Rev, 26*(1), 63-77. https://doi.org/10.1210/er.2003-0040

Bradley, L. A., Young, A., Li, H., Billcheck, H. O., & Wolf, M. J. (2021). Loss of endogenously cycling adult cardiomyocytes worsens myocardial function. *Circulation research, 128*(2), 155-168.

Brock, J., Midwinter, K., Lewis, J., & Martin, P. (1996, Nov). Healing of incisional wounds in the embryonic chick wing bud: characterization of the actin purse-string and demonstration of a requirement for Rho activation. *J Cell Biol, 135*(4), 1097-1107. https://doi.org/10.1083/jcb.135.4.1097

Brown, J. B., Boley, N., Eisman, R., May, G. E., Stoiber, M. H., Duff, M. O., Booth, B. W., Wen, J., Park, S., Suzuki, A. M., Wan, K. H., Yu, C., Zhang, D., Carlson, J. W., Cherbas, L., Eads, B. D., Miller, D., Mockaitis, K., Roberts, J., Davis, C. A., Frise, E., Hammonds, A. S., Olson, S., Shenker, S., Sturgill,

D., Samsonova, A. A., Weiszmann, R., Robinson, G., Hernandez, J., Andrews, J., Bickel, P. J., Carninci, P., Cherbas, P., Gingeras, T. R., Hoskins, R. A., Kaufman, T. C., Lai, E. C., Oliver, B., Perrimon, N., Graveley, B. R., & Celniker, S. E. (2014, 2014/08/01). Diversity and dynamics of the Drosophila transcriptome. *Nature, 512*(7515), 393-399. https://doi.org/10.1038/nature12962

Brukman, N. G., Uygur, B., Podbilewicz, B., & Chernomordik, L. V. (2019). How cells fuse. *Journal of Cell Biology, 218*(5), 1436-1451.

Bryant, D. M., & Mostov, K. E. (2008, Nov). From cells to organs: building polarized tissue. *Nat Rev Mol Cell Biol, 9*(11), 887-901. https://doi.org/10.1038/nrm2523

Buckley, C. D., Tan, J., Anderson, K. L., Hanein, D., Volkmann, N., Weis, W. I., Nelson, W. J., & Dunn, A. R. (2014, Oct 31). Cell adhesion. The minimal cadherin-catenin complex binds to actin filaments under force. *Science, 346*(6209), 1254211. https://doi.org/10.1126/science.1254211

Burbridge, K., Holcombe, J., & Weavers, H. (2021). Metabolically active and polyploid renal tissues rely on graded cytoprotection to drive developmental and homeostatic stress resilience. *Development, 148*(8). https://doi.org/10.1242/dev.197343

Campos, I., Geiger, J. A., Santos, A. C., Carlos, V., & Jacinto, A. (2010). Genetic screen in Drosophila melanogaster uncovers a novel set of genes required for embryonic epithelial repair. *Genetics, 184*(1), 129-140.

Cao, J., Wang, J., Jackman, C. P., Cox, A. H., Trembley, M. A., Balowski, J. J., Cox, B. D., De Simone, A., Dickson, A. L., Di Talia, S., Small, E. M., Kiehart, D. P., Bursac, N., & Poss, K. D. (2017, Sep 25). Tension Creates an Endoreplication Wavefront that Leads Regeneration of Epicardial Tissue. *Dev Cell, 42*(6), 600-615.e604. https://doi.org/10.1016/j.devcel.2017.08.024

Carmichael, S. W. (2014). The tangled web of Langer's lines. *Clinical Anatomy, 27*(2), 162-168.

Carriere, R. (1969). The growth of liver parenchymal nuclei and its endocrine regulation. *International review of cytology, 25*, 201-277.

Casotti, M. C., Meira, D. D., Zetum, A. S. S., Araújo, B. C., Silva, D., Santos, E., Garcia, F. M., Paula, F., Santana, G. M., Louro, L. S., Alves, L. N. R., Braga, R. F. R., Trabach, R., Bernardes, S. S., Louro, T. E. S., Chiela, E. C. F., Lenz, G., Carvalho, E. F., & Louro, I. D. (2023, Mar 26). Computational Biology Helps Understand How Polyploid Giant Cancer Cells Drive Tumor Success. *Genes (Basel), 14*(4). https://doi.org/10.3390/genes14040801

Castro, B., Barolo, S., Bailey, A. M., & Posakony, J. W. (2005, Aug). Lateral inhibition in proneural clusters: cis-regulatory logic and default repression by Suppressor of Hairless. *Development, 132*(15), 3333-3344. https://doi.org/10.1242/dev.01920

Celton-Morizur, S., Merlen, G., Couton, D., Margall-Ducos, G., & Desdouets, C. (2009). The insulin/Akt pathway controls a specific cell division program that leads to generation of binucleated tetraploid liver cells in rodents. *The Journal of clinical investigation, 119*(7), 1880-1887.

Chakraborty, A., Peterson, N. G., King, J. S., Gross, R. T., Pla, M. M., Thennavan, A., Zhou, K. C., DeLuca, S., Bursac, N., Bowles, D. E., Wolf, M. J., & Fox, D. T. (2023, Aug 15). Conserved chamber-specific polyploidy maintains heart function in Drosophila. *Development, 150*(16). https://doi.org/10.1242/dev.201896

Chaplin, D. D. (2010, Feb). Overview of the immune response. *J Allergy Clin Immunol, 125*(2 Suppl 2), S3-23. https://doi.org/10.1016/j.jaci.2009.12.980

Chen, E. H. (2011). Invasive podosomes and myoblast fusion. *Current topics in membranes, 68*, 235-258.

Chen, I. H., Kiang, J. H., Correa, V., Lopez, M. I., Chen, P. Y., McKittrick, J., & Meyers, M. A. (2011, Jul). Armadillo armor: mechanical testing and micro-structural evaluation. *J Mech Behav Biomed Mater, 4*(5), 713-722. https://doi.org/10.1016/j.jmbbm.2010.12.013

Chernomordik, L. V., & Kozlov, M. M. (2008, 2008/07/01). Mechanics of membrane fusion. *Nature Structural & Molecular Biology, 15*(7), 675-683. https://doi.org/10.1038/nsmb.1455

Chiorazzi, M., Rui, L., Yang, Y., Ceribelli, M., Tishbi, N., Maurer, C. W., Ranuncolo, S. M., Zhao, H., Xu, W., & Chan, W.-C. C. (2013). Related F-box proteins control cell death in Caenorhabditis elegans and human lymphoma. *Proceedings of the National Academy of Sciences, 110*(10), 3943-3948.

Chiquet, M., Tunc-Civelek, V., & Sarasa-Renedo, A. (2007). Gene regulation by mechanotransduction in fibroblasts. *Applied Physiology, Nutrition, and Metabolism, 32*(5), 967-973.

Choi, E.-H., & Kim, K. P. (2019, 2019/09/01). E2F1 facilitates DNA break repair by localizing to break sites and enhancing the expression of homologous recombination factors. *Experimental & Molecular Medicine, 51*(9), 1-12. https://doi.org/10.1038/s12276-019-0307-2

Clark, A. G., Miller, A. L., Vaughan, E., Hoi-Ying, E. Y., Penkert, R., & Bement, W. M. (2009). Integration of single and multicellular wound responses. *Current Biology, 19*(16), 1389-1395.

Cochet-Escartin, O., Ranft, J., Silberzan, P., & Marcq, P. (2014, Jan 7). Border forces and friction control epithelial closure dynamics. *Biophys J, 106*(1), 65-73. https://doi.org/10.1016/j.bpj.2013.11.015

Cohen, E., Allen, S. R., Sawyer, J. K., & Fox, D. T. (2018, 2018/08/17). Fizzy-Related dictates A cell cycle switch during organ repair and tissue growth responses in the Drosophila hindgut. *eLife, 7*, e38327. https://doi.org/10.7554/eLife.38327

Cohen, M., Georgiou, M., Stevenson, N. L., Miodownik, M., & Baum, B. (2010, 2010/07/20/). Dynamic Filopodia Transmit Intermittent Delta-Notch Signaling to Drive Pattern Refinement during Lateral Inhibition. *Developmental cell, 19*(1), 78-89. https://doi.org/https://doi.org/10.1016/j.devcel.2010.06.006

Corbel, S. Y., Lee, A., Yi, L., Duenas, J., Brazelton, T. R., Blau, H. M., & Rossi, F. M. (2003, Dec). Contribution of hematopoietic stem cells to skeletal muscle. *Nat Med, 9*(12), 1528-1532. https://doi.org/10.1038/nm959

Cosolo, A., Jaiswal, J., Csordás, G., Grass, I., Uhlirova, M., & Classen, A. K. (2019, Feb 8). JNK-dependent cell cycle stalling in G2 promotes survival and senescence-like phenotypes in tissue stress. *eLife, 8*. https://doi.org/10.7554/eLife.41036

Couturier, L., Mazouni, K., Bernard, F., Besson, C., Reynaud, E., & Schweisguth, F. (2017, Dec 15). Regulation of cortical stability by RhoGEF3 in mitotic Sensory Organ Precursor cells in Drosophila. *Biol Open, 6*(12), 1851-1860. https://doi.org/10.1242/bio.026641

Couturier, L., Mazouni, K., Corson, F., & Schweisguth, F. (2019, 2019/08/02). Regulation of Notch output dynamics via specific E(spl)-HLH factors during bristle patterning in Drosophila. *Nat Commun, 10*(1), 3486. https://doi.org/10.1038/s41467-019-11477-2

Couturier, L., & Schweisguth, F. (2014). Antibody Uptake Assay and In Vivo Imaging to Study Intracellular Trafficking of Notch and Delta in Drosophila. In H. J. Bellen & S. Yamamoto (Eds.), *Notch Signaling: Methods and Protocols* (pp. 79-86). Springer New York. https://doi.org/10.1007/978-1-4939-1139-4_6

Cristo, I., Carvalho, L., Ponte, S., & Jacinto, A. (2018). Novel role for Grainy head in the regulation of cytoskeletal and junctional dynamics during epithelial repair. *Journal of Cell Science, 131*(17), jcs213595. https://doi.org/10.1242/jcs.213595

Danjo, Y., & Gipson, I. K. (1998). Actin 'purse string'filaments are anchored by E-cadherin-mediated adherens junctions at the leading edge of the epithelial wound, providing coordinated cell movement. *Journal of Cell Science, 111*(22), 3323-3332.

Davidson, L. A., Ezin, A. M., & Keller, R. (2002, Nov). Embryonic wound healing by apical contraction and ingression in Xenopus laevis. *Cell Motil Cytoskeleton, 53*(3), 163-176. https://doi.org/10.1002/cm.10070

Davies, P. S., Powell, A. E., Swain, J. R., & Wong, M. H. (2009). Inflammation and Proliferation Act Together to Mediate Intestinal Cell Fusion. *PLoS One, 4*(8), e6530. https://doi.org/10.1371/journal.pone.0006530

De Chiara, L., Conte, C., Semeraro, R., Diaz-Bulnes, P., Angelotti, M. L., Mazzinghi, B., Molli, A., Antonelli, G., Landini, S., Melica, M. E., Peired, A. J., Maggi, L., Donati, M., La Regina, G., Allinovi, M., Ravaglia, F., Guasti, D., Bani, D., Cirillo, L., Becherucci, F., Guzzi, F., Magi, A., Annunziato, F., Lasagni, L., Anders, H. J., Lazzeri, E., & Romagnani, P. (2022, Oct 4). Tubular cell polyploidy protects from lethal acute kidney injury but promotes consequent chronic kidney disease. *Nat Commun, 13*(1), 5805. https://doi.org/10.1038/s41467-022-33110-5

Dehn, A. S., Duhaime, L., Gogna, N., Nishina, P. M., Kelly, K., & Losick, V. P. (2023). Epithelial mechanics are maintained by inhibiting cell fusion with age in Drosophila. *Journal of Cell Science*. https://doi.org/10.1242/jcs.260974

Delaisse, J.-M., Andersen, T. L., Kristensen, H. B., Jensen, P. R., Andreasen, C. M., & Søe, K. (2020). Re-thinking the bone remodeling cycle mechanism and the origin of bone loss. *Bone, 141*, 115628.

Deng, W.-M., Althauser, C., & Ruohola-Baker, H. (2001). Notch-Delta signaling induces a transition from mitotic cell cycle to endocycle in Drosophila follicle cells.

Derks, W., & Bergmann, O. (2020, Feb 14). Polyploidy in Cardiomyocytes: Roadblock to Heart Regeneration? *Circ Res, 126*(4), 552-565. https://doi.org/10.1161/circresaha.119.315408

Desai, L. P., Aryal, A. M., Ceacareanu, B., Hassid, A., & Waters, C. M. (2004). RhoA and Rac1 are both required for efficient wound closure of airway epithelial cells. *American Journal of Physiology-Lung Cellular and Molecular Physiology, 287*(6), L1134-L1144.

Desmoulière, A., Chaponnier, C., & Gabbiani, G. (2005). Tissue repair, contraction, and the myofibroblast. *Wound Repair and Regeneration, 13*(1), 7-12.

Dewhurst, M. R., Ow, J. R., Zafer, G., van Hul, N. K., Wollmann, H., Bisteau, X., Brough, D., Choi, H., & Kaldis, P. (2020). Loss of hepatocyte cell division leads to liver inflammation and fibrosis. *PLoS genetics, 16*(11), e1009084.

Domínguez-Giménez, P., Brown, N. H., & Martín-Bermudo, M. a. D. (2007). Integrin-ECM interactions regulate the changes in cell shape driving the morphogenesis of the Drosophila wing epithelium. *Journal of Cell Science, 120*(6), 1061-1071. https://doi.org/10.1242/jcs.03404

Donne, R., Saroul-Aïnama, M., Cordier, P., Celton-Morizur, S., & Desdouets, C. (2020, 2020/07/01). Polyploidy in liver development, homeostasis and disease. *Nature Reviews Gastroenterology & Hepatology, 17*(7), 391-405. https://doi.org/10.1038/s41575-020-0284-x

Doron, S., & Gorbach, S. L. *Bacterial Infections: Overview*. International Encyclopedia of Public Health. 2008:273-82. doi: 10.1016/B978-012373960-5.00596-7. Epub 2008 Aug 26.

du Roure, O., Saez, A., Buguin, A., Austin, R. H., Chavrier, P., Silberzan, P., & Ladoux, B. (2005, Feb 15). Force mapping in epithelial cell migration. *Proc Natl Acad Sci U S A, 102*(7), 2390-2395. https://doi.org/10.1073/pnas.0408482102

Duan, R., & Gallagher, P. J. (2009). Dependence of myoblast fusion on a cortical actin wall and nonmuscle myosin IIA. *Developmental biology, 325*(2), 374-385.

Duan, R., Kim, J. H., Shilagardi, K., Schiffhauer, E. S., Lee, D. M., Son, S., Li, S., Thomas, C., Luo, T., & Fletcher, D. A. (2018). Spectrin is a mechanoresponsive protein shaping fusogenic synapse architecture during myoblast fusion. *Nature cell biology, 20*(6), 688-698.

Duan, Z., & Luo, Y. (2021). Targeting macrophages in cancer immunotherapy. *Signal transduction and targeted therapy, 6*(1), 127.

Duncan, A. W. (2013). Aneuploidy, polyploidy and ploidy reversal in the liver. Seminars in Cell & Developmental Biology,

Duncan, A. W., Hickey, R. D., Paulk, N. K., Culberson, A. J., Olson, S. B., Finegold, M. J., & Grompe, M. (2009). Ploidy reductions in murine fusion-derived hepatocytes. *PLoS genetics, 5*(2), e1000385.

Duncan, A. W., Newell, A. E. H., Smith, L., Wilson, E. M., Olson, S. B., Thayer, M. J., Strom, S. C., & Grompe, M. (2012). Frequent aneuploidy among normal human hepatocytes. *Gastroenterology, 142*(1), 25-28.

Duncan, A. W., Taylor, M. H., Hickey, R. D., Hanlon Newell, A. E., Lenzi, M. L., Olson, S. B., Finegold, M. J., & Grompe, M. (2010). The ploidy conveyor of mature hepatocytes as a source of genetic variation. *Nature, 467*(7316), 707-710.

Dunnill, C., Patton, T., Brennan, J., Barrett, J., Dryden, M., Cooke, J., Leaper, D., & Georgopoulos, N. T. (2017, Feb). Reactive oxygen species (ROS) and wound healing: the functional role of ROS and emerging ROS-modulating technologies for augmentation of the healing process. *Int Wound J, 14*(1), 89-96. https://doi.org/10.1111/iwj.12557

Duscher, D., Maan, Z. N., Wong, V. W., Rennert, R. C., Januszyk, M., Rodrigues, M., Hu, M., Whitmore, A. J., Whittam, A. J., & Longaker, M. T. (2014). Mechanotransduction and fibrosis. *Journal of biomechanics, 47*(9), 1997-2005.

Dushay, M. S. (2009, Aug). Insect hemolymph clotting. *Cell Mol Life Sci, 66*(16), 2643-2650. https://doi.org/10.1007/s00018-009-0036-0

Dymerska, D., & Marusiak, A. A. (2023, 2023/12/25/). Drivers of cancer metastasis – Arise early and remain present. *Biochimica et Biophysica Acta (BBA) - Reviews on Cancer*, 189060. https://doi.org/https://doi.org/10.1016/j.bbcan.2023.189060

Eaton, S., Auvinen, P., Luo, L., Jan, Y. N., & Simons, K. (1995). CDC42 and Rac1 control different actin-dependent processes in the Drosophila wing disc epithelium. *The Journal of cell biology, 131*(1), 151-164.

Ebert, L., & Pfitzer, P. (1977). Nuclear DNA of myocardial cells in the periphery of infarctions and scars. *Virchows Archiv B, 24*, 209-217.

Eckes, B., Zweers, M. C., Zhang, Z. G., Hallinger, R., Mauch, C., Aumailley, M., & Krieg, T. (2006). Mechanical tension and integrin α2β1 regulate fibroblast functions. Journal of Investigative Dermatology Symposium Proceedings,

Edgar, B. A., & Orr-Weaver, T. L. (2001, May 4). Endoreplication cell cycles: more for less. *Cell, 105*(3), 297-306. https://doi.org/10.1016/s0092-8674(01)00334-8

Eisenhoffer, G. T., Loftus, P. D., Yoshigi, M., Otsuna, H., Chien, C.-B., Morcos, P. A., & Rosenblatt, J. (2012). Crowding induces live cell extrusion to maintain homeostatic cell numbers in epithelia. *Nature, 484*(7395), 546-549.

Elbediwy, A., Vincent-Mistiaen, Z. I., Spencer-Dene, B., Stone, R. K., Boeing, S., Wculek, S. K., Cordero, J., Tan, E. H., Ridgway, R., Brunton, V. G., Sahai, E., Gerhardt, H., Behrens, A., Malanchi, I., Sansom, O. J., & Thompson, B. J. (2016). Integrin signalling regulates YAP and TAZ to control skin homeostasis. *Development, 143*(10), 1674-1687. https://doi.org/10.1242/dev.133728

Enyedi, B., & Niethammer, P. (2015, Jul). Mechanisms of epithelial wound detection. *Trends Cell Biol, 25*(7), 398-407. https://doi.org/10.1016/j.tcb.2015.02.007

Erenpreisa, J., Ivanov, A., Wheatley, S. P., Kosmacek, E. A., Ianzini, F., Anisimov, A. P., Mackey, M., Davis, P. J., Plakhins, G., & Illidge, T. M. (2008). Endopolyploidy in irradiated p53-deficient tumour cell lines: persistence of cell division activity in giant cells expressing Aurora-B kinase. *Cell biology international, 32*(9), 1044-1056.

Erenpreisa, J. A., Cragg, M. S., Fringes, B., Sharakhov, I., & Illidge, T. M. (2000). Release of mitotic descendants by giant cells from irradiated Burkitt's lymphoma cell lines. *Cell biology international, 24*(9), 635-648.

Erickson, M. R. S., Galletta, B. J., & Abmayr, S. M. (1997). Drosophila myoblast city encodes a conserved protein that is essential for myoblast fusion, dorsal closure, and cytoskeletal organization [Article]. *Journal of Cell Biology, 138*(3), 589-603. https://doi.org/10.1083/jcb.138.3.589

Farooqui, R., & Fenteany, G. (2005). Multiple rows of cells behind an epithelial wound edge extend cryptic lamellipodia to collectively drive cell-sheet movement. *Journal of Cell Science, 118*(1), 51-63. https://doi.org/10.1242/jcs.01577

Fenteany, G., Janmey, P. A., & Stossel, T. P. (2000, Jul 13). Signaling pathways and cell mechanics involved in wound closure by epithelial cell sheets. *Curr Biol, 10*(14), 831-838. https://doi.org/10.1016/s0960-9822(00)00579-0

Fernandez-Gonzalez, R., & Zallen, J. A. (2013). Wounded cells drive rapid epidermal repair in the early Drosophila embryo. *Molecular biology of the cell, 24*(20), 3227-3237.

Florian, P., Schöneberg, T., Schulzke, J., Fromm, M., & Gitter, A. (2002). Single-cell epithelial defects close rapidly by an actinomyosin purse string mechanism with functional tight junctions. *The Journal of physiology, 545*(2), 485-499.

Franco, J. J., Atieh, Y., Bryan, C. D., Kwan, K. M., & Eisenhoffer, G. T. (2019, Jul 22). Cellular crowding influences extrusion and proliferation to facilitate epithelial tissue repair. *Mol Biol Cell, 30*(16), 1890-1899. https://doi.org/10.1091/mbc.E18-05-0295

Fristrom, D. (1993). The metamorphic development of the adult epidermis. *The development of Drosophila melanogaster*.

Fu, H., Zhou, H., Yu, X., Xu, J., Zhou, J., Meng, X., Zhao, J., Zhou, Y., Chisholm, A. D., & Xu, S. (2020, Feb 26). Wounding triggers MIRO-1 dependent mitochondrial fragmentation that accelerates epidermal wound closure through oxidative signaling. *Nat Commun, 11*(1), 1050. https://doi.org/10.1038/s41467-020-14885-x

Fuchs, E. (2007, Feb 22). Scratching the surface of skin development. *Nature, 445*(7130), 834-842. https://doi.org/10.1038/nature05659

Fujisawa, Y., Shinoda, N., Chihara, T., & Miura, M. (2020, 2020/08/21/). ROS Regulate Caspase-Dependent Cell Delamination without Apoptosis in the Drosophila Pupal Notum. *iScience, 23*(8), 101413. https://doi.org/https://doi.org/10.1016/j.isci.2020.101413

Fujiwara, T., Bandi, M., Nitta, M., Ivanova, E. V., Bronson, R. T., & Pellman, D. (2005, Oct 13). Cytokinesis failure generating tetraploids promotes tumorigenesis in p53-null cells. *Nature, 437*(7061), 1043-1047. https://doi.org/10.1038/nature04217

Galko, M. J., & Krasnow, M. A. (2004). Cellular and Genetic Analysis of Wound Healing in Drosophila Larvae. *PLoS biology, 2*(8), e239. https://doi.org/10.1371/journal.pbio.0020239

Gandarillas, A. (2012). The mysterious human epidermal cell cycle, or an oncogene-induced differentiation checkpoint. *Cell cycle, 11*(24), 4507-4516.

Gandarillas, A., & Freije, A. (2014). Cycling up the epidermis: reconciling 100 years of debate. *Experimental dermatology, 23*(2), 87-91.

Gauthier, B. R., & Comaills, V. (2021, Jul 6). Nuclear Envelope Integrity in Health and Disease: Consequences on Genome Instability and Inflammation. *Int J Mol Sci, 22*(14). https://doi.org/10.3390/ijms22147281

Gavet, O., & Pines, J. (2010, Apr 20). Progressive activation of CyclinB1-Cdk1 coordinates entry to mitosis. *Dev Cell, 18*(4), 533-543. https://doi.org/10.1016/j.devcel.2010.02.013

Geddis, A. E., Fox, N. E., Tkachenko, E., & Kaushansky, K. (2007, Feb 15). Endomitotic megakaryocytes that form a bipolar spindle exhibit cleavage furrow ingression followed by furrow regression. *Cell cycle, 6*(4), 455-460. https://doi.org/10.4161/cc.6.4.3836

Geisbrecht, E. R., Haralalka, S., Swanson, S. K., Florens, L., Washburn, M. P., & Abmayr, S. M. (2008, 2008/02/01/). Drosophila ELMO/CED-12 interacts with Myoblast city to direct myoblast fusion and ommatidial organization. *Developmental biology, 314*(1), 137-149. https://doi.org/https://doi.org/10.1016/j.ydbio.2007.11.022

Gentric, G., & Desdouets, C. (2014). Polyploidization in liver tissue. *The American journal of pathology, 184*(2), 322-331.

Gentric, G., Maillet, V., Paradis, V., Couton, D., L'Hermitte, A., Panasyuk, G., Fromenty, B., Celton-Morizur, S., & Desdouets, C. (2015, Mar 2). Oxidative stress promotes pathologic polyploidization in nonalcoholic fatty liver disease. *J Clin Invest, 125*(3), 981-992. https://doi.org/10.1172/jci73957

Ghanaati, S., Barbeck, M., Lorenz, J., Stuebinger, S., Seitz, O., Landes, C., Kovács, A. F., Kirkpatrick, C. J., & Sader, R. A. (2013). Synthetic bone substitute material comparable with xenogeneic material for bone tissue regeneration in oral cancer patients: First and preliminary histological, histomorphometrical and clinical results. *Annals of maxillofacial surgery, 3*(2), 126.

Ghosh, T. S., Shanahan, F., & O'Toole, P. W. (2022, Sep). The gut microbiome as a modulator of healthy ageing. *Nat Rev Gastroenterol Hepatol, 19*(9), 565-584. https://doi.org/10.1038/s41575-022-00605-x

Gildor, B., Massarwa, R. a., Shilo, B. Z., & Schejter, E. D. (2009, 2009/09/01). The SCAR and WASp nucleation‐promoting factors act sequentially to mediate Drosophila myoblast fusion. *EMBO reports, 10*(9), 1043-1050-1050. https://doi.org/https://doi.org/10.1038/embor.2009.129

Gjelsvik, K., Besen-McNally, R., & Losick, V. (2019). Solving the polyploid mystery in health and disease. *Trends in Genetics, 35*(1), 6-14.

Goldstein, B., & Macara, I. G. (2007). The PAR proteins: fundamental players in animal cell polarization. *Developmental cell, 13*(5), 609-622.

González-Rosa, J. M., Sharpe, M., Field, D., Soonpaa, M. H., Field, L. J., Burns, C. E., & Burns, C. G. (2018, Feb 26). Myocardial Polyploidization Creates a Barrier to Heart Regeneration in Zebrafish. *Dev Cell, 44*(4), 433-446.e437. https://doi.org/10.1016/j.devcel.2018.01.021

Gordon, W. R., Zimmerman, B., He, L., Miles, L. J., Huang, J., Tiyanont, K., McArthur, D. G., Aster, J. C., Perrimon, N., & Loparo, J. J. (2015). Mechanical allostery: evidence for a force requirement in the proteolytic activation of Notch. *Developmental cell, 33*(6), 729-736.

Grendler, J., Lowgren, S., Mills, M., & Losick, V. P. (2019, Aug 2). Wound-induced polyploidization is driven by Myc and supports tissue repair in the presence of DNA damage. *Development, 146*(15). https://doi.org/10.1242/dev.173005

Grinnell, F., & Petroll, W. M. (2010). Cell motility and mechanics in three-dimensional collagen matrices. *Annual review of cell and developmental biology, 26*, 335-361.

Gu, Y., Forostyan, T., Sabbadini, R., & Rosenblatt, J. (2011). Epithelial cell extrusion requires the sphingosine-1-phosphate receptor 2 pathway. *Journal of Cell Biology, 193*(4), 667-676.

Gudipaty, S. A., Lindblom, J., Loftus, P. D., Redd, M. J., Edes, K., Davey, C., Krishnegowda, V., & Rosenblatt, J. (2017). Mechanical stretch triggers rapid epithelial cell division through Piezo1. *Nature, 543*(7643), 118-121.

Guidotti, J.-E., Brégerie, O., Robert, A., Debey, P., Brechot, C., & Desdouets, C. (2003). Liver cell polyploidization: a pivotal role for binuclear hepatocytes. *Journal of Biological Chemistry, 278*(21), 19095-19101.

Guirao, B., Rigaud, S. U., Bosveld, F., Bailles, A., López-Gay, J., Ishihara, S., Sugimura, K., Graner, F., & Bellaïche, Y. (2015, 2015/12/12). Unified quantitative characterization of epithelial tissue development. *eLife, 4*, e08519. https://doi.org/10.7554/eLife.08519

[Record #150 is using a reference type undefined in this output style.]

Hakeda-Suzuki, S., Ng, J., Tzu, J., Dietzl, G., Sun, Y., Harms, M., Nardine, T., Luo, L., & Dickson, B. J. (2002). Rac function and regulation during Drosophila development [Letter]. *Nature, 416*(6879), 438-442. https://doi.org/10.1038/416438a

Halaoui, R., & McCaffrey, L. (2015, 2015/02/01). Rewiring cell polarity signaling in cancer. *Oncogene, 34*(8), 939-950. https://doi.org/10.1038/onc.2014.59

Han, I., Nassar, L. S., Page-McCaw, A., & Hutson, M. S. (2023, Jun 3). After wounding, a G-protein coupled receptor restores tension to epithelial cells in a dynamic inward-traveling wave. *bioRxiv*. https://doi.org/10.1101/2023.05.31.543122

Hao, Y., Zhou, Y., Yu, Y., Zheng, M., Weng, K., Kou, Z., Liang, J., Zhang, Q., Tang, X., Xu, P., Link, B. A., Yao, K., & Zou, J. (2020). Interplay of MPP5a with Rab11 synergistically builds epithelial apical polarity and zonula adherens. *Development, 147*(22). https://doi.org/10.1242/dev.184457

Hartenstein, V., & Posakony, J. W. (1989). Development of adult sensilla on the wing and notum of Drosophila melanogaster. *Development, 107*(2), 389-405. https://doi.org/10.1242/dev.107.2.389

Hartsock, A., & Nelson, W. J. (2008). Adherens and tight junctions: structure, function and connections to the actin cytoskeleton. *Biochimica et Biophysica Acta (BBA)-Biomembranes, 1778*(3), 660-669.

Hassel, C., Zhang, B., Dixon, M., & Calvi, B. R. (2014, Jan). Induction of endocycles represses apoptosis independently of differentiation and predisposes cells to genome instability. *Development, 141*(1), 112-123. https://doi.org/10.1242/dev.098871

Havens, C. G., & Walter, J. C. (2009). Docking of a specialized PIP Box onto chromatin-bound PCNA creates a degron for the ubiquitin ligase CRL4Cdt2. *Molecular cell, 35*(1), 93-104.

Hesse, M., Raulf, A., Pilz, G.-A., Haberlandt, C., Klein, A. M., Jabs, R., Zaehres, H., Fügemann, C. J., Zimmermann, K., & Trebicka, J. (2012). Direct visualization of cell division using high-resolution imaging of M-phase of the cell cycle. *Nature communications, 3*(1), 1076.

Hillman, R., & Lesnik, L. H. (1970). Cuticle formation in the embryo of Drosophila melanogaster. *Journal of Morphology, 131*(4), 383-395. https://doi.org/https://doi.org/10.1002/jmor.1051310403

Horn, A., Raavicharla, S., Shah, S., Cox, D., & Jaiswal, J. K. (2020, May 4). Mitochondrial fragmentation enables localized signaling required for cell repair. *J Cell Biol, 219*(5). https://doi.org/10.1083/jcb.201909154

Hsu, S. h., Delgado, E. R., Otero, P. A., Teng, K. y., Kutay, H., Meehan, K. M., Moroney, J. B., Monga, J. K., Hand, N. J., & Friedman, J. R. (2016). MicroRNA-122 regulates polyploidization in the murine liver. *Hepatology, 64*(2), 599-615.

Hu, M. S., Borrelli, M. R., Hong, W. X., Malhotra, S., Cheung, A. T. M., Ransom, R. C., Rennert, R. C., Morrison, S. D., Lorenz, H. P., & Longaker, M. T. (2018, Jan 2). Embryonic skin development and repair. *Organogenesis, 14*(1), 46-63. https://doi.org/10.1080/15476278.2017.1421882

Hynes, R. O. (2002, 2002/09/20/). Integrins: Bidirectional, Allosteric Signaling Machines. *Cell, 110*(6), 673-687. https://doi.org/https://doi.org/10.1016/S0092-8674(02)00971-6

Hynes, R. O., & Zhao, Q. (2000). The evolution of cell adhesion. *The Journal of cell biology, 150*(2), F89-F96.

Illidge, T. M., Cragg, M. S., Fringes, B., Olive, P., & Erenpreisa, J. A. (2000). Polyploid giant cells provide a survival mechanism for p53 mutant cells after DNA damage. *Cell Biol Int, 24*(9), 621-633. https://doi.org/10.1006/cbir.2000.0557

Iosilevskii, Y., & Podbilewicz, B. (2021). Chapter Seven - Programmed cell fusion in development and homeostasis. In S. Jarriault & B. Podbilewicz (Eds.), *Current Topics in Developmental Biology* (Vol. 144, pp. 215-244). Academic Press. https://doi.org/https://doi.org/10.1016/bs.ctdb.2020.12.013

James T. O'Connor, E. K. S., M. Shane Hutson, Andrea Page-McCaw. (In revision at STAR Protocols). Mounting Drosophila pupae for laser ablation and live imaging of the dorsal thorax [Review ]. *STAR Protocols*.

Jiao, Y., Yu, Y., Zheng, M., Yan, M., Wang, J., Zhang, Y., & Zhang, S. (2024, Feb). Dormant cancer cells and polyploid giant cancer cells: The roots of cancer recurrence and metastasis. *Clin Transl Med, 14*(2), e1567. https://doi.org/10.1002/ctm2.1567

Jin, P., Duan, R., Luo, F., Zhang, G., Hong, Sabrina N., & Chen, Elizabeth H. (2011, 2011/05/17/). Competition between Blown Fuse and WASP for WIP Binding Regulates the Dynamics of WASP-Dependent Actin Polymerization In Vivo. *Developmental cell, 20*(5), 623-638. https://doi.org/https://doi.org/10.1016/j.devcel.2011.04.007

Johansson, C. B., Youssef, S., Koleckar, K., Holbrook, C., Doyonnas, R., Corbel, S. Y., Steinman, L., Rossi, F. M., & Blau, H. M. (2008). Extensive fusion of haematopoietic cells with Purkinje neurons in response to chronic inflammation. *Nature cell biology, 10*(5), 575-583.

Jopling, C., Sleep, E., Raya, M., Martí, M., Raya, A., & Belmonte, J. C. I. (2010). Zebrafish heart regeneration occurs by cardiomyocyte dedifferentiation and proliferation. *Nature, 464*(7288), 606-609.

Kadi, A., Fawzi-Grancher, S., Lakisic, G., Stoltz, J., & Muller, S. (2008). Effect of cyclic stretching and TGF-β on the SMAD pathway in fibroblasts. *Bio-medical Materials and Engineering, 18*(s1), 77-86.

Kaipa, B. R., Shao, H., Schäfer, G., Trinkewitz, T., Groth, V., Liu, J., Beck, L., Bogdan, S., Abmayr, S. M., & Önel, S.-F. (2013). Dock mediates Scar- and WASp-dependent actin polymerization through interaction with cell adhesion molecules in founder cells and fusion-competent myoblasts. *Journal of Cell Science, 126*(1), 360-372. https://doi.org/10.1242/jcs.113860

Kamran, Z., Zellner, K., Kyriazes, H., Kraus, C. M., Reynier, J. B., & Malamy, J. E. (2017, Dec 19). In vivo imaging of epithelial wound healing in the cnidarian Clytia hemisphaerica demonstrates early evolution of purse string and cell crawling closure mechanisms. *BMC Dev Biol, 17*(1), 17. https://doi.org/10.1186/s12861-017-0160-2

Kashgari, G., Huang, Y., & Andersen, B. (2018). Embryonic Development of the Epidermis. In *Reference Module in Biomedical Sciences*. Elsevier. https://doi.org/https://doi.org/10.1016/B978-0-12-801238-3.65811-7

Kasperski, A. (2022). Life entrapped in a network of atavistic attractors: How to find a rescue. *International Journal of Molecular Sciences, 23*(7), 4017.

Kawamori, A., Shimaji, K., & Yamaguchi, M. (2012). Dynamics of endoreplication during Drosophila posterior scutellar macrochaete development. *PLoS One, 7*(6), e38714-e38714. https://doi.org/10.1371/journal.pone.0038714

Kaznowski, C. E., Schneiderman, H. A., & Bryant, P. J. (1985, 1985/01/01/). Cuticle secretion during larval growth in Drosophila melanogaster. *Journal of Insect Physiology, 31*(10), 801-813. https://doi.org/https://doi.org/10.1016/0022-1910(85)90073-3

Khandelwal, P., Abraham, S. N., & Apodaca, G. (2009, Dec). Cell biology and physiology of the uroepithelium. *Am J Physiol Renal Physiol, 297*(6), F1477-1501. https://doi.org/10.1152/ajprenal.00327.2009

Kiehart, D. P., Galbraith, C. G., Edwards, K. A., Rickoll, W. L., & Montague, R. A. (2000, Apr 17). Multiple forces contribute to cell sheet morphogenesis for dorsal closure in Drosophila. *J Cell Biol, 149*(2), 471-490. https://doi.org/10.1083/jcb.149.2.471

Kiehart, D. P., Tokutake, Y., Chang, M.-S., Hutson, M. S., Wiemann, J., Peralta, X. G., Toyama, Y., Wells, A. R., Rodriguez, A., & Edwards, G. S. (2006). Chapter 9 - Ultraviolet Laser Microbeam for Dissection

of Drosophila Embryos. In J. E. Celis (Ed.), *Cell Biology (Third Edition)* (pp. 87-103). Academic Press. https://doi.org/https://doi.org/10.1016/B978-012164730-8/50137-4

Kikuchi, K. (2014). Advances in understanding the mechanism of zebrafish heart regeneration. *Stem cell research, 13*(3), 542-555.

Kikuchi, K., Holdway, J. E., Werdich, A. A., Anderson, R. M., Fang, Y., Egnaczyk, G. F., Evans, T., MacRae, C. A., Stainier, D. Y., & Poss, K. D. (2010). Primary contribution to zebrafish heart regeneration by gata4+ cardiomyocytes. *Nature, 464*(7288), 601-605.

Kim, J. H., & Chen, E. H. (2019, Sep 16). The fusogenic synapse at a glance. *J Cell Sci, 132*(18). https://doi.org/10.1242/jcs.213124

Kim, J. H., Jin, P., Duan, R., & Chen, E. H. (2015, Jun). Mechanisms of myoblast fusion during muscle development. *Curr Opin Genet Dev, 32*, 162-170. https://doi.org/10.1016/j.gde.2015.03.006

Kim, J. H., Jin, P., Duan, R., & Chen, E. H. (2015). Mechanisms of myoblast fusion during muscle development. *Current opinion in genetics & development, 32*, 162-170. https://doi.org/10.1016/j.gde.2015.03.006

Kim, J. H., Ren, Y., Ng, W. P., Li, S., Son, S., Kee, Y.-S., Zhang, S., Zhang, G., Fletcher, D. A., & Robinson, D. N. (2015). Mechanical tension drives cell membrane fusion. *Developmental cell, 32*(5), 561-573.

Kim, J. H., Ren, Y., Ng, W. P., Li, S., Son, S., Kee, Y. S., Zhang, S., Zhang, G., Fletcher, D. A., Robinson, D. N., & Chen, E. H. (2015, Mar 9). Mechanical tension drives cell membrane fusion. *Dev Cell, 32*(5), 561-573. https://doi.org/10.1016/j.devcel.2015.01.005

Kim, N.-G., & Gumbiner, B. M. (2015). Adhesion to fibronectin regulates Hippo signaling via the FAK–Src–PI3K pathway. *Journal of Cell Biology, 210*(3), 503-515. https://doi.org/10.1083/jcb.201501025

Kim, S., Shilagardi, K., Zhang, S., Hong, S. N., Sens, K. L., Bo, J., Gonzalez, G. A., & Chen, E. H. (2007, 2007/04/01/). A Critical Function for the Actin Cytoskeleton in Targeted Exocytosis of Prefusion Vesicles during Myoblast Fusion. *Developmental cell, 12*(4), 571-586. https://doi.org/https://doi.org/10.1016/j.devcel.2007.02.019

Klarlund, J. K. (2012). Dual modes of motility at the leading edge of migrating epithelial cell sheets. *Proceedings of the National Academy of Sciences, 109*(39), 15799-15804. https://doi.org/doi:10.1073/pnas.1210992109

Klinovska, K., Sebkova, N., & Dvorakova-Hortova, K. (2014, Jun 13). Sperm-egg fusion: a molecular enigma of mammalian reproduction. *Int J Mol Sci, 15*(6), 10652-10668. https://doi.org/10.3390/ijms150610652

Klunder, L. J., Faber, K. N., Dijkstra, G., & van, I. S. C. D. (2017, Jul 5). Mechanisms of Cell Polarity-Controlled Epithelial Homeostasis and Immunity in the Intestine. *Cold Spring Harb Perspect Biol, 9*(7). https://doi.org/10.1101/cshperspect.a027888

Kollmannsberger, P., Bidan, C. M., Dunlop, J. W. C., Fratzl, P., & Vogel, V. (2018). Tensile forces drive a reversible fibroblast-to-myofibroblast transition during tissue growth in engineered clefts. *Science Advances, 4*(1), eaao4881. https://doi.org/doi:10.1126/sciadv.aao4881

Koto, A., Kuranaga, E., & Miura, M. (2011, 2011/02/22/). Apoptosis Ensures Spacing Pattern Formation of Drosophila Sensory Organs. *Current Biology, 21*(4), 278-287. https://doi.org/https://doi.org/10.1016/j.cub.2011.01.015

Kovbasnjuk, O., Leader, J. P., Weinstein, A. M., & Spring, K. R. (1998). Water does not flow across the tight junctions of MDCK cell epithelium. *Proceedings of the National Academy of Sciences, 95*(11), 6526-6530. https://doi.org/doi:10.1073/pnas.95.11.6526

Kudryavtsev, B., Kudryavtseva, M., Sakuta, G., & Stein, G. (1993). Human hepatocyte polyploidization kinetics in the course of life cycle. *Virchows Archiv B, 64*, 387-393.

Kuri, P., Rice, G., & Rompolas, P. (2019). Chapter Three - Molecular aspects governing epidermal stem cell niches. In M. Perez-Moreno (Ed.), *Advances in Stem Cells and their Niches* (Vol. 3, pp. 73-113). Elsevier. https://doi.org/https://doi.org/10.1016/bs.asn.2019.05.001

Lai, S. L., & Lee, T. (2006, May). Genetic mosaic with dual binary transcriptional systems in Drosophila. *Nat Neurosci, 9*(5), 703-709. https://doi.org/10.1038/nn1681

Landén, N. X., Li, D., & Ståhle, M. (2016). Transition from inflammation to proliferation: a critical step during wound healing. *Cellular and Molecular Life Sciences, 73*, 3861-3885.

Lang, L., & Schnittger, A. (2020, Apr). Endoreplication - a means to an end in cell growth and stress response. *Curr Opin Plant Biol, 54*, 85-92. https://doi.org/10.1016/j.pbi.2020.02.006

Laprise, P., Beronja, S., Silva-Gagliardi, N. F., Pellikka, M., Jensen, A. M., McGlade, C. J., & Tepass, U. (2006). The FERM protein Yurt is a negative regulatory component of the Crumbs complex that controls epithelial polarity and apical membrane size. *Developmental cell, 11*(3), 363-374.

Laprise, P., Lau, K. M., Harris, K. P., Silva-Gagliardi, N. F., Paul, S. M., Beronja, S., Beitel, G. J., McGlade, C. J., & Tepass, U. (2009). Yurt, Coracle, Neurexin IV and the Na+, K+-ATPase form a novel group of epithelial polarity proteins. *Nature, 459*(7250), 1141-1145.

Lattner, J., Leng, W., Knust, E., Brankatschk, M., & Flores-Benitez, D. (2019, 2019/11/07). Crumbs organizes the transport machinery by regulating apical levels of PI(4,5)P2 in Drosophila. *eLife, 8*, e50900. https://doi.org/10.7554/eLife.50900

Lazzeri, E., Angelotti, M. L., Peired, A., Conte, C., Marschner, J. A., Maggi, L., Mazzinghi, B., Lombardi, D., Melica, M. E., & Nardi, S. (2018). Endocycle-related tubular cell hypertrophy and progenitor proliferation recover renal function after acute kidney injury. *Nature communications, 9*(1), 1344.

Leach, J. P., & Morrisey, E. E. (2018, December 1, 2018). Repairing the lungs one breath at a time: How dedicated or facultative are you? *Genes & development, 32*(23-24), 1461-1471. https://doi.org/10.1101/gad.319418.118

Lee, D. M., & Chen, E. H. (2019, Dec 3). Drosophila Myoblast Fusion: Invasion and Resistance for the Ultimate Union. *Annu Rev Genet, 53*, 67-91. https://doi.org/10.1146/annurev-genet-120116-024603

Lee, H. O., Davidson, J. M., & Duronio, R. J. (2009, Nov 1). Endoreplication: polyploidy with purpose. *Genes Dev, 23*(21), 2461-2477. https://doi.org/10.1101/gad.1829209

Lehka, L., & Rędowicz, M. J. (2020, 2020/08/01/). Mechanisms regulating myoblast fusion: A multilevel interplay. *Seminars in Cell & Developmental Biology, 104*, 81-92. https://doi.org/https://doi.org/10.1016/j.semcdb.2020.02.004

Leikam, C., Hufnagel, A., Otto, C., Murphy, D., Mühling, B., Kneitz, S., Nanda, I., Schmid, M., Wagner, T., & Haferkamp, S. (2015). In vitro evidence for senescent multinucleated melanocytes as a source for tumor-initiating cells. *Cell death & disease, 6*(4), e1711-e1711.

Leroy, H., Han, M., Woottum, M., Bracq, L., Bouchet, J., Xie, M., & Benichou, S. (2020, Dec 17). Virus-Mediated Cell-Cell Fusion. *Int J Mol Sci, 21*(24). https://doi.org/10.3390/ijms21249644

Levayer, R., Dupont, C., & Moreno, E. (2016). Tissue crowding induces caspase-dependent competition for space. *Current Biology, 26*(5), 670-677.

Levayer, R., Dupont, C., & Moreno, E. (2016, Mar 7). Tissue Crowding Induces Caspase-Dependent Competition for Space. *Curr Biol, 26*(5), 670-677. https://doi.org/10.1016/j.cub.2015.12.072

Lhoták, Š., Elavathil, L. J., Vukmirović-Popović, S., Duivenvoorden, W. C., Tozer, R. G., & Singh, G. (2000). Immunolocalization of matrix metalloproteinases and their inhibitors in clinical specimens of bone metastasis from breast carcinoma. *Clinical & Experimental Metastasis, 18*, 463-470.

Li, H., Janssens, J., De Waegeneer, M., Kolluru, S. S., Davie, K., Gardeux, V., Saelens, W., David, F. P. A., Brbić, M., Spanier, K., Leskovec, J., McLaughlin, C. N., Xie, Q., Jones, R. C., Brueckner, K., Shim, J., Tattikota, S. G., Schnorrer, F., Rust, K., Nystul, T. G., Carvalho-Santos, Z., Ribeiro, C., Pal, S., Mahadevaraju, S., Przytycka, T. M., Allen, A. M., Goodwin, S. F., Berry, C. W., Fuller, M. T., White-Cooper, H., Matunis, E. L., DiNardo, S., Galenza, A., O'Brien, L. E., Dow, J. A. T., Consortium§, F., Jasper, H., Oliver, B., Perrimon, N., Deplancke, B., Quake, S. R., Luo, L., Aerts, S., Agarwal, D., Ahmed-Braimah, Y., Arbeitman, M., Ariss, M. M., Augsburger, J., Ayush, K., Baker, C. C., Banisch, T., Birker, K., Bodmer, R., Bolival, B., Brantley, S. E., Brill, J. A., Brown, N. C., Buehner, N. A., Cai, X. T., Cardoso-Figueiredo, R., Casares, F., Chang, A., Clandinin, T. R., Crasta, S., Desplan, C., Detweiler, A. M., Dhakan, D. B., Donà, E., Engert, S., Floc'hlay, S., George, N., González-Segarra, A. J., Groves, A. K., Gumbin, S., Guo, Y., Harris, D. E., Heifetz, Y., Holtz, S. L., Horns, F., Hudry, B., Hung, R.-J., Jan, Y. N., Jaszczak, J. S., Jefferis, G. S. X. E., Karkanias, J., Karr, T. L., Katheder, N. S., Kezos, J., Kim, A. A., Kim, S. K., Kockel, L., Konstantinides, N., Kornberg, T. B., Krause, H. M., Labott, A. T., Laturney, M., Lehmann, R., Leinwand, S., Li, J., Li, J. S. S., Li, K., Li, K., Li, L., Li, T., Litovchenko, M., Liu, H.-H., Liu, Y., Lu, T.-C., Manning, J., Mase, A., Matera-Vatnick, M., Matias, N. R., McDonough-Goldstein, C. E., McGeever, A., McLachlan, A. D., Moreno-Roman, P., Neff, N., Neville, M., Ngo, S., Nielsen, T., O'Brien, C. E., Osumi-Sutherland, D., Özel, M. N., Papatheodorou, I., Petkovic, M., Pilgrim, C., Pisco, A. O., Reisenman, C., Sanders, E. N., dos Santos, G., Scott, K., Sherlekar, A., Shiu, P., Sims, D., Sit, R. V., Slaidina, M., Smith, H. E., Sterne, G., Su, Y.-H., Sutton, D., Tamayo, M., Tan, M., Tastekin, I., Treiber, C., Vacek, D., Vogler, G., Waddell, S., Wang, W., Wilson, R. I., Wolfner, M. F., Wong, Y.-C. E., Xie, A., Xu, J., Yamamoto, S., Yan, J., Yao, Z., Yoda, K., Zhu, R., & Zinzen, R. P. (2022). Fly Cell Atlas: A single-nucleus transcriptomic atlas of the adult fruit fly. *Science, 375*(6584), eabk2432. https://doi.org/doi:10.1126/science.abk2432

Li, J., Zhang, Y. P., & Kirsner, R. S. (2003). Angiogenesis in wound repair: angiogenic growth factors and the extracellular matrix. *Microscopy research and technique, 60*(1), 107-114.

Lin, W. C., Lin, F. T., & Nevins, J. R. (2001, Jul 15). Selective induction of E2F1 in response to DNA damage, mediated by ATM-dependent phosphorylation. *Genes Dev, 15*(14), 1833-1844.

Lin, Y.-H., Zhang, S., Zhu, M., Lu, T., Chen, K., Wen, Z., Wang, S., Xiao, G., Luo, D., & Jia, Y. (2020). Mice with increased numbers of polyploid hepatocytes maintain regenerative capacity but develop fewer hepatocellular carcinomas following chronic liver injury. *Gastroenterology, 158*(6), 1698-1712. e1614.

Lindström, A., Midtbö, K., Arnesson, L. G., Garvin, S., & Shabo, I. (2017, Aug 1). Fusion between M2-macrophages and cancer cells results in a subpopulation of radioresistant cells with enhanced DNA-repair capacity. *Oncotarget, 8*(31), 51370-51386. https://doi.org/10.18632/oncotarget.17986

Liu, J. (2020, Feb). The "life code": A theory that unifies the human life cycle and the origin of human tumors. *Semin Cancer Biol, 60*, 380-397. https://doi.org/10.1016/j.semcancer.2019.09.005

Liu, Z., Yue, S., Chen, X., Kubin, T., & Braun, T. (2010). Regulation of cardiomyocyte polyploidy and multinucleation by CyclinG1. *Circulation research, 106*(9), 1498-1506.

Loncar, D., & Singer, S. J. (1995, Mar 14). Cell membrane formation during the cellularization of the syncytial blastoderm of Drosophila. *Proc Natl Acad Sci U S A, 92*(6), 2199-2203. https://doi.org/10.1073/pnas.92.6.2199

López-Schier, H., & Johnston, D. S. (2001). Delta signaling from the germ line controls the proliferation and differentiation of the somatic follicle cells during Drosophila oogenesis. *Genes & development, 15*(11), 1393-1405.

Lorenz, J., Kubesch, A., Korzinskas, T., Barbeck, M., Landes, C., Sader, R. A., Kirkpatrick, C. J., & Ghanaati, S. (2015). TRAP-positive multinucleated giant cells are foreign body giant cells rather than osteoclasts: results from a split-mouth study in humans. *Journal of Oral Implantology, 41*(6), e257-e266.

Losick, V. P. (2016). Wound-Induced Polyploidy Is Required for Tissue Repair. *Advances in wound care, 5*(6), 271-278. https://doi.org/10.1089/wound.2014.0545

Losick, V. P., Fox, D. T., & Spradling, A. C. (2013, Nov 18). Polyploidization and cell fusion contribute to wound healing in the adult Drosophila epithelium. *Curr Biol, 23*(22), 2224-2232. https://doi.org/10.1016/j.cub.2013.09.029

Losick, V. P., Jun, A. S., & Spradling, A. C. (2016). Wound-Induced Polyploidization: Regulation by Hippo and JNK Signaling and Conservation in Mammals. *PLOS ONE, 11*(3), e0151251. https://doi.org/10.1371/journal.pone.0151251

Loubéry, S., Seum, C., Moraleda, A., Daeden, A., Fürthauer, M., & Gonzalez-Gaitan, M. (2014). Uninflatable and Notch Control the Targeting of Sara Endosomes during Asymmetric Division. *Current Biology, 24*(18), 2142-2148. https://doi.org/10.1016/j.cub.2014.07.054

Luo, L., Liao, Y. J., Jan, L. Y., & Jan, Y. N. (1994). Distinct morphogenetic functions of similar small GTPases: Drosophila Drac1 is involved in axonal outgrowth and myoblast fusion. *Genes & development, 8*(15), 1787-1802. http://genesdev.cshlp.org/content/8/15/1787.abstract

M'Boneko, V., & Merker, H. J. (1988). Development and morphology of the periderm of mouse embryos (days 9-12 of gestation). *Acta Anat (Basel), 133*(4), 325-336. https://doi.org/10.1159/000146662

MacDonald, B. T., Tamai, K., & He, X. (2009, Jul). Wnt/beta-catenin signaling: components, mechanisms, and diseases. *Dev Cell, 17*(1), 9-26. https://doi.org/10.1016/j.devcel.2009.06.016

Mack, J. J., Mosqueiro, T. S., Archer, B. J., Jones, W. M., Sunshine, H., Faas, G. C., Briot, A., Aragón, R. L., Su, T., & Romay, M. C. (2017). NOTCH1 is a mechanosensor in adult arteries. *Nature communications, 8*(1), 1620.

MacLauchlan, S., Skokos, E. A., Meznarich, N., Zhu, D. H., Raoof, S., Shipley, J. M., Senior, R. M., Bornstein, P., & Kyriakides, T. R. (2009). Macrophage fusion, giant cell formation, and the foreign body response require matrix metalloproteinase 9. *Journal of Leucocyte Biology, 85*(4), 617-626.

Madra, S., Styles, J., & Smith, A. G. (1995). Perturbation of hepatocyte nuclear populations induced by iron and polychlorinated biphenyls in C57BL/10ScSn mice during carcinogenesis. *Carcinogenesis, 16*(4), 719-727.

Mandel, L. J., Bacallao, R., & Zampighi, G. (1993, Feb 11). Uncoupling of the molecular 'fence' and paracellular 'gate' functions in epithelial tight junctions. *Nature, 361*(6412), 552-555. https://doi.org/10.1038/361552a0

Marchetti, M., Fanti, L., Berloco, M., & Pimpinelli, S. (2003). Differential expression of the Drosophila BX-C in polytene chromosomes in cells of larval fat bodies: a cytological approach to identifying in vivo targets of the homeotic Ubx, Abd-A and Abd-B proteins.

Marinari, E., Mehonic, A., Curran, S., Gale, J., Duke, T., & Baum, B. (2012). Live-cell delamination counterbalances epithelial growth to limit tissue overcrowding. *Nature, 484*(7395), 542-545.

Markvoort, A. J., & Marrink, S. J. (2011). Chapter 11 - Lipid Acrobatics in the Membrane Fusion Arena. In L. V. Chernomordik & M. M. Kozlov (Eds.), *Current Topics in Membranes* (Vol. 68, pp. 259-294). Academic Press. https://doi.org/https://doi.org/10.1016/B978-0-12-385891-7.00011-8

Martin-Blanco, E., Pastor-Pareja, J. C., & Garcia-Bellido, A. (2000). JNK and Decapentaplegic Signaling Control Adhesiveness and Cytoskeleton Dynamics during Thorax Closure in Drosophila. *Proceedings of the National Academy of Sciences of the United States of America, 97*(14), 7888-7893. http://www.jstor.org.proxy.library.vanderbilt.edu/stable/123020

Martin, P., & Lewis, J. (1992, Nov 12). Actin cables and epidermal movement in embryonic wound healing. *Nature, 360*(6400), 179-183. https://doi.org/10.1038/360179a0

Martin, P., Nobes, C. D., McCluskey, J. T., & Lewis, J. (1994). Repair of excisional wounds in the embryo. *Eye, 8*, 155-160.

Massarwa, R. a., Carmon, S., Shilo, B.-Z., & Schejter, E. D. (2007, 2007/04/01/). WIP/WASp-Based Actin-Polymerization Machinery Is Essential for Myoblast Fusion in Drosophila. *Developmental cell, 12*(4), 557-569. https://doi.org/https://doi.org/10.1016/j.devcel.2007.01.016

Matsumoto, T. (2022, Aug 20). Implications of Polyploidy and Ploidy Alterations in Hepatocytes in Liver Injuries and Cancers. *Int J Mol Sci, 23*(16). https://doi.org/10.3390/ijms23169409

Matsumoto, T., Wakefield, L., & Grompe, M. (2021). The significance of polyploid hepatocytes during aging process. *Cellular and Molecular Gastroenterology and Hepatology, 11*(5), 1347.

Matsumoto, T., Wakefield, L., Tarlow, B. D., & Grompe, M. (2020). In vivo lineage tracing of polyploid hepatocytes reveals extensive proliferation during liver regeneration. *Cell stem cell, 26*(1), 34-47. e33.

Maynard, R. L., & Downes, N. (2019). Chapter 24 - The Skin or the Integument. In R. L. Maynard & N. Downes (Eds.), *Anatomy and Histology of the Laboratory Rat in Toxicology and Biomedical Research* (pp. 303-315). Academic Press. https://doi.org/https://doi.org/10.1016/B978-0-12-811837-5.00024-1

McClure, K. D., & Schubiger, G. (2005). Developmental analysis and squamous morphogenesis of the peripodial epithelium in Drosophila imaginal discs.

McNeil, P. L., & Steinhardt, R. A. (2003). Plasma membrane disruption: repair, prevention, adaptation. *Annu Rev Cell Dev Biol, 19*, 697-731. https://doi.org/10.1146/annurev.cellbio.19.111301.140101

Médina, E., Williams, J., Klipfell, E., Zarnescu, D., Thomas, C. M., & Le Bivic, A. (2002, Sep 2). Crumbs interacts with moesin and beta(Heavy)-spectrin in the apical membrane skeleton of Drosophila. *J Cell Biol, 158*(5), 941-951. https://doi.org/10.1083/jcb.200203080

Meghana, C., Ramdas, N., Hameed, F. M., Rao, M., Shivashankar, G. V., & Narasimha, M. (2011). Integrin adhesion drives the emergent polarization of active cytoskeletal stresses to pattern cell delamination. *Proceedings of the National Academy of Sciences, 108*(22), 9107-9112. https://doi.org/doi:10.1073/pnas.1018652108

Mehrotra, S., Maqbool, S. B., Kolpakas, A., Murnen, K., & Calvi, B. R. (2008). Endocycling cells do not apoptose in response to DNA rereplication genotoxic stress. *Genes & development, 22*(22), 3158-3171.

Melzer, C., von der Ohe, J., & Hass, R. (2018). In Vitro Fusion of Normal and Neoplastic Breast Epithelial Cells with Human Mesenchymal Stroma/Stem Cells Partially Involves Tumor Necrosis Factor Receptor Signaling. *Stem Cells, 36*(7), 977-989. https://doi.org/10.1002/stem.2819

Mescher, A. L. (2018). In *Junqueira's Basic Histology: Text and Atlas, 15e*. McGraw-Hill Education. accessmedicine.mhmedical.com/content.aspx?aid=1153706400

Miller, P. W., Clarke, D. N., Weis, W. I., Lowe, C. J., & Nelson, W. J. (2013). The evolutionary origin of epithelial cell-cell adhesion mechanisms. *Curr Top Membr, 72*, 267-311. https://doi.org/10.1016/b978-0-12-417027-8.00008-8

Mirastschijski, U., Schnabel, R., Claes, J., Schneider, W., Ågren, M. S., Haaksma, C., & Tomasek, J. J. (2010). Matrix metalloproteinase inhibition delays wound healing and blocks the latent transforming growth factor-β1-promoted myofibroblast formation and function. *Wound Repair and Regeneration, 18*(2), 223-234.

Mirth, C. (2005). Ecdysteroid control of metamorphosis in the differentiating adult leg structures of Drosophila melanogaster. *Developmental biology, 278*(1), 163-174.

Mirzayans, R., Andrais, B., & Murray, D. (2018). Roles of polyploid/multinucleated giant cancer cells in metastasis and disease relapse following anticancer treatment. *Cancers, 10*(4), 118.

Mirzayans, R., & Murray, D. (2020a). Do TUNEL and other apoptosis assays detect cell death in preclinical studies? *International Journal of Molecular Sciences, 21*(23), 9090.

Mirzayans, R., & Murray, D. (2020b). Intratumor heterogeneity and therapy resistance: Contributions of dormancy, apoptosis reversal (anastasis) and cell fusion to disease recurrence. *International Journal of Molecular Sciences, 21*(4), 1308.

Miyaoka, Y., Ebato, K., Kato, H., Arakawa, S., Shimizu, S., & Miyajima, A. (2012). Hypertrophy and unconventional cell division of hepatocytes underlie liver regeneration. *Current Biology, 22*(13), 1166-1175.

Mohler, W. A., Shemer, G., del Campo, J. J., Valansi, C., Opoku-Serebuoh, E., Scranton, V., Assaf, N., White, J. G., & Podbilewicz, B. (2002). The type I membrane protein EFF-1 is essential for developmental cell fusion. *Developmental cell, 2*(3), 355-362.

Moll, R., Moll, I., & Wiest, W. (1982). Changes in the pattern of cytokeratin polypeptides in epidermis and hair follicles during skin development in human fetuses. *Differentiation, 23*(2), 170-178. https://doi.org/10.1111/j.1432-0436.1982.tb01280.x

Møller, A. M., Delaissé, J.-M., Olesen, J. B., Canto, L. M., Rogatto, S. R., Madsen, J. S., & Søe, K. (2020). Fusion potential of human osteoclasts in vitro reflects age, menopause, and in vivo bone resorption levels of their donors—a possible involvement of DC-STAMP. *International Journal of Molecular Sciences, 21*(17), 6368.

Møller, A. M. J., Delaissé, J.-M., Olesen, J. B., Madsen, J. S., Canto, L. M., Bechmann, T., Rogatto, S. R., & Søe, K. (2020). Aging and menopause reprogram osteoclast precursors for aggressive bone resorption. *Bone research, 8*(1), 27.

Mollova, M., Bersell, K., Walsh, S., Savla, J., Das, L. T., Park, S.-Y., Silberstein, L. E., Dos Remedios, C. G., Graham, D., & Colan, S. (2013). Cardiomyocyte proliferation contributes to heart growth in young humans. *Proceedings of the National Academy of Sciences, 110*(4), 1446-1451.

Monier, B., Gettings, M., Gay, G., Mangeat, T., Schott, S., Guarner, A., & Suzanne, M. (2015). Apico-basal forces exerted by apoptotic cells drive epithelium folding. *Nature, 518*(7538), 245-248.

Morais-de-Sá, E., Mirouse, V., & St Johnston, D. (2010, 2010/04/30/). aPKC Phosphorylation of Bazooka Defines the Apical/Lateral Border in Drosophila Epithelial Cells. *Cell, 141*(3), 509-523. https://doi.org/https://doi.org/10.1016/j.cell.2010.02.040

Moreira, C., Regan, J., Zaidman-Rémy, A., Jacinto, A., & Prag, S. (2011, 06/17). Drosophila Hemocyte Migration: An In Vivo Assay for Directional Cell Migration. *Methods in molecular biology (Clifton, N.J.), 769*, 249-260. https://doi.org/10.1007/978-1-61779-207-6_17

Morris, S. C. (1993, 1993/01/01). The fossil record and the early evolution of the Metazoa. *Nature, 361*(6409), 219-225. https://doi.org/10.1038/361219a0

Mosieniak, G., Sliwinska, M. A., Alster, O., Strzeszewska, A., Sunderland, P., Piechota, M., Was, H., & Sikora, E. (2015, 2015/12/01/). Polyploidy Formation in Doxorubicin-Treated Cancer Cells Can Favor Escape from Senescence. *Neoplasia, 17*(12), 882-893. https://doi.org/https://doi.org/10.1016/j.neo.2015.11.008

Mukherjee, S., Ali, A. M., Murty, V. V., & Raza, A. (2022). Mutation in SF3B1 gene promotes formation of polyploid giant cells in Leukemia cells. *Medical Oncology, 39*(6), 65.

Muramatsu, Y., Yamada, T., Moralejo, D. H., Mochizuki, H., Sogawa, K., & Matsumoto, K. (2000). Increased polyploid incidence is associated with abnormal copper accumulation in the liver of LEC mutant rat. *Research Communications in Molecular Pathology and Pharmacology, 107*(1-2), 129-136.

Nagata, Y., Muro, Y., & Todokoro, K. (1997). Thrombopoietin-induced polyploidization of bone marrow megakaryocytes is due to a unique regulatory mechanism in late mitosis. *The Journal of cell biology, 139*(2), 449-457.

Nandakumar, S., Grushko, O., & Buttitta, L. A. (2020, Aug 25). Polyploidy in the adult Drosophila brain. *Elife, 9*. https://doi.org/10.7554/eLife.54385

Niculescu, V. F. (2022). Cancer genes and cancer stem cells in tumorigenesis: Evolutionary deep homology and controversies. *Genes & Diseases, 9*(5), 1234-1247.

Nieto, M. A., Huang, Ruby Y.-J., Jackson, Rebecca A., & Thiery, Jean P. (2016). EMT: 2016. *Cell, 166*(1), 21-45. https://doi.org/10.1016/j.cell.2016.06.028

Niu, N., Zhang, J., Zhang, N., Mercado-Uribe, I., Tao, F., Han, Z., Pathak, S., Multani, A. S., Kuang, J., Yao, J., Bast, R. C., Sood, A. K., Hung, M. C., & Liu, J. (2016, Dec 19). Linking genomic reorganization to tumor initiation via the giant cell cycle. *Oncogenesis, 5*(12), e281. https://doi.org/10.1038/oncsis.2016.75

Noma, K., Goncharov, A., Ellisman, M. H., & Jin, Y. (2017, 2017/08/02). Microtubule-dependent ribosome localization in C. elegans neurons. *Elife, 6*, e26376. https://doi.org/10.7554/eLife.26376

Nordman, J., Li, S., Eng, T., MacAlpine, D., & Orr-Weaver, T. L. (2011). Developmental control of the DNA replication and transcription programs. *Genome research, 21*(2), 175-181.

Noubissi, F. K., Harkness, T., Alexander, C. M., & Ogle, B. M. (2015, 2015/09/01). Apoptosis-induced cancer cell fusion: a mechanism of breast cancer metastasis [https://doi.org/10.1096/fj.15-271098]. *The FASEB Journal, 29*(9), 4036-4045. https://doi.org/https://doi.org/10.1096/fj.15-271098

Nygren, J. M., Jovinge, S., Breitbach, M., Säwén, P., Röll, W., Hescheler, J., Taneera, J., Fleischmann, B. K., & Jacobsen, S. E. (2004, May). Bone marrow-derived hematopoietic cells generate cardiomyocytes at a low frequency through cell fusion, but not transdifferentiation. *Nat Med, 10*(5), 494-501. https://doi.org/10.1038/nm1040

Nygren, J. M., Liuba, K., Breitbach, M., Stott, S., Thorén, L., Roell, W., Geisen, C., Sasse, P., Kirik, D., & Björklund, A. (2008). Myeloid and lymphoid contribution to non-haematopoietic lineages through irradiation-induced heterotypic cell fusion. *Nature cell biology, 10*(5), 584-592.

O'Connor, J. T., Shannon, E. K., Hutson, M. S., & Page-McCaw, A. (2022, Jun 17). Mounting Drosophila pupae for laser ablation and live imaging of the dorsal thorax. *STAR Protoc, 3*(2), 101396. https://doi.org/10.1016/j.xpro.2022.101396

O'Connor, J. T., Stevens, A. C., Shannon, E. K., Akbar, F. B., LaFever, K. S., Narayanan, N. P., Gailey, C. D., Hutson, M. S., & Page-McCaw, A. (2021, Aug 9). Proteolytic activation of Growth-blocking peptides triggers calcium responses through the GPCR Mthl10 during epithelial wound detection. *Dev Cell, 56*(15), 2160-2175.e2165. https://doi.org/10.1016/j.devcel.2021.06.020

O'Connor, J., Akbar, F. B., Hutson, M. S., & Page-McCaw, A. (2021). Zones of cellular damage around pulsed-laser wounds. *PLOS ONE, 16*(9), e0253032. https://doi.org/10.1371/journal.pone.0253032

Ogawa, R., Okai, K., Tokumura, F., Mori, K., Ohmori, Y., Huang, C., Hyakusoku, H., & Akaishi, S. (2012). The relationship between skin stretching/contraction and pathologic scarring: the important role of mechanical forces in keloid generation. *Wound Repair and Regeneration, 20*(2), 149-157.

Ogden, A., Rida, P. C. G., Knudsen, B. S., Kucuk, O., & Aneja, R. (2015, 2015/10/28/). Docetaxel-induced polyploidization may underlie chemoresistance and disease relapse. *Cancer Letters, 367*(2), 89-92. https://doi.org/https://doi.org/10.1016/j.canlet.2015.06.025

Ogura, Y., Wen, F.-L., Sami, M. M., Shibata, T., & Hayashi, S. (2018, 2018/07/16/). A Switch-like Activation Relay of EGFR-ERK Signaling Regulates a Wave of Cellular Contractility for Epithelial Invagination. *Developmental Cell, 46*(2), 162-172.e165. https://doi.org/https://doi.org/10.1016/j.devcel.2018.06.004

Omelchenko, T., Vasiliev, J. M., Gelfand, I. M., Feder, H. H., & Bonder, E. M. (2003). Rho-dependent formation of epithelial "leader" cells during wound healing. *Proceedings of the National Academy of Sciences, 100*(19), 10788-10793. https://doi.org/doi:10.1073/pnas.1834401100

Orr-Weaver, T. L. (2015). When bigger is better: the role of polyploidy in organogenesis. *Trends in genetics : TIG, 31*(6), 307-315. https://doi.org/10.1016/j.tig.2015.03.011

Øvrebø, J. I., & Edgar, B. A. (2018, Jul 18). Polyploidy in tissue homeostasis and regeneration. *Development, 145*(14). https://doi.org/10.1242/dev.156034

Ow, J. R., Caldez, M. J., Zafer, G., Foo, J. C., Li, H. Y., Ghosh, S., Wollmann, H., Cazenave-Gassiot, A., Ong, C. B., & Wenk, M. R. (2020). Remodeling of whole-body lipid metabolism and a diabetic-like phenotype caused by loss of CDK1 and hepatocyte division. *eLife, 9*, e63835.

Palta, S., Saroa, R., & Palta, A. (2014, Sep). Overview of the coagulation system. *Indian J Anaesth, 58*(5), 515-523. https://doi.org/10.4103/0019-5049.144643

Pan, Y., Yu, Y., Wang, X., & Zhang, T. (2020). Tumor-associated macrophages in tumor immunity. *Frontiers in immunology, 11*, 583084.

Pandit, S. K., Westendorp, B., Nantasanti, S., Van Liere, E., Tooten, P. C., Cornelissen, P. W., Toussaint, M. J., Lamers, W. H., & De Bruin, A. (2012). E2F8 is essential for polyploidization in mammalian cells. *Nature cell biology, 14*(11), 1181-1191.

Park, S., Gonzalez, D. G., Guirao, B., Boucher, J. D., Cockburn, K., Marsh, E. D., Mesa, K. R., Brown, S., Rompolas, P., Haberman, A. M., Bellaïche, Y., & Greco, V. (2017, Mar 1). Tissue-scale coordination of cellular behaviour promotes epidermal wound repair in live mice. *Nat Cell Biol, 19*(2), 155-163. https://doi.org/10.1038/ncb3472

Pastor-Pareja, J. C., Grawe, F., Martín-Blanco, E., & García-Bellido, A. (2004, 2004/09/01/). Invasive Cell Behavior during Drosophila Imaginal Disc Eversion Is Mediated by the JNK Signaling Cascade. *Developmental cell, 7*(3), 387-399. https://doi.org/https://doi.org/10.1016/j.devcel.2004.07.022

Patterson, M., Barske, L., Van Handel, B., Rau, C. D., Gan, P., Sharma, A., Parikh, S., Denholtz, M., Huang, Y., & Yamaguchi, Y. (2017). Frequency of mononuclear diploid cardiomyocytes underlies natural variation in heart regeneration. *Nature genetics, 49*(9), 1346-1353.

Pawelek, J., Chakraborty, A., Lazova, R., Yilmaz, Y., Cooper, D., Brash, D., & Handerson, T. (2006). Co-opting macrophage traits in cancer progression: a consequence of tumor cell fusion? *Infection and inflammation: impacts on oncogenesis, 13*, 138-155.

Pawelek, J. M., & Chakraborty, A. K. (2008). Fusion of tumour cells with bone marrow-derived cells: a unifying explanation for metastasis. *Nature Reviews Cancer, 8*(5), 377-386.

Pereira, M., Ko, J.-H., Logan, J., Protheroe, H., Kim, K.-B., Tan, A. L. M., Croucher, P. I., Park, K.-S., Rotival, M., & Petretto, E. (2020). A trans-eQTL network regulates osteoclast multinucleation and bone mass. *eLife, 9*, e55549.

Perez-Moreno, M., & Fuchs, E. (2006, Nov). Catenins: keeping cells from getting their signals crossed. *Dev Cell, 11*(5), 601-612. https://doi.org/10.1016/j.devcel.2006.10.010

Perret, E., Leung, A., Feracci, H., & Evans, E. (2004, Nov 23). Trans-bonded pairs of E-cadherin exhibit a remarkable hierarchy of mechanical strengths. *Proc Natl Acad Sci U S A, 101*(47), 16472-16477. https://doi.org/10.1073/pnas.0402085101

Petrany, M. J., & Millay, D. P. (2019, Dec). Cell Fusion: Merging Membranes and Making Muscle. *Trends Cell Biol, 29*(12), 964-973. https://doi.org/10.1016/j.tcb.2019.09.002

Pieczynski, J., & Margolis, B. (2011, 2011/03//). Protein complexes that control renal epithelial polarity. *American journal of physiology. Renal physiology, 300*(3), F589-601. https://doi.org/10.1152/ajprenal.00615.2010

Pienta, K. J., Hammarlund, E. U., Austin, R. H., Axelrod, R., Brown, J. S., & Amend, S. R. (2022, Jun). Cancer cells employ an evolutionarily conserved polyploidization program to resist therapy. *Semin Cancer Biol, 81*, 145-159. https://doi.org/10.1016/j.semcancer.2020.11.016

Pignoni, F., & Zipursky, S. L. (1997). Induction of Drosophila eye development by Decapentaplegic. *Development, 124*(2), 271-278. https://doi.org/10.1242/dev.124.2.271

Piper, K., Boyde, A., & Jones, S. J. (1992). The relationship between the number of nuclei of an osteoclast and its resorptive capability in vitro. *Anatomy and embryology, 186*, 291-299.

Podbilewicz, B., Leikina, E., Sapir, A., Valansi, C., Suissa, M., Shemer, G., & Chernomordik, L. V. (2006). The C. elegans developmental fusogen EFF-1 mediates homotypic fusion in heterologous cells and in vivo. *Developmental Cell, 11*(4), 471-481.

Podbilewicz, B., & White, J. G. (1994, Feb). Cell fusions in the developing epithelial of C. elegans. *Dev Biol, 161*(2), 408-424. https://doi.org/10.1006/dbio.1994.1041

Porrello, E. R., Mahmoud, A. I., Simpson, E., Hill, J. A., Richardson, J. A., Olson, E. N., & Sadek, H. A. (2011). Transient regenerative potential of the neonatal mouse heart. *Science, 331*(6020), 1078-1080.

Poujade, M., Grasland-Mongrain, E., Hertzog, A., Jouanneau, J., Chavrier, P., Ladoux, B., Buguin, A., & Silberzan, P. (2007). Collective migration of an epithelial monolayer in response to a model wound. *Proceedings of the National Academy of Sciences, 104*(41), 15988-15993. https://doi.org/doi:10.1073/pnas.0705062104

Powell, A. D., & Marrion, N. V. (2007). Resolution of fusion pore formation in a cell-attached patch. *Journal of neuroscience methods, 162*(1-2), 272-281.

Powell, A. E., Anderson, E. C., Davies, P. S., Silk, A. D., Pelz, C., Impey, S., & Wong, M. H. (2011). Fusion between Intestinal epithelial cells and macrophages in a cancer context results in nuclear reprogramming. *Cancer research, 71*(4), 1497-1505.

Powell, A. E., Anderson, E. C., Davies, P. S., Silk, A. D., Pelz, C., Impey, S., & Wong, M. H. (2011, Feb 15). Fusion between Intestinal epithelial cells and macrophages in a cancer context results in nuclear reprogramming. *Cancer Res, 71*(4), 1497-1505. https://doi.org/10.1158/0008-5472.Can-10-3223

Puig, P. E., Guilly, M. N., Bouchot, A., Droin, N., Cathelin, D., Bouyer, F., Favier, L., Ghiringhelli, F., Kroemer, G., & Solary, E. (2008). Tumor cells can escape DNA-damaging cisplatin through DNA endoreduplication and reversible polyploidy. *Cell biology international, 32*(9), 1031-1043.

Qu, Y., Zhang, L., Rong, Z., He, T., & Zhang, S. (2013, Oct 15). Number of glioma polyploid giant cancer cells (PGCCs) associated with vasculogenic mimicry formation and tumor grade in human glioma. *J Exp Clin Cancer Res, 32*(1), 75. https://doi.org/10.1186/1756-9966-32-75

Ramos-Lewis, W., & Page-McCaw, A. (2019). Basement membrane mechanics shape development: Lessons from the fly. *Matrix Biology, 75*, 72-81.

Rasmussen, J. P., English, K., Tenlen, J. R., & Priess, J. R. (2008). Notch signaling and morphogenesis of single-cell tubes in the C. elegans digestive tract. *Developmental cell, 14*(4), 559-569.

Ravid, K., Lu, J., Zimmet, J. M., & Jones, M. R. (2002). Roads to polyploidy: the megakaryocyte example. *Journal of cellular physiology, 190*(1), 7-20.

Razzell, W., Wood, W., & Martin, P. (2014). Recapitulation of morphogenetic cell shape changes enables wound re-epithelialisation. *Development, 141*(9), 1814-1820.

Reed, B. H., Wilk, R., Schöck, F., & Lipshitz, H. D. (2004). Integrin-dependent apposition of Drosophila extraembryonic membranes promotes morphogenesis and prevents anoikis. *Current Biology, 14*(5), 372-380.

Renaud, S. J., & Jeyarajah, M. J. (2022, 2022/07/20). How trophoblasts fuse: an in-depth look into placental syncytiotrophoblast formation. *Cellular and Molecular Life Sciences, 79*(8), 433. https://doi.org/10.1007/s00018-022-04475-z

Riabinina, O., & Potter, C. J. (2016). The Q-System: A Versatile Expression System for Drosophila. *Methods Mol Biol, 1478*, 53-78. https://doi.org/10.1007/978-1-4939-6371-3_3

Richardson, B. E., Beckett, K., Nowak, S. J., & Baylies, M. K. (2007). SCAR/WAVE and Arp2/3 are crucial for cytoskeletal remodeling at the site of myoblast fusion. *Development, 134*(24), 4357-4367. https://doi.org/10.1242/dev.010678

Richter, M., Deligiannis, I., Yin, K., Danese, A., Lleshi, E., Coupland, P., Vallejos, C. A., Matchett, K., Henderson, N., & Colome-Tatche, M. (2021). Single-nucleus RNA-seq2 reveals functional crosstalk between liver zonation and ploidy. *Nature communications, 12*(1), 4264.

Riddiford, L. M., Truman, J. W., Mirth, C. K., & Shen, Y.-c. (2010). A role for juvenile hormone in the prepupal development of Drosophila melanogaster. *Development, 137*(7), 1117-1126.

Rivera, J., Hosseini, M. S., Restrepo, D., Murata, S., Vasile, D., Parkinson, D. Y., Barnard, H. S., Arakaki, A., Zavattieri, P., & Kisailus, D. (2020). Toughening mechanisms of the elytra of the diabolical ironclad beetle. *Nature, 586*(7830), 543-548.

Rodriguez-Boulan, E., & Macara, I. G. (2014). Organization and execution of the epithelial polarity programme. *Nature reviews Molecular cell biology, 15*(4), 225-242.

Rohnalter, V., Roth, K., Finkernagel, F., Adhikary, T., Obert, J., Dorzweiler, K., Bensberg, M., Müller-Brüsselbach, S., & Müller, R. (2015). A multi-stage process including transient polyploidization and EMT precedes the emergence of chemoresistent ovarian carcinoma cells with a dedifferentiated and pro-inflammatory secretory phenotype. *Oncotarget, 6*(37), 40005.

Rosenblatt, J., Raff, M. C., & Cramer, L. P. (2001). An epithelial cell destined for apoptosis signals its neighbors to extrude it by an actin-and myosin-dependent mechanism. *Current Biology, 11*(23), 1847-1857.

Rothenberg, K. E., & Fernandez-Gonzalez, R. (2019, Jun 1). Forceful closure: cytoskeletal networks in embryonic wound repair. *Mol Biol Cell, 30*(12), 1353-1358. https://doi.org/10.1091/mbc.E18-04-0248

Ruiz-Gómez, M., Coutts, N., Price, A., Taylor, M. V., & Bate, M. (2000, 2000/07/21/). Drosophila Dumbfounded: A Myoblast Attractant Essential for Fusion. *Cell, 102*(2), 189-198. https://doi.org/https://doi.org/10.1016/S0092-8674(00)00024-6

Rushton, E., Drysdale, R., Abmayr, S. M., Michelson, A. M., & Bate, M. (1995). Mutations in a novel gene, myoblast city, provide evidence in support of the founder cell hypothesis for Drosophila muscle development. *Development, 121*(7), 1979-1988. https://doi.org/10.1242/dev.121.7.1979

Russo, J. M., Florian, P., Shen, L., Graham, W. V., Tretiakova, M. S., Gitter, A. H., Mrsny, R. J., & Turner, J. R. (2005, Apr). Distinct temporal-spatial roles for rho kinase and myosin light chain kinase in epithelial purse-string wound closure. *Gastroenterology, 128*(4), 987-1001. https://doi.org/10.1053/j.gastro.2005.01.004

Saltel, F., Chabadel, A., Zhao, Y., Lafage-Proust, M. H., Clézardin, P., Jurdic, P., & Bonnelye, E. (2006). Transmigration: a new property of mature multinucleated osteoclasts. *Journal of bone and mineral research, 21*(12), 1913-1923.

Sapir, A., Choi, J., Leikina, E., Avinoam, O., Valansi, C., Chernomordik, L. V., Newman, A. P., & Podbilewicz, B. (2007). AFF-1, a FOS-1-regulated fusogen, mediates fusion of the anchor cell in C. elegans. *Developmental cell, 12*(5), 683-698.

Sasso, J. M., Ammar, R. M., Tenchov, R., Lemmel, S., Kelber, O., Grieswelle, M., & Zhou, Q. A. (2023, May 17). Gut Microbiome-Brain Alliance: A Landscape View into Mental and Gastrointestinal Health and Disorders. *ACS Chem Neurosci, 14*(10), 1717-1763. https://doi.org/10.1021/acschemneuro.3c00127

Sawant, M., Hinz, B., Schönborn, K., Zeinert, I., Eckes, B., Krieg, T., & Schuster, R. (2021). A story of fibers and stress: Matrix-embedded signals for fibroblast activation in the skin. *Wound Repair and Regeneration, 29*(4), 515-530.

Scepanovic, G., Hunter, M. V., Kafri, R., & Fernandez-Gonzalez, R. (2021, 2021/10/19/). p38-mediated cell growth and survival drive rapid embryonic wound repair. *Cell Reports, 37*(3), 109874. https://doi.org/https://doi.org/10.1016/j.celrep.2021.109874

Schaeffer, V., Althauser, C., Shcherbata, H. R., Deng, W. M., & Ruohola-Baker, H. (2004, Apr 6). Notch-dependent Fizzy-related/Hec1/Cdh1 expression is required for the mitotic-to-endocycle transition in Drosophila follicle cells. *Curr Biol, 14*(7), 630-636. https://doi.org/10.1016/j.cub.2004.03.040

Schäfer, G., Weber, S., Holz, A., Bogdan, S., Schumacher, S., Müller, A., Renkawitz-Pohl, R., & Önel, S.-F. (2007, 2007/04/15/). The Wiskott–Aldrich syndrome protein (WASP) is essential for myoblast fusion in Drosophila. *Developmental biology, 304*(2), 664-674. https://doi.org/https://doi.org/10.1016/j.ydbio.2007.01.015

Schlüter, M. A., & Margolis, B. (2012, May 15). Apicobasal polarity in the kidney. *Exp Cell Res, 318*(9), 1033-1039. https://doi.org/10.1016/j.yexcr.2012.02.028

Schröter, R. H., Lier, S., Holz, A., Bogdan, S., Klämbt, C., Beck, L., & Renkawitz-Pohl, R. (2004). kette and blown fuse interact genetically during the second fusion step of myogenesis in Drosophila [Article]. *Development, 131*(18), 4501-4509. https://doi.org/10.1242/dev.01309

Sens, K. L., Zhang, S., Jin, P., Duan, R., Zhang, G., Luo, F., Parachini, L., & Chen, E. H. (2010, Nov 29). An invasive podosome-like structure promotes fusion pore formation during myoblast fusion. *J Cell Biol, 191*(5), 1013-1027. https://doi.org/10.1083/jcb.201006006

Sens, K. L., Zhang, S., Jin, P., Duan, R., Zhang, G., Luo, F., Parachini, L., & Chen, E. H. (2010). An invasive podosome-like structure promotes fusion pore formation during myoblast fusion. *Journal of Cell Biology, 191*(5), 1013-1027.

Senyo, S. E., Steinhauser, M. L., Pizzimenti, C. L., Yang, V. K., Cai, L., Wang, M., Wu, T.-D., Guerquin-Kern, J.-L., Lechene, C. P., & Lee, R. T. (2013). Mammalian heart renewal by pre-existing cardiomyocytes. *Nature, 493*(7432), 433-436.

Severin, E., Willers, R., & Bettecken, T. (1984). Flow cytometric analysis of mouse hepatocyte ploidy: II. The development of polyploidy pattern in four mice strains with different life spans. *Cell and tissue research, 238*, 649-652.

Shabo, I., Midtbö, K., Andersson, H., Åkerlund, E., Olsson, H., Wegman, P., Gunnarsson, C., & Lindström, A. (2015). Macrophage traits in cancer cells are induced by macrophage-cancer cell fusion and cannot be explained by cellular interaction. *BMC cancer, 15*(1), 1-11.

Shannon, E. K., Stevens, A., Edrington, W., Zhao, Y., Jayasinghe, A. K., Page-McCaw, A., & Hutson, M. S. (2017, Oct 3). Multiple Mechanisms Drive Calcium Signal Dynamics around Laser-Induced Epithelial Wounds. *Biophys J, 113*(7), 1623-1635. https://doi.org/10.1016/j.bpj.2017.07.022

Shannon, E. K., Stevens, A., Edrington, W., Zhao, Y., Jayasinghe, A. K., Page-McCaw, A., & Hutson, M. S. (2017, Oct 03). Multiple Mechanisms Drive Calcium Signal Dynamics around Laser-Induced Epithelial Wounds. *Biophysical Journal, 113*(7), 1623-1635. https://doi.org/10.1016/j.bpj.2017.07.022

Shcherbata, H. R., Althauser, C., Findley, S. D., & Ruohola-Baker, H. (2004). The mitotic-to-endocycle switch in Drosophila follicle cells is executed by Notch-dependent regulation of G1/S, G2/M and M/G1 cell-cycle transitions.

Shemer, G., Suissa, M., Kolotuev, I., Nguyen, K. C., Hall, D. H., & Podbilewicz, B. (2004). EFF-1 is sufficient to initiate and execute tissue-specific cell fusion in C. elegans. *Current Biology, 14*(17), 1587-1591.

Shibutani, S. T., de la Cruz, A. F. A., Tran, V., Turbyfill, W. J., Reis, T., Edgar, B. A., & Duronio, R. J. (2008). Intrinsic negative cell cycle regulation provided by PIP box-and Cul4Cdt2-mediated destruction of E2f1 during S phase. *Developmental cell, 15*(6), 890-900.

Sigal, S. H., Rajvanshi, P., Gorla, G. R., Sokhi, R. P., Saxena, R., Gebhard Jr, D. R., Reid, L. M., & Gupta, S. (1999). Partial hepatectomy-induced polyploidy attenuates hepatocyte replication and activates cell aging events. *American Journal of Physiology-Gastrointestinal and Liver Physiology, 276*(5), G1260-G1272.

Silhavy, T. J., Kahne, D., & Walker, S. (2010, May). The bacterial cell envelope. *Cold Spring Harb Perspect Biol, 2*(5), a000414. https://doi.org/10.1101/cshperspect.a000414

Silk, A. D., Gast, C. E., Davies, P. S., Fakhari, F. D., Vanderbeek, G. E., Mori, M., & Wong, M. H. (2013). Fusion between hematopoietic and epithelial cells in adult human intestine. *PLOS ONE, 8*(1), e55572.

Sims, N. A., & Martin, T. J. (2020). Osteoclasts provide coupling signals to osteoblast lineage cells through multiple mechanisms. *Annual review of physiology, 82*, 507-529.

Sindrilaru, A., & Scharffetter-Kochanek, K. (2013). Disclosure of the culprits: macrophages—versatile regulators of wound healing. *Advances in wound care, 2*(7), 357-368.

Sladky, V. C., Knapp, K., Soratroi, C., Heppke, J., Eichin, F., Rocamora-Reverte, L., Szabo, T. G., Bongiovanni, L., Westendorp, B., & Moreno, E. (2020). E2F-family members engage the PIDDosome to limit hepatocyte ploidy in liver development and regeneration. *Developmental cell, 52*(3), 335-349. e337.

Slattum, G., McGee, K. M., & Rosenblatt, J. (2009). P115 RhoGEF and microtubules decide the direction apoptotic cells extrude from an epithelium. *Journal of Cell Biology, 186*(5), 693-702.

Søe, K. (2020, Oct 19). Osteoclast Fusion: Physiological Regulation of Multinucleation through Heterogeneity-Potential Implications for Drug Sensitivity. *Int J Mol Sci, 21*(20). https://doi.org/10.3390/ijms21207717

Søe, K., Andersen, T. L., Hinge, M., Rolighed, L., Marcussen, N., & Delaisse, J.-M. (2019). Coordination of fusion and trafficking of pre-osteoclasts at the marrow–bone interface. *Calcified Tissue International, 105*(4), 430-445.

Søe, K., Delaisse, J.-M., & Borggaard, X. G. (2021). Osteoclast formation at the bone marrow/bone surface interface: Importance of structural elements, matrix, and intercellular communication. Seminars in Cell & Developmental Biology,

Song, Y., Zhao, Y., Deng, Z., Zhao, R., & Huang, Q. (2021). Stress-Induced Polyploid Giant Cancer Cells: Unique Way of Formation and Non-Negligible Characteristics. *Frontiers in oncology, 11*, 724781. https://doi.org/10.3389/fonc.2021.724781

Soonpaa, M., & Field, L. J. (1997). Assessment of cardiomyocyte DNA synthesis in normal and injured adult mouse hearts. *American Journal of Physiology-Heart and Circulatory Physiology, 272*(1), H220-H226.

Soonpaa, M. H., Kim, K. K., Pajak, L., Franklin, M., & Field, L. J. (1996). Cardiomyocyte DNA synthesis and binucleation during murine development. *American Journal of Physiology-Heart and Circulatory Physiology, 271*(5), H2183-H2189.

Sorg, H., Tilkorn, D. J., Hager, S., Hauser, J., & Mirastschijski, U. (2017). Skin wound healing: an update on the current knowledge and concepts. *European Surgical Research, 58*(1-2), 81-94.

Soto, X., Li, J., Lea, R., Dubaissi, E., Papalopulu, N., & Amaya, E. (2013). Inositol kinase and its product accelerate wound healing by modulating calcium levels, Rho GTPases, and F-actin assembly. *Proceedings of the National Academy of Sciences, 110*(27), 11029-11034.

Spradling, A., & Orr-Weaver, T. (1987). Regulation of DNA replication during Drosophila development. *Annual review of genetics, 21*(1), 373-403.

Srinivas, B. P., Woo, J., Leong, W. Y., & Roy, S. (2007, 2007/06/01). A conserved molecular pathway mediates myoblast fusion in insects and vertebrates. *Nature genetics, 39*(6), 781-786. https://doi.org/10.1038/ng2055

Stern, C. D. (2005, May). Neural induction: old problem, new findings, yet more questions. *Development, 132*(9), 2007-2021. https://doi.org/10.1242/dev.01794

Stone, C. E., Hall, D. H., & Sundaram, M. V. (2009). Lipocalin signaling controls unicellular tube development in the Caenorhabditis elegans excretory system. *Developmental biology, 329*(2), 201-211.

Strünkelnberg, M., Bonengel, B., Moda, L. M., Hertenstein, A., de Couet, H. G., Ramos, R. G. P., & Fischbach, K.-F. (2001). rst and its paralogue kirre act redundantly during embryonic muscle development in Drosophila. *Development, 128*(21), 4229-4239. https://doi.org/10.1242/dev.128.21.4229

Sui, L., Pflugfelder, G. O., & Shen, J. (2012). The Dorsocross T-box transcription factors promote tissue morphogenesis in the Drosophila wing imaginal disc. *Development, 139*(15), 2773-2782.

Sulston, J. E., Schierenberg, E., White, J. G., & Thomson, J. N. (1983). The embryonic cell lineage of the nematode Caenorhabditis elegans. *Developmental biology, 100*(1), 64-119.

Sun, J., & Deng, W. M. (2007, Mar). Hindsight mediates the role of notch in suppressing hedgehog signaling and cell proliferation. *Dev Cell, 12*(3), 431-442. https://doi.org/10.1016/j.devcel.2007.02.003

Sundaram, M., Guernsey, D. L., Rajaraman, M. M., & Rajaraman, R. (2004). Neosis: a novel type of cell division in cancer. *Cancer biology & therapy, 3*(2), 207-218.

Suraneni, P., Rubinstein, B., Unruh, J. R., Durnin, M., Hanein, D., & Li, R. (2012). The Arp2/3 complex is required for lamellipodia extension and directional fibroblast cell migration. *Journal of Cell Biology, 197*(2), 239-251. https://doi.org/10.1083/jcb.201112113

Takase, N., Koma, Y.-i., Urakawa, N., Nishio, M., Arai, N., Akiyama, H., Shigeoka, M., Kakeji, Y., & Yokozaki, H. (2016). NCAM-and FGF-2-mediated FGFR1 signaling in the tumor microenvironment of esophageal cancer regulates the survival and migration of tumor-associated macrophages and cancer cells. *Cancer letters, 380*(1), 47-58.

Tamada, M., Perez, T. D., Nelson, W. J., & Sheetz, M. P. (2007). Two distinct modes of myosin assembly and dynamics during epithelial wound closure. *Journal of Cell Biology, 176*(1), 27-33. https://doi.org/10.1083/jcb.200609116

Tamada, M., Perez, T. D., Nelson, W. J., & Sheetz, M. P. (2007, Jan 1). Two distinct modes of myosin assembly and dynamics during epithelial wound closure. *J Cell Biol, 176*(1), 27-33. https://doi.org/10.1083/jcb.200609116

Tamori, Y., & Deng, W. M. (2013, May 28). Tissue repair through cell competition and compensatory cellular hypertrophy in postmitotic epithelia. *Dev Cell, 25*(4), 350-363. https://doi.org/10.1016/j.devcel.2013.04.013

Tanentzapf, G., & Tepass, U. (2003). Interactions between the crumbs, lethal giant larvae and bazooka pathways in epithelial polarization. *Nature cell biology, 5*(1), 46-52.

Tanimizu, N., & Mitaka, T. (2017, Aug 1). Epithelial Morphogenesis during Liver Development. *Cold Spring Harb Perspect Biol, 9*(8). https://doi.org/10.1101/cshperspect.a027862

Tepass, U. (2012). The apical polarity protein network in Drosophila epithelial cells: regulation of polarity, junctions, morphogenesis, cell growth, and survival. *Annual review of cell and developmental biology, 28*, 655-685.

Tepass, U., Tanentzapf, G., Ward, R., & Fehon, R. (2001). Epithelial cell polarity and cell junctions in Drosophila. *Annual review of genetics, 35*(1), 747-784.

Tetley, R. J., Staddon, M. F., Heller, D., Hoppe, A., Banerjee, S., & Mao, Y. (2019). Tissue Fluidity Promotes Epithelial Wound Healing. *Nature physics, 15*(11), 1195-1203. https://doi.org/10.1038/s41567-019-0618-1

Thulabandu, V., Chen, D., & Atit, R. P. (2018). Dermal fibroblast in cutaneous development and healing. *Wiley Interdisciplinary Reviews: Developmental Biology, 7*(2), e307.

Tonnesen, M. G., Feng, X., & Clark, R. A. (2000). Angiogenesis in wound healing. Journal of investigative dermatology symposium proceedings,

Toyama, Y., Peralta, X. G., Wells, A. R., Kiehart, D. P., & Edwards, G. S. (2008). Apoptotic force and tissue dynamics during Drosophila embryogenesis. *Science, 321*(5896), 1683-1686.

Toyoda, H., Bregerie, O., Vallet, A., Nalpas, B., Pivert, G., Brechot, C., & Desdouets, C. (2005a). Changes to hepatocyte ploidy and binuclearity profiles during human chronic viral hepatitis. *Gut, 54*(2), 297.

Toyoda, H., Bregerie, O., Vallet, A., Nalpas, B., Pivert, G., Brechot, C., & Desdouets, C. (2005b). Changes to hepatocyte ploidy and binuclearity profiles during human chronic viral hepatitis. *Gut, 54*(2), 297-302.

Trakala, M., Rodríguez-Acebes, S., Maroto, M., Symonds, C. E., Santamaría, D., Ortega, S., Barbacid, M., Méndez, J., & Malumbres, M. (2015). Functional reprogramming of polyploidization in megakaryocytes. *Developmental cell, 32*(2), 155-167.

Trepat, X., Wasserman, M. R., Angelini, T. E., Millet, E., Weitz, D. A., Butler, J. P., & Fredberg, J. J. (2009, 2009/06/01). Physical forces during collective cell migration. *Nature Physics, 5*(6), 426-430. https://doi.org/10.1038/nphys1269

Tripathi, B. K., & Irvine, K. D. (2022, Apr 4). The wing imaginal disc. *Genetics, 220*(4). https://doi.org/10.1093/genetics/iyac020

Truman, J. W. (2019). The evolution of insect metamorphosis. *Current Biology, 29*(23), R1252-R1268.

Truman, J. W., & Riddiford, L. M. (1999). The origins of insect metamorphosis. *Nature, 401*(6752), 447-452.

Unhavaithaya, Y., & Orr-Weaver, T. L. (2012). Polyploidization of glia in neural development links tissue growth to blood–brain barrier integrity. *Genes & development, 26*(1), 31.

Valon, L., Davidović, A., Levillayer, F., Villars, A., Chouly, M., Cerqueira-Campos, F., & Levayer, R. (2021). Robustness of epithelial sealing is an emerging property of local ERK feedback driven by cell elimination. *Developmental Cell, 56*(12), 1700-1711.e1708. https://doi.org/10.1016/j.devcel.2021.05.006

Vincent, J. F. V. (2002, 2002/10/01/). Arthropod cuticle: a natural composite shell system. *Composites Part A: Applied Science and Manufacturing, 33*(10), 1311-1315. https://doi.org/https://doi.org/10.1016/S1359-835X(02)00167-7

Vinogradov, A., Anatskaya, O., & Kudryavtsev, B. (2001). Relationship of hepatocyte ploidy levels with body size and growth rate in mammals. *Genome, 44*(3), 350-360.

Vivien, C. J., Hudson, J. E., & Porrello, E. R. (2016). Evolution, comparative biology and ontogeny of vertebrate heart regeneration. *NPJ Regenerative medicine, 1*(1), 1-14.

Walck-Shannon, E., & Hardin, J. (2014, 2014/01/01). Cell intercalation from top to bottom. *Nature reviews Molecular cell biology, 15*(1), 34-48. https://doi.org/10.1038/nrm3723

Wang, B., Liu, K., Lin, F.-T., & Lin, W.-C. (2004). A role for 14-3-3τ in E2F1 stabilization and DNA damage-induced apoptosis. *Journal of Biological Chemistry, 279*(52), 54140-54152.

Wang, J., Batourina, E., Schneider, K., Souza, S., Swayne, T., Liu, C., George, C. D., Tate, T., Dan, H., & Wiessner, G. (2018). Polyploid superficial cells that maintain the urothelial barrier are produced via incomplete cytokinesis and endoreplication. *Cell Reports, 25*(2), 464-477. e464.

Wang, J., Batourina, E., Schneider, K., Souza, S., Swayne, T., Liu, C., George, C. D., Tate, T., Dan, H., Wiessner, G., Zhuravlev, Y., Canman, J. C., Mysorekar, I. U., & Mendelsohn, C. L. (2018, Oct 9). Polyploid Superficial Cells that Maintain the Urothelial Barrier Are Produced via Incomplete Cytokinesis and Endoreplication. *Cell Rep, 25*(2), 464-477.e464. https://doi.org/10.1016/j.celrep.2018.09.042

Wang, J. G., Miyazu, M., Xiang, P., Li, S. N., Sokabe, M., & Naruse, K. (2005). Stretch-induced cell proliferation is mediated by FAK-MAPK pathway. *Life sciences, 76*(24), 2817-2825.

Wang, Q., Wu, P. C., Dong, D. Z., Ivanova, I., Chu, E., Zeliadt, S., Vesselle, H., & Wu, D. Y. (2013). Polyploidy road to therapy-induced cellular senescence and escape. *International Journal of Cancer, 132*(7), 1505-1515.

Wang, X. F., Yang, S. A., Gong, S., Chang, C. H., Portilla, J. M., Chatterjee, D., Irianto, J., Bao, H., Huang, Y. C., & Deng, W. M. (2021, Jul 12). Polyploid mitosis and depolyploidization promote chromosomal instability and tumor progression in a Notch-induced tumor model. *Dev Cell, 56*(13), 1976-1988.e1974. https://doi.org/10.1016/j.devcel.2021.05.017

Wang, Y., Antunes, M., Anderson, A. E., Kadrmas, J. L., Jacinto, A., & Galko, M. J. (2015, Aug 31). Integrin Adhesions Suppress Syncytium Formation in the Drosophila Larval Epidermis. *Curr Biol, 25*(17), 2215-2227. https://doi.org/10.1016/j.cub.2015.07.031

Wang, Y., Wang, Y., & Zheng, W. (2013). Cytologic changes of ovarian epithelial cancer induced by neoadjuvant chemotherapy. *Int J Clin Exp Pathol, 6*(10), 2121-2128.

Waters, C. M., Roan, E., & Navajas, D. (2012, Jan). Mechanobiology in lung epithelial cells: measurements, perturbations, and responses. *Compr Physiol, 2*(1), 1-29. https://doi.org/10.1002/cphy.c100090

Weihua, Z., Lin, Q., Ramoth, A. J., Fan, D., & Fidler, I. J. (2011, Sep 1). Formation of solid tumors by a single multinucleated cancer cell. *Cancer, 117*(17), 4092-4099. https://doi.org/10.1002/cncr.26021

Weihua, Z., Lin, Q., Ramoth, A. J., Fan, D., & Fidler, I. J. (2011). Formation of solid tumors by a single multinucleated cancer cell. *Cancer, 117*(17), 4092-4099.

Weng, A., Maciel Herrerias, M., Watanabe, S., Welch, L. C., Flozak, A. S., Grant, R. A., Aillon, R. P., Dada, L. A., Han, S. H., Hinchcliff, M., Misharin, A. V., Budinger, G. R. S., & Gottardi, C. J. (2022, May). Lung

Injury Induces Alveolar Type 2 Cell Hypertrophy and Polyploidy with Implications for Repair and Regeneration. *Am J Respir Cell Mol Biol, 66*(5), 564-576. https://doi.org/10.1165/rcmb.2021-0356OC

Wheatley, D. (1972). Binucleation in mammalian liver: Studies on the control of cytokinesis in vivo. *Experimental cell research, 74*(2), 455-465.

Wheatley, D. (2008, 2008/09/01). Growing evidence of the repopulation of regressed tumours by the division of giant cells. *Cell Biology International, 32*(9), 1029-1030. https://doi.org/10.1016/j.cellbi.2008.06.001

White, J. S., LaFever, K. S., & Page-McCaw, A. (2022, 2022/04/06/). Dissecting, Fixing, and Visualizing the Drosophila Pupal Notum. *JoVE*(182), e63682. https://doi.org/doi:10.3791/63682

White, J. S., Su, J. J., Ruark, E. M., Hua, J., Hutson, M. S., & Page-McCaw, A. (2023, Oct 26). Wound-Induced Syncytia Outpace Mononucleate Neighbors during Drosophila Wound Repair. *bioRxiv*. https://doi.org/10.1101/2023.06.25.546442

Wilkinson, P. D., Alencastro, F., Delgado, E. R., Leek, M. P., Weirich, M. P., Otero, P. A., Roy, N., Brown, W. K., Oertel, M., & Duncan, A. W. (2019, Jun). Polyploid Hepatocytes Facilitate Adaptation and Regeneration to Chronic Liver Injury. *Am J Pathol, 189*(6), 1241-1255. https://doi.org/10.1016/j.ajpath.2019.02.008

Winding, B., Misander, H., Sveigaard, C., Therkildsen, B., Jakobsen, M., Overgaard, T., Oursler, M. J., & Foged, N. T. (2000). Human breast cancer cells induce angiogenesis, recruitment, and activation of osteoclasts in osteolytic metastasis. *Journal of cancer research and clinical oncology, 126*, 631-640.

Wong, V. W., Levi, K., Akaishi, S., Schultz, G., & Dauskardt, R. H. (2012). Scar zones: region-specific differences in skin tension may determine incisional scar formation. *Plastic and reconstructive surgery, 129*(6), 1272-1276.

Wood, W., Jacinto, A., Grose, R., Woolner, S., Gale, J., Wilson, C., & Martin, P. (2002). Wound healing recapitulates morphogenesis in Drosophila embryos. *Nature cell biology, 4*(11), 907-912.

Wood, W., Jacinto, A., Grose, R., Woolner, S., Gale, J., Wilson, C., & Martin, P. (2002, Nov). Wound healing recapitulates morphogenesis in Drosophila embryos. *Nat Cell Biol, 4*(11), 907-912. https://doi.org/10.1038/ncb875

Xiang, J., Bandura, J., Zhang, P., Jin, Y., Reuter, H., & Edgar, B. A. (2017, 2017/05/09). EGFR-dependent TOR-independent endocycles support Drosophila gut epithelial regeneration. *Nature communications, 8*(1), 15125. https://doi.org/10.1038/ncomms15125

Xu, S., & Chisholm, A. D. (2011, Dec 6). A Gαq-$Ca^{2+}$ signaling pathway promotes actin-mediated epidermal wound closure in C. elegans. *Curr Biol, 21*(23), 1960-1967. https://doi.org/10.1016/j.cub.2011.10.050

Yamanaka, T., & Ohno, S. (2008). Role of Lgl/Dlg/Scribble in the regulation of epithelial junction, polarity and growth. *Front Biosci, 13*(6), 693-707.

Ye, X. (2020, Feb). Uterine Luminal Epithelium as the Transient Gateway for Embryo Implantation. *Trends Endocrinol Metab, 31*(2), 165-180. https://doi.org/10.1016/j.tem.2019.11.008

Yeh, E., Zhou, L., Rudzik, N., & Boulianne, G. L. (2000). Neuralized functions cell autonomously to regulate Drosophila sense organ development. *The EMBO journal, 19*(17), 4827-4837. https://doi.org/10.1093/emboj/19.17.4827

Zanet, J., Freije, A., Ruiz, M., Coulon, V., Sanz, J. R., Chiesa, J., & Gandarillas, A. (2010). A mitosis block links active cell cycle with human epidermal differentiation and results in endoreplication. *PLOS ONE, 5*(12), e15701.

Zeitlinger, J., & Bohmann*, D. (1999). Thorax closure in Drosophila: involvement of Fos and the JNK pathway. *Development, 126*(17), 3947-3956.

Zemans, R. L. (2022, May). Polyploidy in Lung Regeneration: Double Trouble or Dynamic Duo? *Am J Respir Cell Mol Biol, 66*(5), 481-483. https://doi.org/10.1165/rcmb.2022-0062ED

Zhang, B., Mehrotra, S., Ng, W. L., & Calvi, B. R. (2014, Sep). Low levels of p53 protein and chromatin silencing of p53 target genes repress apoptosis in Drosophila endocycling cells. *PLoS Genet, 10*(9), e1004581. https://doi.org/10.1371/journal.pgen.1004581

Zhang, D., Wang, Y., & Zhang, S. (2014). Asymmetric cell division in polyploid giant cancer cells and low eukaryotic cells. *BioMed Research International, 2014*.

Zhang, H., Ma, H., Yang, X., Fan, L., Tian, S., Niu, R., Yan, M., Zheng, M., & Zhang, S. (2021). Cell Fusion-Related Proteins and Signaling Pathways, and Their Roles in the Development and Progression of Cancer. *Frontiers in cell and developmental biology, 9*, 809668. https://doi.org/10.3389/fcell.2021.809668

Zhang, J., Ma, Y., Taylor, S. S., & Tsien, R. Y. (2001). Genetically encoded reporters of protein kinase A activity reveal impact of substrate tethering. *Proceedings of the National Academy of Sciences, 98*(26), 14997-15002.

Zhang, S., Mercado-Uribe, I., Xing, Z., Sun, B., Kuang, J., & Liu, J. (2014). Generation of cancer stem-like cells through the formation of polyploid giant cancer cells. *Oncogene, 33*(1), 116-128.

Zhang, S., Mercado-Uribe, I., & Liu, J. (2014). Tumor stroma and differentiated cancer cells can be originated directly from polyploid giant cancer cells induced by paclitaxel. *International Journal of Cancer, 134*(3), 508-518.

Zhang, S., Zhou, K., Luo, X., Li, L., Tu, H.-C., Sehgal, A., Nguyen, L. H., Zhang, Y., Gopal, P., & Tarlow, B. D. (2018). The polyploid state plays a tumor-suppressive role in the liver. *Developmental cell, 44*(4), 447-459. e445.

Zhang, Y.-W., Jones, T. L., Martin, S. E., Caplen, N. J., & Pommier, Y. (2009). Implication of checkpoint kinase-dependent up-regulation of ribonucleotide reductase R2 in DNA damage response. *Journal of Biological Chemistry, 284*(27), 18085-18095.

Zhao, Q., Zhang, K., Li, Z., Zhang, H., Fu, F., Fu, J., Zheng, M., & Zhang, S. (2021). High Migration and Invasion Ability of PGCCs and Their Daughter Cells Associated With the Nuclear Localization of S100A10 Modified by SUMOylation. *Frontiers in cell and developmental biology, 9*, 696871. https://doi.org/10.3389/fcell.2021.696871

Zhou, J., Tang, Z., Gao, S., Li, C., Feng, Y., & Zhou, X. (2020). Tumor-associated macrophages: recent insights and therapies. *Frontiers in oncology, 10*, 188.

Zicha, D., Dobbie, I. M., Holt, M. R., Monypenny, J., Soong, D. Y., Gray, C., & Dunn, G. A. (2003, Apr 4). Rapid actin transport during cell protrusion. *Science, 300*(5616), 142-145. https://doi.org/10.1126/science.1082026

Zielke, N., Edgar, B. A., & DePamphilis, M. L. (2013, Jan 1). Endoreplication. *Cold Spring Harb Perspect Biol, 5*(1), a012948. https://doi.org/10.1101/cshperspect.a012948

Zielke, N., Kim, K. J., Tran, V., Shibutani, S. T., Bravo, M.-J., Nagarajan, S., Van Straaten, M., Woods, B., Von Dassow, G., & Rottig, C. (2011). Control of Drosophila endocycles by E2F and CRL4CDT2. *Nature, 480*(7375), 123-127.

Zielke, N., Korzelius, J., van Straaten, M., Bender, K., Schuhknecht, Gregor F. P., Dutta, D., Xiang, J., & Edgar, Bruce A. (2014, 2014/04/24/). Fly-FUCCI: A Versatile Tool for Studying Cell Proliferation in Complex Tissues. *Cell Reports, 7*(2), 588-598. https://doi.org/https://doi.org/10.1016/j.celrep.2014.03.020